Studies on Antiobesity-related Compound in Okinawan Medicinal Plant *Peucedanum japonicum* Thunb: Identification and its Mechanisms of Action

沖縄産薬草ボタンボウフウの
抗肥満成分に関する研究
-化学構造とその作用機構の解明-

N.N.R. Nilushi Nugara

2016

Studies on Antiobesity-related Compound in Okinawan Medicinal Plant *Peucedanum japonicum* Thunb: Identification and its Mechanisms of Action

沖縄産薬草ボタンボウフウの

抗肥満成分に関する研究

-化学構造とその作用機構の解明-

N.N.R. Nilushi Nugara

A dissertation submitted to the United Graduate School of Agricultural Sciences, Kagoshima University, Japan

In partial fulfillment of the requirements
for the degree of

Doctor of Agriculture

2016

Acknowledgments

This dissertation would not have been possible without the guidance of several individuals who in one way or another contributed and extended their valuable assistance in the completion of this study.

It is with immense gratitude that I acknowledge the support and guidance received by my Major Advisory Supervisor, Prof. Hirosuke Oku, Tropical Biosphere Research Center (TBRC), Center of Molecular Biosciences (COMB), University of the Ryukyus. Prof. Oku has been my inspiration and guidance in my life during the stay in Japan. Knowing my role as a student and a mom, he always understood my all situations, and stood beside me whenever I needed his help.

It gives me great pleasure in acknowledging Prof. Koji Nagao, Faculty of Agriculture, Saga University; Prof. Ryo Takano and Asst. Prof. Hironori Iwasaki, Faculty of Agriculture, University of the Ryukyus for their immense comments, suggestions and support throughout my research period. Special thanks to my thesis reviewers Prof. Akira Ohtsuka, Faculty of Agriculture, Kagoshima University and Associate Prof. Konishi Teruko, Faculty of Agriculture, University of the Ryukyus and Faculty of Agriculture, Kagoshima University.

My sincere gratitude goes to Dr. Masashi Inafuku, for his advices, guidance and kind consideration on me at all times as a senior, researcher, friend and a brother. Not forgetting Dr. Natthanan Nukitrangsan, and Dr. Takafumi Okabe, who offered a helping hand to me at the beginning of my study. Heartiest gratitude to Dr. Seikoh Saitoh for his wonderful assistance and guidance in Next Generation Sequencing and Analyses.

Special thanks to my dearest friend Dr. Leila El Bassi for being so dear to me and guiding me throughout even during her absence with me in Japan. A big thank you to Mr. Naoyuki Taira, and to all my previous and present lab members for their support and making my lab experience a memorable one. Special thanks to all staff members at the Center of Molecular Biosciences for their kind assistance during my study period.

I recognize that this research would have not been possible without the financial assistance of Ministry of Education, Culture, Sports, Science and Technology, Japan, and express my heartfelt gratitude for the enormous financial support given to me.

Finally, I take this opportunity to praise the “Lord Jesus Christ” for making me who I am today, also my beloved husband, for his unconditional love, dedication and invaluable support and my ever-loving daughters for their love and sweet smile. A big ‘thank you’ to my mom and dad for all their encouragement and mostly believing in me.

Table of contents

List of Figures

List of Tables

List of abbreviations

ACC: acetyl CoA carboxylase

ACL: ATP citrate lyase

ACTB: Actin, beta, cytoplasmic

AMPK: AMP-activated protein kinase

ATGL: Adipose triglyceride lipase

BAT: Brown adipose tissue

BCS: Bovine calf serum

BMI: Body mass index

CA: Carbonic anhydrase

CC: Open column chromatography

C/EBPα: CCAAT/enhancer binding protein alpha

CGA: Chlorogenic acid

ChREBP: Carbohydrate-responsive element binding protein

CPT1: Carnitine palmitoyltransferase 1

CREB: cAMP response element-binding protein

Cyp a: Cyclophilin a

CYP7A1: Cytochrome P450, family 7, subfamily a, polypeptide 1

DMEM: Dulbecco's modified Eagle's medium

DEX: Dexamethasone

EE: Ethanol extract of PJT

EI-MS: electron ionization mass spectrometry

ERK: Extracellular-signal regulated kinase

FABP4: Fatty acid binding protein 4

FAS: Fatty acid synthase

FBS: Fetal bovine serum

FDR: False discovery rate

FFA: Free fatty acids

FXRα: Farnesoid X receptor α

GAPDH: Glyceraldehyde-3-phosphate dehydrogenase

GC-MS: Gas chromatogram mass spectrometry

GLUT: Glucose transporter

HFD: High fat diet

HMBC: Heteronuclear multiple bond correlation

HMG-CoA: 3-hydroxy-3-methyl-glutaryl-coenyme A

HMQC: Heteronuclear multiple quantum coherence

HOMA: Homeostasis model assessment

HP: Hexane phase of PJT EE

HDL: High density lipoprotein

HSL: Hormone sensitive lipase

IBMX: 3-isobutyl-1-methylxanthine

IGF: Insulin like growth factor

IGFBP: Insulin like growth factor binding protein

IL: Interleukin

INSIG2: Insulin induced gene 2

IPA: Ingenuity pathway analysis

IR: Insulin resistance

IRS-1: Insulin receptor substrate 1

LPL: Lipoprotein lipase

MAPK: Mitogen activated protein kinase

MCE: Mitotic clonal expansion

MCP: Monocyte ckemoattractant protein

MTS: 3-(4,5-dimethylthiazol-2-yl)- 5-(3-carboxymethoxyphenyl)-2-(4-sulfophenyl)-2H-

tetrazolium

NEFA: Nonesterified fatty acids

NGS: Next generation sequencing

PBEF1: Pre-b-cell colony-enhancing factor 1 (Visferin)

PEG1/MEST: Paternally expressed gene 1 (Peg1)/mesoderm specific transcript (Mest)

PGC1α: Peroxisome proliferator activated receptor gamma coactivator 1-alpha

PI3K: Phosphoinositide 3 kinase

PJT: *Peucedanum japonicum* Thunb

PK (A/G): Protein kinase (A or G)

PPAR: Peroxisome proliferator activated receptor gamma

qPCR: Quantitative reverse transcriptase real-time polymerase chain reaction

RORC: RAR-related orphan receptor gamma C

SCD: stearoyl-CoA desaturase

SERPINA12: Serine (or cystein) peptidase inhibitor, clade A (Vastin) (alpha-1antiproteinase, antitrypsin), member 12

SREBP: Sterol regulatory element-binding protein

TC: Total Cholesterol

TFA: Trifluoroacetic acid

TG: Triglyceride

TNFα: Tumor necrosis factor alpha

UCP: Uncoupling protein

VLDL: Very low density lipoprotein

WAT: White adipose tissue

WHO: World health organization

WP: Water phase of PJT EE

Abstract

Obesity and overweight are major health concerns worldwide due to their contribution in numerous metabolic disorders. Previous studies on *Peucedanum japonicum* Thunb (PJT) have reported anti-obesity properties available in PJT powder. However, PJT as a crude extract restricted in-depth investigations on mechanisms related to anti-obesity. In this thesis, partial purification of PJT, isolation of the active compound responsible for anti-obesity 'pteryxin' in PJT and its characterization were investigated.

The first experiment examined the anti-obesity activities of partially purified fractions of PJT *in vitro*. This study focused on the lipid accumulation in 3T3-L1 adipocytes, HepG2 hepatocytes and glucose consumption in C2C12 muscle cells. The gene modulation pattern in each cell type due to ethanol extract (EE), hexane phase (HP) and water phase (WP) of PJT was examined. The HP significantly downregulated lipogenic gene expressions in hepatocytes, inhibited TG accumulation, and decreased the size of 3T3-L1 adipocytes. In C2C12 myotubes, HP tended to enhance energy expenditure. The results suggested that PJT HP possessing the characteristics of anti-obesity during the partial purification.

The second experiment isolated the active compound from PJT HP responsible for anti-obesity, namely pteryxin, a previously known coumarin in PJT. The dose dependent effect on the triglyceride (TG) content, and the gene expressions related to adipogenesis, energy expenditure and lipogenesis due to pteryxin were examined *in vitro*. Pteryxin dose-dependently suppressed TG content in both 3T3-L1 and HepG2 cells. Key lipogenic transcription factors were downregulated in pteryxin-treated 3T3-L1 and HepG2 cells. The energy expenditure was upregulated due to pteryxin. This study demonstrated that pteryxin in PJT play the key role in regulating lipid metabolism related gene network *in vitro*.

Next, the efficacy of pteryxin containing PJT extracts against obesity in C57BL/6 mice fed a high-fat diet was assesses. The PJT EE was fractionated in to HP and WP. The pteryxin content in each fraction was quantified by HPLC. The pteryxin-rich HP and EE attenuated the body weight of mice after 4 weeks. HP suppressed blood glucose, TG content and showed a downregulatory trend in insulin resistance. The highest marked reduction in epididymal white adipose tissue weight was observed due to the HP diet.

The TG formation and storage in liver were reduced. This study demonstrated that pteryxin in HP plays an important role in regulating lipid metabolism-related gene expression and energy expenditure *in vivo*.

Finally, I investigated the molecular mechanisms of pteryxin in attenuating adipogenesis. Pteryxin was used at low (20 μg/mL) and high (50 μg/mL) doses in 3T3-L1 cells either during the entire adipogenesis or only during the proliferation stage and performed next generation sequencing (NGS), qPCR, and protein expressions related to different doses of pteryxin. I found that pteryxin at two different doses attenuate adipogenesis, however, pteryxin at 20 μg/mL, downregulated lipogenic genes and increased lipolysis. The 50 μg/mL pteryxin completely suppressed adipocyte differentiation in 3T3-L1 adipocytes. The NGS data analysis suggested that pteryxin at 50 μg/mL downregulated Wnt5a non-canonical pathway. I found that ERK1/2, AMPK activities play a major role in the adipogenesis inhibition in the presence of 20 and 50 μg/mL pteryxin, respectively.

In conclusion, these results provide great insight on the unique characteristics of pteryxin in the anti-adipogenic process in order to utilize pteryxin as an anti-obesity drug in the pharmaceutical industry in the near future.

沖縄産薬草ボタンボウフウの抗肥満成分に関する研究

-化学構造とその作用機構の解明-

高脂血症、高血圧、糖尿病、動脈硬化症などの生活習慣病の発症に対して肥満、特に腹腔内脂肪の蓄積は重要な危険因子であることから、安全な肥満改善食材の開発が強く求められている。

沖縄県で伝統的に野菜／薬草として食されているボタンボウフウ（*Peucedanum japonicum* Thunb）には、抗肥満作用があることがこれまでの研究において明らかにされている。しかしながら、これまでの知見は粗抽出物を用いた結果であり、抗肥満作用の詳細なメカニズムについては明らかにされていない。そこで、本研究はボタンボウフウ抽出物中の抗肥満成分の同定とその作用メカニズムを明らかにすることを目的とした。

まず、ボタンボウフウのエタノール粗抽出物をヘキサンと水で分配した部分精製画分の抗肥満作用を脂肪細胞、肝細胞及び筋肉細胞を用いた培養試験により検証した。このうち、ヘキサン画分により強い抗肥満作用が検出され、脂肪細胞及び肝細胞においては脂質合成が抑制され、筋肉細胞においてはエネルギー消費が亢進される傾向にあった。さらに、抗肥満成分は比較的疎水性の化合物であることがヘキサン画分の HPLC 分析により示唆された。

次に、ヘキサン画分の抗肥満成分を各種クロマトグラフィーの組み合わせにより単離し、有効成分をピラノクマリンの一種であるプテリキシンと同定した。プテリキシンは脂質合成関連転写因子の発現抑制とエネルギー消費の促進により、脂肪細胞及び肝細胞の中性脂肪濃度を用量依存的に低下させることが明らかになった。

引き続き、ボタンボウフウのエタノール抽出物をヘキサンと水で分配した部分精製画分の抗肥満作用を動物試験により検証した。プテリキシン濃度の高いヘキサン画分は体重、血清グルコース、中性脂肪濃度を低下させ、インシュリン抵抗性を改善させる傾向にあった。また、ヘキサン画分は内臓及び肝臓脂肪濃度も低下させた。これらの結果は、長命草中のプテリキシンが生体においても抗肥満作用を示すことを支持するものと考えられた。

最後に、脂肪細胞におけるプテリキシンの抗肥満作用の分子機構を解析した。プテリキシンは低用量及び高用量いずれでも ERK1/2 及び AMPK 経路を介して脂質合成を抑制した。一方、高用量では脂肪細胞の分化が完全に抑制され、これには非古典的 Wnt5a 経路の関与が示唆された。

本研究により、沖縄産薬草ボタンボウフウの抗肥満成分とその作用機構が明らかになった。これらは、ボタンボウフウ或はその有効成分であるプテリキシンを用いた安全な抗肥満剤の開発に貢献する成果と判断された。

CHAPTER I

General Introduction

1.1 Global Perspective on Metabolic Syndrome

Metabolic syndrome represent a cluster of risk factors that raises the risk for cardiovascular diseases and diabetes. The risk factors include obesity, hypertension, dyslipidemia, and hyperglycemia (Borch-Johnsen, 2007). These syndrome or diseases were earlier considered as high in occurrence in developed countries. However, the stagnation or increment of the prevalence of these diseases in developing countries have increased dominantly along with the global transition over the years. Metabolic syndrome is an attractive scientific and commercial factor due to its high morbidity and mortality. Thus, immediate attention should be required for preventive measures of these risk factors.

Among these, obesity and overweight is increasing worldwide and has become an overwhelming threat to large communities. The World Health Organization (WHO) showed that, in 2014, more than 1.9 billion adults, the age of 18 and over, were overweight (Fig. 1-1). Of these, more than 600 million were obese (WHO, 2014b).

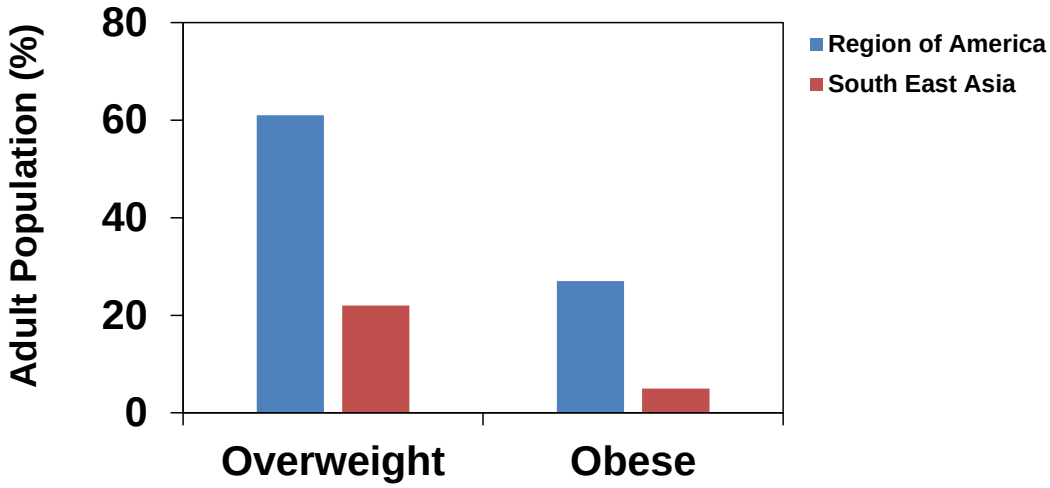

Figure 1-1 Comparison between the highest and least overweight and obese population prevalence regions in the world

Source: World Health Organization; 2014

The prevalence of childhood overweight is increasing worldwide, especially in Africa and Asia. Between the year 2000 and 2013, the prevalence of overweight in children aged under 5 years, increased from 11% to 19% in some countries in southern Africa and from 3% to 7% in South-East Asia. In 2013, there were an estimated 18 million overweight children aged under 5 years in Asia. It is estimated that the prevalence of overweight in children aged under 5 years will rise to 11% worldwide by 2025, if the current trends continue (WHO, 2014a).

1.2 Prevalence of Obesity and occurrence in Japan

The WHO has standardized overweight and obesity by using body mass index (BMI) ≥ 25 to be overweight and ≥ 30 to be obese. However, due to the high tendency of exceeding the risk of type 2 diabetes and cardiovascular diseases due to the availability of high visceral fat in human body at BMI 25, the Japan Society on Obesity Study has bench-marked 25 as the obese limit of BMI (Japan Society on Obesity Study, 2014).

According to a survey conducted by the Ministry of Health, Labor and Welfare, Japan, obesity risk was higher in adults 40 years and over, and continued to increase yearly during the last two decades. Furthermore, it also revealed that Okinawa was ranked as No. 1 for the highest prevalence of obesity amongst the 47 prefectures in all Japan in the 2010 (Fig. 1-2). The second highest prevalence was observed in Miyazaki and the least were in Tottori, Shiga, Fukui and Yamaguchi (Ministry of Health, Labour and Welfare, Japan, 2010). The following figure illustrates the selected highest and lowest prevalence of obesity in prefectures in Japan.

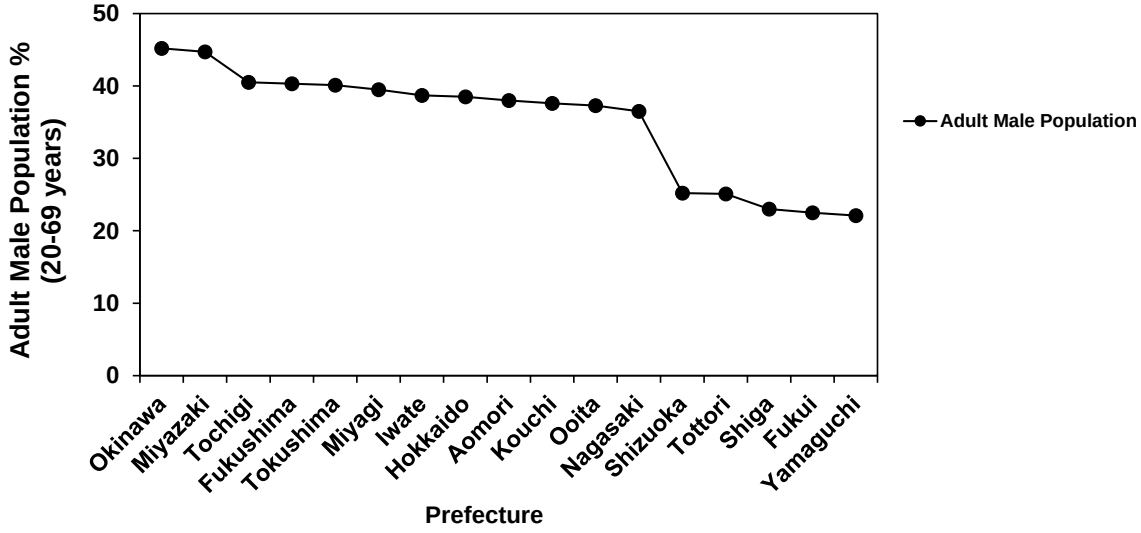

Figure 1-2 Highest and lowest obese adult male population prevalence regions in Japan

Source: Ministry of Health, Labor and Welfare; 2010

1.3 Causes for Obesity

Lack of energy balance in the body plays a pivotal role in obesity and overweight. The accumulation of excess body fat occurs by the greater energy intake than the energy expenditure. A high-fat diet (HFD) enriched with saturated fatty acids, which may affect body weight by controlling satiety and metabolic efficiency, or by modulating insulin secretion and action (Liu *et al.*, 2003). On the other hand, there are many other factors that are affecting obesity such as an inactive life style (Papandreou *et al.*, 2007), environment where the society has become overloaded with their busy schedules and has poor access to healthy food. A person with an inactive life style could spend hours watching television, seated in front of a computer, or even relying on cars instead of walking. This way, the amount of calories burnt are less, allowing a retention of energy in the body. Moreover, genes and family history (Lin *et al.*, 2010), health condition of a person, sleep (Dixon *et al.*, 2007) and certain medicines that are used for depression also have been found to contribute towards obesity (Uguz *et al.*, 2015).

1.4 Physiological Roles of Adipose Tissue during Obesity

Adipose tissue is a complex organ that regulates energy homeostasis in the body. However, the over accumulation of fat in the adipose tissue is characterized as obesity (Nakamura *et al.*, 2013; Rosen and Spiegelman, 2000). Furthermore, the adipose tissue function as an endocrine organ that is capable of producing and secreting a variety of factors including free fatty acids (FFA), leptin, adiponectin, tumor necrosis factor-α (*TNF-α*) and interleukin-6 (*IL-6*) ultimately influence on the metabolic homeostasis. Thus, the adipose cells had been used as a study model since 1970s due to its authentic key features against other cell lines (Green and Kehinde, 1975). While many studies focus on the adipogenesis by the development of white adipose tissue (WAT) (Than *et al.*, 2012; Park *et al.*, 2012; Hung *et al.*, 2005), recent research also focus on the brown adipose tissue (BAT), which the physiological role is the opposite to that of WAT (Vitali *et al.*, 2012; Fisher *et al.*, 2012). Thus, it confers beneficial effects on adiposity, insulin resistance and hyperlipidaemia at least in mice (Bartelt and Heeren, 2014).

Figure 1-3 illustrates the cellular interactions that participates in the inflammatory pathways along with the obesity-associated comorbidities. Insulin, which is the key hormone involved in the control of glucose and lipid homeostasis. The adipose tissue-derived inflammatory cytokines and the insulin resistance may promote the tumorogenesis. In the presence of cold or β3-agonism, the WAT poses the ability to be converted to BAT and reverse the action by a HFD or thermoneutrality. The abbreviated genes are as follows: *LPL*; lipoprotein lipase, *TNFα*; tumor necrosis factor α, *IL-6*; interleukin-6, *MCP-1*; monocyte ckemoattractant protein-1, *HSL*; hormone sensitive lipase, *PGC1α*; peroxisome proliferator-activated receptor-gamma coactivator, *PPAR*; peroxisome proliferator-activated receptor, *CREB*; cAMP response element-binding protein, *UCP*; uncoupled protein, *GLUT*; glucose transporter, *ACL*; ATP citrate lyase, *FAS*; fatty acid synthase, *SCD*; stearoyl-CoA desaturase, *ATGL*; adipose triglyceride lipase, *SREBP*; sterol regulatory element binding protein, *ChREBP*; carbohydrate-responsive element binding protein, PKA; protein kinase A, MAPK; mitogen activated protein kinase, PKG; protein kinase G, AMPK; AMP-activated protein kinase, FFA; free fatty acids, IR; insulin resistance, IGFBP; insulin like growth factor binding proteins,

TG; triglyceride, VLDL; very low density lipoprotein, HDL-C; high density lipoprotein-cholesterol.

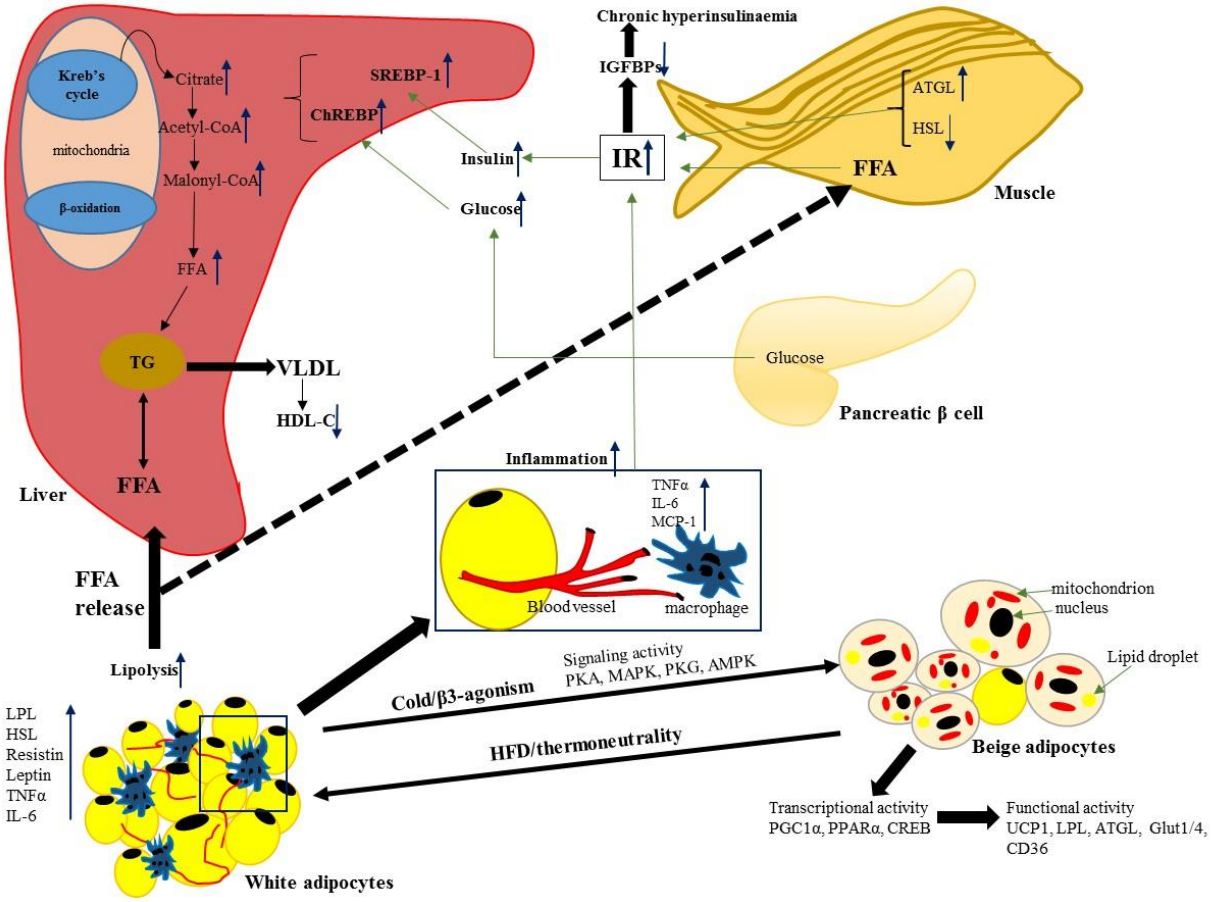

Figure 1-3 Mechanisms linking excess adiposity in the body.

1.5 Treatments for Obesity

A weight loss between 5-10% of initial body weight has been recommended as the threshold by National Institute of Health, USA (Padwal and Majumdar, 2007). There are various obesity treatment drugs available on the market, one of these is orlistat (Xenical), which reduces intestinal fat absorption through inhibition of pancreatic lipase ((Drew *et al.*, 2007; Thurairajah *et al.*, 2005). The other is sibutramine (Reductil), which is an anorectic or appetite suppressant (Lean, 2001). Both drugs have side-effects, including increased blood pressure, dry mouth, constipation, headache, and insomnia (De Simone and D' Addeo, 2008; Slovacek *et al.*, 2008; Thurairajah *et al.*, 2005). Studies of many anti-obesity drugs have been notable for their high attrition rates and lack of data on obesity-related mortality.

At present, because of the dissatisfaction with high costs and potentially hazardous side-effects, the potential of natural products for treating obesity is under exploration, and this may be an excellent alternative strategy.

1.6 *Peucedanum japonicum* Thunb (PJT), a Plant with an Impact

Peucedanum japonicum Thunb (PJT), also known as "Chomeiso" (長命草) is a medicinal plant belonging to the family of Apiaceae, which is distributed in southern Japan, China and Taiwan (Fig. 1-4).

Figure 1-4 *Peucedanum japonicum* Thunb (PJT)

The roots of this plant have been used as a folk medicine for cold and neuralgic diseases in Taiwan (Chen *et al.*, 1996b), also used as a basal ingredient in many dishes in Okinawa. A number of studies have reported on the physiological activities of PJT including antioxidant activity (Hisamoto *et al.*, 2003), tyrosinase inhibitory effect (Hisamoto *et al.*, 2004), and antiplatelet aggregation activity (Chen *et al.*, 1996b) *in vitro*. Many studies have demonstrated that phenolic compounds available in plant extracts exhibit anti-obesity activity in obese animal models and C57BL/6 mice (Wang *et al.*, 2011; Chan *et al.*, 1999; Kim *et al.*, 2008; Chung *et al.*, 2012). PJT leaves too consist of phenolic compounds including rutin and chlorogenic acid analogues (Hisamoto *et al.*, 2004).

1.7 PJT as an Obesity Treatment

Early studies on PJT have found its usefulness as a natural agent to reduce obesity (Okabe *et al.*, 2011) and Nukitrangsan et al. confirmed 10% PJT powder can inhibit the absorption of triacylglycerol (TG) and cholesterol (TC) in the alimentary tract of C57BL/6 mice model (Nukitrangsan *et al.*, 2011). Therefore, it was speculated that the fiber component in PJT is largely responsible for the anti-obesity activity. However, a compensatory decrease in dietary cellulose does not decisively address the question whether fiber or other phytochemical components are responsible for the anti-obesity activity in PJT. Therefore, further examination was carried out to partially identify the fraction containing the anti-obesity activity and it was found that ethanol extract of PJT has an ability to lower the lipid levels by modulating obesity related gene expression levels in liver, adipose tissue and muscle (Nukitrangsan *et al.*, 2012b). It was also revealed that ethanol extract of PJT not only specific for anti-obesity, yet also plays an important role in anti-diabetic activity (Nukitrangsan *et al.*, 2012a) .

Yet, *in vivo* studies may have a limiting approach in order to gain insight on molecular mechanisms involved with PJT in the anti-obesity process. Therefore, it was a timely requirement to address the actual mechanisms of PJT by *in vitro* studies which will be the most appropriate to unveil the unexplored.

1.8 *In vitro* based studies using Cell Models

3T3-L1 preadipocytes are frequently used to study the function of adipocytes. This cell line isolated from non-clonal Swiss 3T3 cells and is already committed to the adipocytic lineage (Green and Kehinde, 1975). Differentiated 3T3-L1 preadipocytes consist of similar characteristics to that of adipocytes from animal tissue. Peroxisome proliferator-activated receptor γ (*PPARγ*) and CCAAT-enhancer-binding proteins (*C/EBP*s) are the crucial transcription factors in adipogenesis (Rosen and MacDougald, 2006). *PPARγ*, is considered as the *master regulator* of adipogenesis. There are many studies that have shown significant downregulation of *PPARγ* by plant extracts and concluded to be useful natural agents for obesity treatments (Taxvig *et al.*, 2012; Chang *et al.*, 2011; Kim *et al.*, 2012). On the other hand, *PPARγ* also has a crucial role in regulating lipid metabolism in mature adipocytes (Lehrke and Lazar, 2005). Targeted deletion of *PPARγ* in fat tissue has resulted in reduction of adipocytes number (He *et al.*, 2003), elevated levels of plasma non-esterified fatty acids and TG, and decreased levels of plasma leptin and adiponectin. Furthermore, these mice were also significantly susceptible to HFD induced steatosis (fatty liver), hyperinsulinemia, and insulin insensitivity in fat and liver. Therefore, these contradicting findings suggest the capabilities of *PPARγ* that can act differently based on the type of plant extract.

In my studies, I selected the 3T3-L1 cell line, HepG2, hepatoma cell line and C2C12 muscle cell model for investigations of the activity of PJT and its related mechanisms *in vitro.* The 3T3-L1 cell model is a widely used cell line for adipocyte differentiation and its fibroblast appearance can be changed to an adipocyte phenotype in the presence of a differentiation induction cocktail which consist of isobutylmethylxanthine, dexamethasone and insulin. The mature adipocytes are able to store lipid as droplets and this could be used for assessing the TG accumulation in the cells (Green and Kehinde, 1975; Mackall *et al.*, 1976).

The HepG2 cell line is a perpetual cell obtained from the liver of a 15 years old human male adolescent suffering from hepatocellular carcinoma. HepG2 having an epithelial morphology either grow as a monolayer or as aggregates. Many studies have used this cell model for screening of hepatic lipid accumulation and related lipogenic activity (Lee *et al.*, 2010; Hwang *et al.*, 2011).

C2C12 is a mouse myoblast cell line originally obtained from the thigh muscle of the C3H mice after crush injury. These cells are capable of differentiation into muscle-like cells, it takes more than one week to achieve the differentiation. However, this cell line is used for the measurement of glucose consumption *in vitro* (Hayata *et al.*, 2008; Shen *et al.*, 2012).

1.9 Outline of the Studies

1. An investigation of the effect of partially purified *Peucedanum japonicum* Thunb extracts on anti-obesity *in vitro* using 3T3-L1, HepG2 and C2C12 cell lines. Gene expression analyses were given special attention to reveal the underlying mechanisms related to PJT (Chapter II).
2. An identification of the active compound, a coumarin, Pteryxin, in the hexane phase of the *Peucedanum japonicum* Thunb and its mechanisms of action against adipogenesis (Chapter III). The main focus of this study was to elucidate the compound responsible for repressing adipogenesis and to examine the activity against anti-obesity *in vitro*.
3. An investigation of the effect of pteryxin content and ethanol extract, hexane phase, and water phase of *Peucedanum japonicum* Thunb in C57BL/6 male mice in order to explore the activity of these fractions *in vivo* (Chapter IV). This study was carried out to examine the uninterrupted activities of pteryxin containing fractions in a live murine model.
4. An examination of the multifaceted pteryxin-mediated molecular mechanisms to inhibit adipogenesis in 3T3-L1 cell line (Chapter V). This study focused on the molecular mechanisms, upstream and downstream target points and gene modulations due to a low and high dose of pteryxin *in vitro*.

CHAPTER II

Anti-obesity effects of partially purified *Peucedanum japonicum* Thunb extracts: An *in vitro* study

Introduction

Obesity has become one of the most critical medical issues worldwide due to its close relationship with type 2 diabetes, fatty liver disease, and other critical metabolic disorders (Yun, 2010; Ahn *et al.*, 2012). Sedentary life style and a high calorie diet are the most prominent factors involved in the development of obesity. Therefore, obesity constitutes a major public health problem worldwide.

There are several pharmacological substances available globally as anti-obesity drugs, yet they consist of many side effects such as dry mouth, constipation and insomnia (Matson and Fallon, 2012). On the other hand, natural products have been used for treating obesity in many Asian countries for centuries. Especially China and India have taken the lead in this field.

Peucedanum japonicum Thunb (PJT), belonging to the family Apiaceae (earlier known as Umbelliferae), originates from southern Japan, China, and Taiwan. PJT leaves have been used traditionally to treat cold and cough in the Okinawa Island, Japan. In village areas of Okinawa, the leaves are used as a raw ingredient for many dishes. Our previous studies have reported on the anti-obesity properties of PJT powder (Okabe *et al.*, 2011). In further studies, the anti-obesity activity of PJT was found to be due to lipase inhibition, and thus ethanol extract of PJT (EE) being characterized as anti-diabetic activity (Nukitrangsan *et al.*, 2012b; Nukitrangsan *et al.*, 2012a; Nukitrangsan *et al.*, 2011). However, a persisting limitation is that PJT crude extracts restrict in-depth investigations on the mechanisms related to anti-obesity.

Therefore, in the present study, I investigated the following:

1. Inhibitory effects of partially purified EE on obesity *in vitro*.
2. The target stage of adipocyte differentiation for the maximum inhibition of lipid accumulation.
3. Related gene modulation pattern in adipogenesis.
4. Profiling of PJT extracts by HPLC.

2.1 Materials and methods

2.1.1 Preparation of PJT extracts

The origin of PJT was harvested from the Yonaguni Island, Okinawa, Japan. PJT leaves and stems were freeze-dried and ground by Yonagunijima Yakusoen Co. Okinawa, Japan. The dried powder of PJT was analyzed by the Japan Food Research Laboratories (Tokyo, Japan). The yield of EE was ~11% of the starting material. EE was further suspended in water and partitioned into *n*-hexane (4×1: 1 v/v). The approximate yields of the hexane phase (HP) and the residual water phase (WP) were 3.3% and 7.0%, respectively (based on the starting material). All extracts were stored at −80°C for further use (Fig. 2-1).

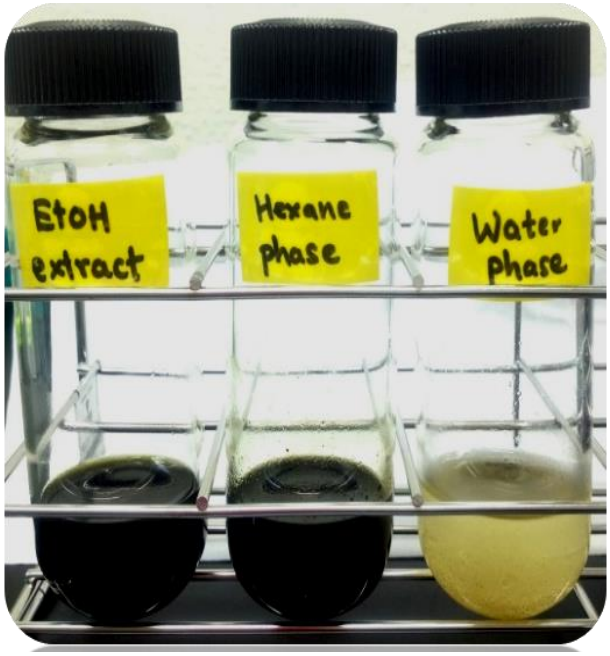

Figure 2-1 PJT ethanol extract fractionation to hexane and residual water phases.

2.1.2 Cell culture

3T3-L1 preadipocytes were grown in Dulbecco's modified Eagle's medium (DMEM) and 10% bovine calf serum (BCS) and avoided complete confluence before initiating differentiation. For adipogenesis, the confluent fibroblasts were maintained for another 2 days (defined as Day 0). Differentiation was induced with standard differentiation inducers 0.5 mM 3-isobutyl-1-methylxanthine (IBMX), 0.25 µM dexamethasone (DEX) and 1.72 mM insulin for 48 h (from Day 0–2) (Koyama *et al.*, 2012). On Day 2, the culture medium was changed to the maintenance medium containing DMEM, 10% fetal bovine serum (FBS), 10 µg/mL insulin, EE (25 or 50 µg/mL), HP (6 or 11 µg/mL), or WP (19 or 37 µg/mL) from Day 2–6. The control group was maintained in the basic maintenance medium without PJT treatments. The non-differentiated (preadipocytes) cells were maintained in DMEM supplemented with 10% FBS from Day 0-6 with no differentiation induction. To study the acting stage of HP in the adipocyte development, cell cultures were supplemented with HP (50 µg/mL) at different time intervals as shown below in Fig. 2-2.

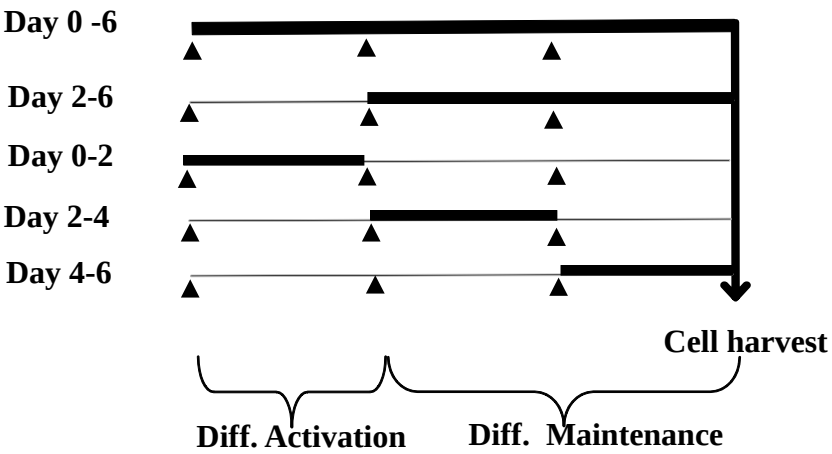

Figure 2-2 Schematic diagram of the addition of hexane phase (50 µg/mL) at different time points during the adipogenesis process in 3T3-L1 cells.

HepG2 cells were maintained in DMEM supplemented with 100 U/ml penicillin, 100 µg/ml streptomycin, and 10% FBS in an atmosphere of 5% CO_2 at 37°C. For experiments, the cells were incubated in complete medium to 70% confluence, and maintained in serum-free DMEM overnight (Zang *et al.*, 2004). HepG2 cells were then cultured with or without insulin (1 µM) for 12 h and subsequently treated with or without insulin and/or EE (50 µg/mL), HP (11 µg/mL), or WP (37 µg/mL) for another 12 h.

For C2C12 myocytes, cells were cultured in complete medium for 24 h as for HepG2, where the cells reach 80% confluence. Then DMEM supplemented with 2% horse serum was used to induce differentiation for 4-5 days with medium change every 48 h (Canto *et al.*, 2009). For the measurement of glucose consumption, the culture medium was replaced by DMEM supplemented with 0.25% (w/v) bovine serum albumin. Then, cells were treated with PJT extracts for 24 h. The glucose concentration in the medium was determined by the glucose oxidase method after 24 h.

For the cell viability check, each type of cells were cultured in 96-well plates and assessed by using the 3-(4,5-dimethylthiazol-2-yl)-5-(3-carboxymethoxyphenyl)-2-(4-sulfophenyl)-2H-tetrazolium (MTS) solution 20 µL per well for 24 h (HepG2, C2C12 cells) and 48 h, and 6 days for 3T3-L1 cells. Once added the MTS solution, absorbance were measured at 0, 5, 10, 15, 20 and 30 min incubation time intervals (Zhang *et al.*, 2012). Dulbecco's modified Eagle's medium (DMEM), and fetal bovine serum (FBS), were purchased from Wako Pure Chemical Industries Ltd. (Osaka, Japan). Heat inactivated horse serum (HS) and bovine calf serum (BCS) were purchased from Life Technologies (Grand Island, NY, USA).

2.1.3 Triglyceride Analysis

At the end of each treatment period, 3T3-L1 and HepG2 cells were washed with phosphate buffer solution (PBS; Wako Pure Chemical Industries Ltd.) and harvested with the use of accutase (Innovative Cell Technologies, Inc., San Diego, CA). Total lipids were extracted according to the Bligh and Dyer method (Bligh and Dyer, 1959), and TG content was quantified using a commercial enzymatic kit (Wako Pure Chemical Industries Ltd.) according to the manufacturer's instructions. The content of cellular protein was determined using the Quant-iT protein assay kit (Life Technologies).

2.1.4 Quantitative real-time PCR

First strand cDNA was synthesized with 2 μg of total RNA as a template using High capacity RNA-to-cDNA kit (Applied Biosystems, CA, USA). The quantitative real-time reverse transcriptase-polymerase chain reaction (qPCR) was performed on the Step One Plus ™ Real-Time PCR System (Applied Biosystems) with the following parameters:

1st step - one cycle of 95°C for 20 s

2nd step - 40 cycles of 95°C for 3 s

3rd step - 60°C for 30 s

4th step - A melting curve analysis

95°C for 15 s

60°C for 60 s

0.3°C increase every 15 s to determine primer specificity (**Table 2-1** and **2-2**). The mRNA levels of all genes were normalized using actin, beta, cytoplasmic (*ACTB*), glyceraldehyde-3-phosphate dehydrogenase (*GAPDH*), and cyclophilin a (*CYPa*) as the internal controls for 3T3-L1, HepG2, and C2C12, respectively.

Table 2-1 Primer sequences used for qPCR *in vitro* murine cell lines

Gene	Description	Primer sequence	Product	Accession no.
RORC	RAR-related orphan receptor γ	(F)5'-TCC TGC CAC CTT GAG TAT AGT C-3'	80	NM_011281
		(R)5'-GTA AGT TGG CCG TCA GTG CTA-3'		
PPARα	peroxisome proliferator	(F)5'-CCT CAG GGT ACC ACT ACG GAG T-3'	69	NM_011144
	activated receptor α	(R)5'-GCC GAA TAG TTC GCC GAA-3'		
PPARγ	peroxisome proliferator	(F)5'-AGG CCG AGA AGG AGA AGC TGT TG-3'	276	NM_011146
	activated receptor γ	(R)5'-TGG CCA CCT CTT TGC TGT GCT C-3'		
FAS	fatty acid synthase	(F)5'-TGC TCC CAG CTG CAG GC-3'	91	AF_127033
		(R)5'-GCC CGG TAG CTC TGG GTG TA-3'		
FXRα	farnesoid X receptor α	(F)5'-CCC TGC TTG ATG TGC TAC AA-3'	189	NM_001163700.1
		(R)5'-GTG TCC ATC ACT GCA CAT C-3'		
SREBP-1	sterol regulatory element	(F)5'-GCG CCA TGG ACG AGC TG-3'	205	NM_011480
	binding protein-1	(R)5'-TTG GCA CCT GGG CTG CT-3'		
C/EBPα	CCAAT/enhancer	(F)5'-TGG ACA AGA ACA GCA ACG AGT AC-3'	257	NM_007678
	binding protein α	(R)5'-GCA GTT GCC CAT GGC CTT GAC-3'		
PEG1/MEST	paternally expressed gene 1/	(F)5'-GTT TTT CAC CTA CAA AGG CCT ACG-3'	52	NM_008590
	Mesoderm specific transcript	(R)5'-CAC ACC GAC AGA ATC TTG GTA GAA-3'		
LPL	lipoprotein lipase	(F)5'-AGG GCT CTG CCT GAG TTG TA-3'	199	NM_008509
		(R)5'-AGA AAT CTC GAA GGC CTG GT-3'		
UCP2	uncoupling protein 2	(F)5'-CAG GTC ACT GTG CCC TTA CCA T-3'	101	NM_011671

		(R)5’-CAC TAC GTT CCA GGA TCC CAA G-3’		
UCP3	uncoupling protein 3	(F)5’-CCA CCT TAG GGC AAG AAC GA-3’	76	AB010742
		(R)5’-GGT ACG ACC CTG AGA TGA GAA AA-3’		
GLUT4	glucose transporter	(F)5’-CTG CAA AGC GTA GGT ACC AA-3’	87	BC014282
	type 4	(R)5’-CCT CCC GCC CTT AGT TG-3’		
IRS-1	insulin receptor substrate 1	(F)5’-CCA GAG TCA AGC CTC ACA CA-3’	179	NM_010570.4
		(R)5’-GAA GAC TGC TGC TGC TGT TG-3’		
FABP4	fatty acid binding protein 4	(F)5’-AGC ATC ATA ACC CTA GAT GG-3’	115	NM_024406.2
		(R)5’-CAT AAC ACA TTC CAC CAC CAG C-3’		
CPT1α	carnitine plamitoytransferase	(F)5’-AAA GAT CAA TCG GAC CCT AGA CA-3’	124	NM_013495
	1-alpha	(R)5’-CAG CGA GTA GCG CAT AGT CA-3’		
GAPDH	glyceraldehydes-3-phosphate	(F)5’-ACC CAG AAG ACT GTG GAT GG-3’	172	NM_008084
	dehydrogenase	(R)5’-ACA CAT TGG GGG TAG GAA CA-3’		
ACTB	actin, beta, cytoplasmic	(F)5’-CAG AAG GAG ATT ACT GCT CTG GCT-3’	93	NM_007393
		(R)5’-GGA GCC ACC GAT CCA CAC A-3’		
CYPa	cyclophilin a	(F)5’-GGG TTC CTC CTT TCA CAG AAT TAT T-3’	78	AF171073
		(R)5’-CCG CCA GTG CCA TTA TGG-3’		

Table 2-2 Primer sequences used for qPCR *in vitro* human cell lines

Gene	Description	Primer sequence	Product	Accession no.
SREBF-1	sterol regulatory element	(F)5'-GCC CCT GTA ACG ACC ACT GTG A-3'	84	NM_001005291.2
	Binding transcription factor 1	(R)5'-CAG CGA GTC TGC CTT GAT G-3'		
PPARα	peroxisome proliferator	(F)5'-CGT CCT GGC CTT CTA AAC GTA G-3'	234	NM_001001928.2
	activated receptor α	(R)5'-CCT GTA GAT CTC CTG CAG TAG -3'		
FASN	fatty acid synthase	(F)5'-TCG TGG GCT ACA GCA TGG T -3'	80	NM_011281
		(R)5'- GCC CTC TGA AGT CGA AGA AG-3'		
FXRα	farnesoid X receptor α	(F)5'-GAC TTT GGA CCA TGA AGA C -3'	104	NM_005123.3
		(R)5'-GCC CAG ACG GAA GTT TCT TAT TG-3'		
GAPDH	glyceraldehydes-3-phosphate	(F)5'-ACC CAG AAG ACT GTG GAT GG-3'	172	NM_008084
	dehydrogenase	(R)5'-ACA CAT TGG GGG TAG GAA CA-3'		

2.1.5 Glucose Consumption

When experiments were conducted, the differentiation culture medium was replaced by DMEM supplemented with 0.25% (w/v) bovine serum albumin (control), and insulin 0.1 μmol/L (as positive control). The glucose concentration in medium was determined by the glucose oxidase method after 24 h of treatment. Briefly, the glucose concentration of the wells with cells was subtracted from the glucose concentration of the blank wells to obtain the amount of glucose consumption (Shen *et al.*, 2012; Yin *et al.*, 2002).

2.1.6 HPLC analyses for PJT extracts

EE, HP, and WP were dissolved in 50% methanol, applied to an ODS column (ODS-HG-5, 150 × 4.6 mm I.D., Nomura Chemical, Seto, Japan) and analyzed using the Shimadzu HPLC 10A system (Shimadzu, Kyoto, Japan). The mobile phases were 0.2% trifluoroacetic acid (TFA) in 10% methanol as the starting eluent and 0.2% TFA in 70% methanol as the limiting eluent. Samples were analyzed using the gradient program of the limiting eluent as follows: 0–5 min, 50% to 100%, and 5–40 min, 100% with a flow rate of 0.5 mL/min at a wavelength of 323 nm.

2.1.7 Statistical analyses

All results were expressed as the mean ± S.E.M. The statistical significance of the difference between the means of control and treatment groups was determined by Dunnett's test. The significance of the difference between the means of two groups was determined by Student's *t*–test. Differences were considered significant at $p < 0.05$.

2.2 Results

2.2.1 Effect of PJT extracts on 3T3-L1 adipocytes

The preliminary results indicated that EE inhibited lipid accumulation in adipocytes in a dose-dependent manner (Fig. 2-3A). Subsequent Oil Red O staining indicated that EE decreased the lipid accumulation compared to the control cells upon differentiation (Fig. 2-3B).

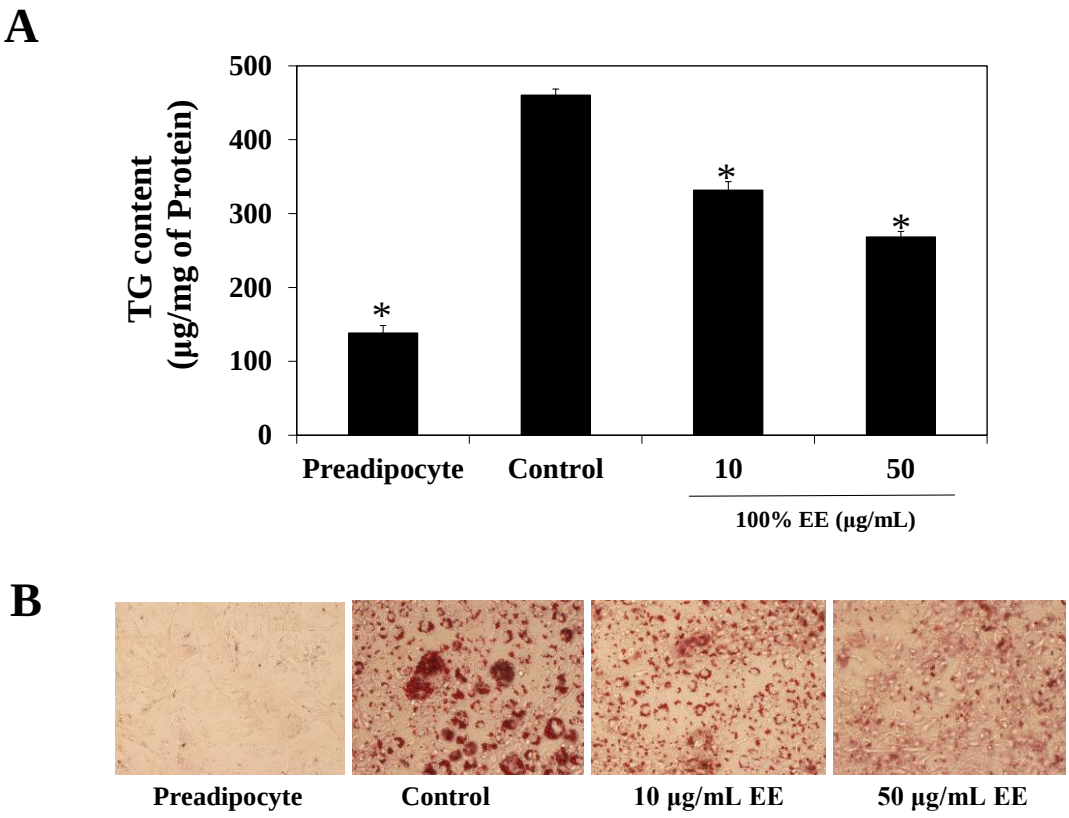

Figure 2-3 Dose dependency effect of PJT 100% EE on 3T3-L1 cells. The cells were incubated with treatments from Day 0–6. The harvested cells were tested for lipid accumulation by TG assay per mg of protein (A). After the Day 6, the cellular droplets were stained with Oil Red O (magnification × 20). Asterisk denotes a statistical significant difference against the control (Dunnett's test; *$p < 0.05$).

The EE was further fractionated into HP and WP and tested in 3T3-L1 adipocytes. A dose-dependent inhibition in the lipid accumulation was observed in EE and HP compared to that of the control (Fig. 2-4A). When the HP concentration was doubled, the lipid accumulation in cells was further reduced by 37.6%. Under the conditions of my study, the treatments produced no detectable cell toxicity for all cell types.

In concordance with the previous *in vivo* results (Nukitrangsan *et al.*, 2012a), EE-treated cells showed a 2.4-fold increase in *PPARγ* expression. The *PPARγ* mRNA levels showed a 2.6-fold increase due to HP (Fig. 2-4B). Lipoprotein lipase (*LPL*) showed 2.7-fold increase due to the EE and HP-treatments and fatty acid transport gene, fatty acid binding protein 4 (*FABP4*) (Strand *et al.*, 2012), showed a 3.4-fold increase by EE and HP, and a 2-fold increase by WP-treatment. A decreasing trend was observed in fatty acid synthase (*FAS*) expression by the HP and was the lowest when compared with EE and WP. The *C/EBPα* expression was upregulated significantly by EE, and uncoupling protein 2 (*UCP2*), involved in uncoupling thermogenesis (Lee *et al.*, 2011), was significantly upregulated by EE and HP. In addition, insulin receptor substrate-1 (*IRS-1*) expression tended to be downregulated in the HP-treated adipocytes. EE increased the glucose transporter 4 (*GLUT4*) expression significantly and *IRS-1*, to a much lower extent.

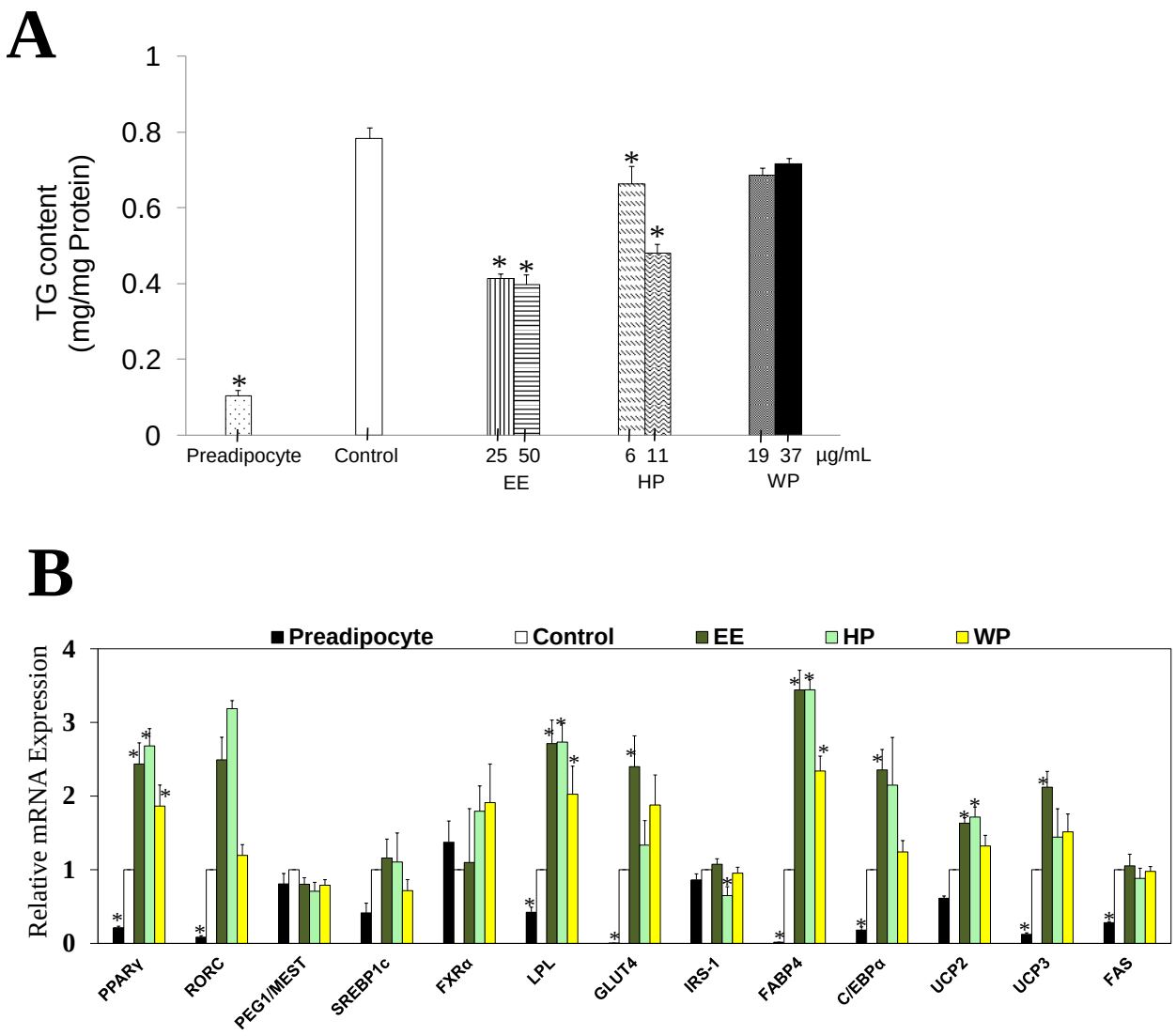

Figure 2-4 Effect of PJT extracts on lipid accumulation in adipocytes. TG content was expressed as total triglyceride per cellular protein (A). 3T3-L1 preadipocytes were treated with EE, HP, or WP (50 μg/mL) during Day 2–6. Gene expressions were examined by qPCR with values expressed as fold-change over control (B). Data are shown as mean ± S.E.M. of three independent experiments. Asterisk indicates significance tested against the control, *$p < 0.05$ vs. the control or †$p < 0.05$ between two concentrations in the same group.

2.2.2 Effect of HP during the adipogenesis process at different time intervals

It was found that HP reduced the lipid accumulation in adipocytes. This prompted to examine the maximum inhibitory point in adipogenesis due to the HP (Fig. 2-2). The HP had the ability to significantly inhibit the TG content during early to late stage (Day 0–6) and intermediate to late stage (Day 2–6) of the differentiation process by 24.4% and 14.9%, respectively (Fig. 2-5A). Day 2–4 increased the lipid accumulation than any other HP-treatment scheme, with values comparable to that of the control. Day 0–6 showed a 2.5-fold upregulation in *PPARγ* expression (Fig. 2-5B). The expression was stimulated 1.6-fold by Day 2–6 treatment, and conversely decreased by 0.3-fold in Day 2–4. The HP-treatment led to a significant decrease in paternally expressed gene 1 (Peg1)/mesoderm specific transcript (Mest) (*PEG1/MEST*) expression during the entire adipogenic process. Both schemes of Day 0–6 and Day 2–6 led to a 2-fold increase in RAR related orphan receptor gamma (*RORC*) and a 0.5-fold decrease in *FAS*.

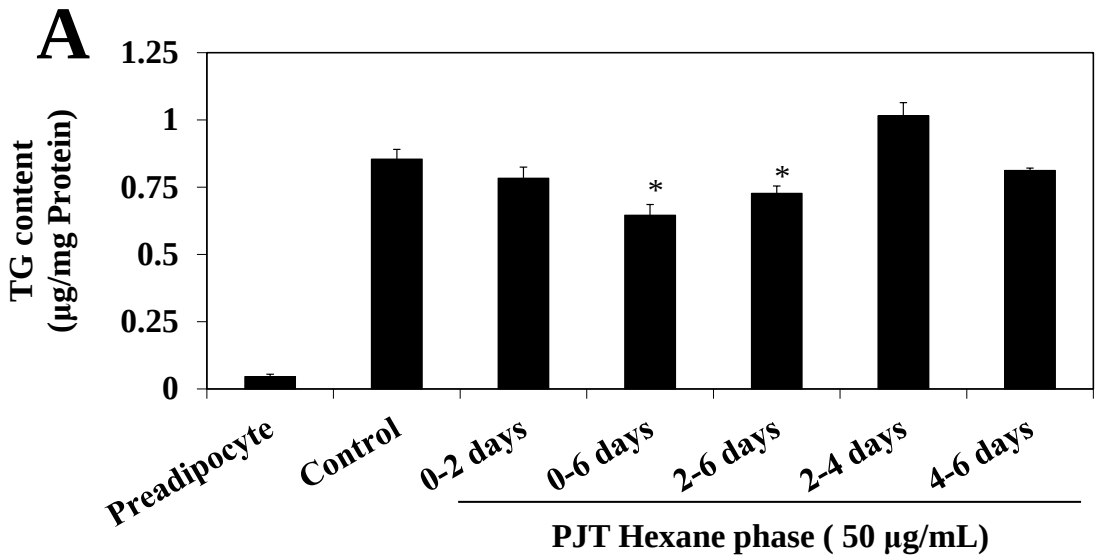

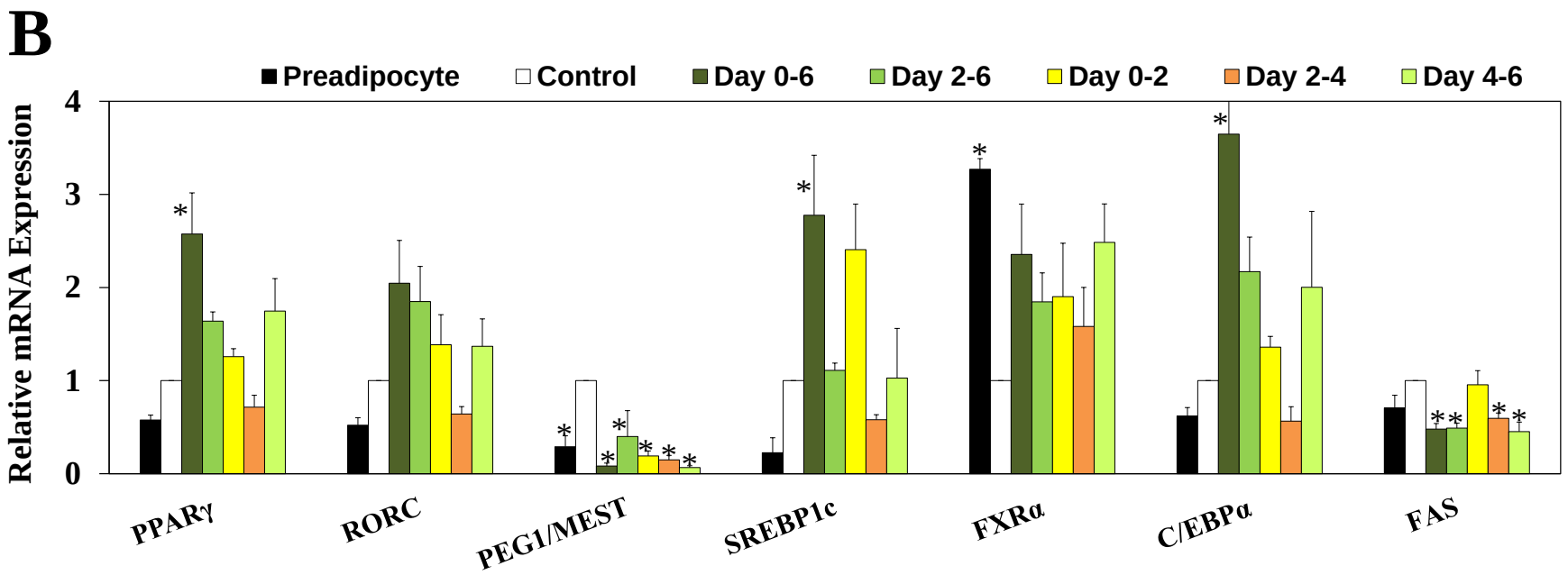

Figure 2-5 Effect of PJT extracts on adipocyte differentiation was evaluated. A schematic representation of the experimental design to assess the effect of HP (50 μg/mL) at various time intervals (thick lines) during adipogenesis (A). TG content was measured (B). HP (50 μg/mL) was added at different time points during adipogenesis. Several target genes were assessed by qPCR and values are expressed as fold-change over control (C). All data are represented as mean ± S.E.M. in three independent experiments. *$p < 0.05$ vs. the control.

2.2.3 Effect of PJT extracts on HepG2 hepatocytes

The lipid accumulation in HepG2 cells was suppressed by PJT EE (25 µg/mL), HP (6 µg/mL; Fig. 2-6A). EE and HP were able to suppress the lipid accumulation in hepatocytes by 11.4% and 9.4%, respectively. However, for a better performance, the concentration of each extract was doubled since no cell cytotoxicity was found.

With the doubled concentration of the extracts, the lipid accumulation in the HepG2 hepatocytes was significantly reduced due to EE and HP by 30.8% and 10.8%, respectively in the absence of insulin (Fig. 2-6B).

This study focused on the expression of sterol regulatory element-binding protein (*SREBP*) and *FAS* as target points of fatty liver (Hwang *et al.*, 2011; Horton *et al.*, 2002). *SREBP1c* expression was suppressed 0.3- and 0.6-fold due to EE and HP, respectively (Fig. 2-6C). PJT extracts significantly reduced *FAS* expression, with the highest degree of attenuation by HP. In concordance with previous data, the farnesoid X receptor alpha (*FXRα*) expression level was upregulated by EE (Nukitrangsan *et al.*, 2012b), with a 2-fold increase in HP.

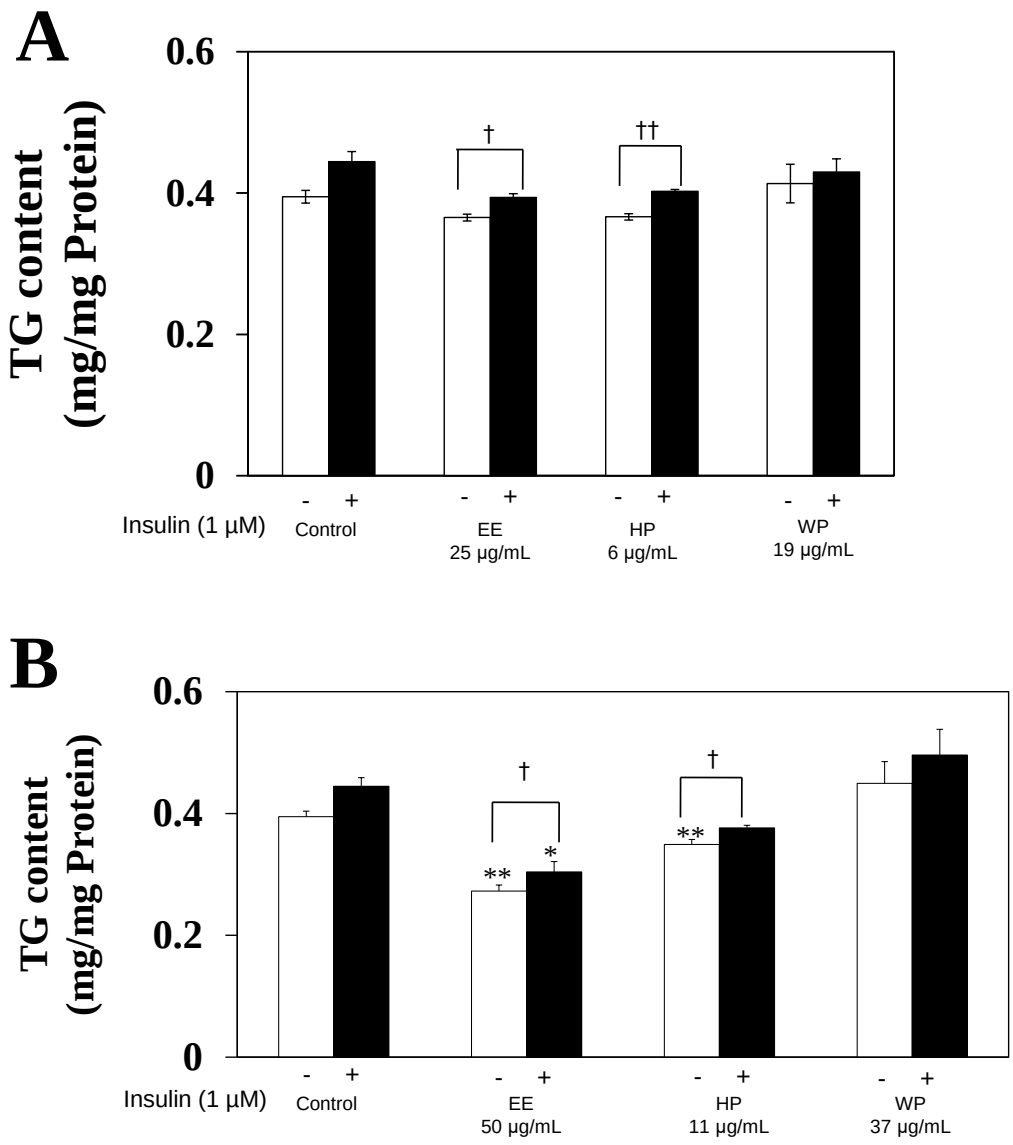
A
TG content
(mg/mg Protein)
0.6
0.4
0.2
0
†
††
- + - + - + - +
Insulin (1 μM)
Control
EE
25 μg/mL
HP
6 μg/mL
WP
19 μg/mL
B
TG content
(mg/mg Protein)
0.6
0.4
0.2
0
†
†
**
*
**
- + - + - + - +
Insulin (1 μM)
Control
EE
50 μg/mL
HP
11 μg/mL
WP
37 μg/mL

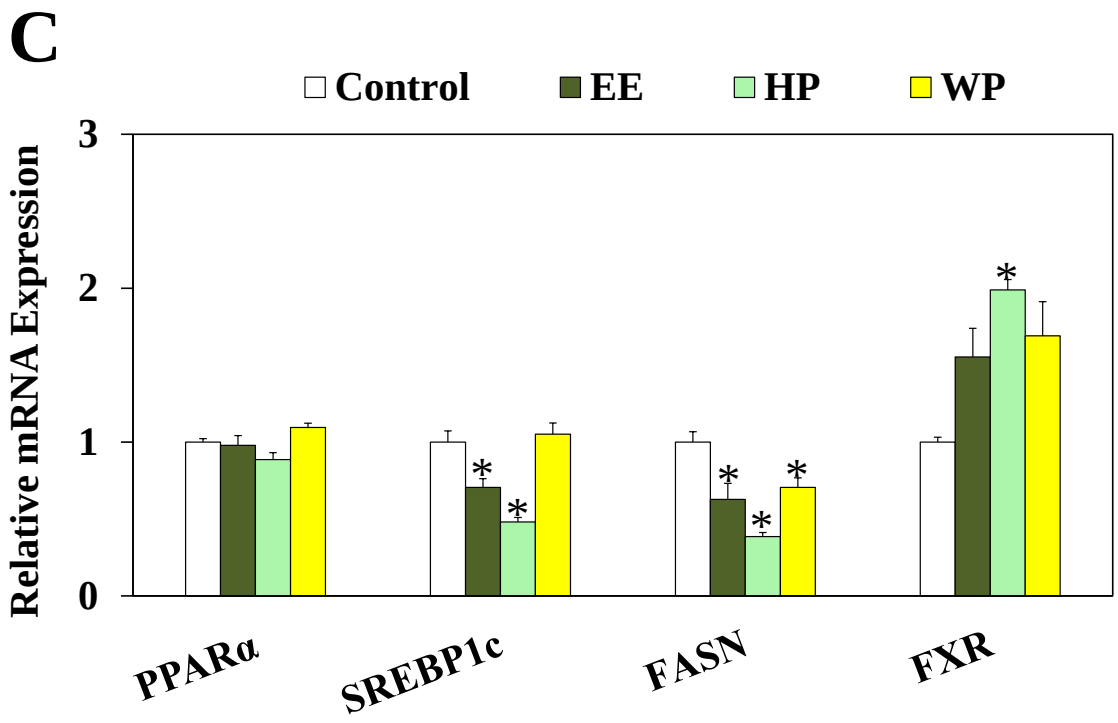

Figure 2-6 Effect of PJT extracts in HepG2 cells. The serum-starved HepG2 cells were treated with EE (25 μg/mL), HP (6 μg/mL), or WP (19 μg/mL) for 12 h and evaluated for the TG content (A) and doubled the concentrations up to EE (50 μg/mL), HP (11 μg/mL), or WP (37 μg/mL) for 12 h and evaluated for the TG content (B). Cells were treated with 50 μg/mL of EE, HP or WP for 24 h. Total RNA were extracted, cDNA were synthesized and performed qPCR analysis with values expressed as fold-change over control (C). Data are shown as mean ± S.E.M. of three independent experiments. *$p < 0.05$ vs. the control with insulin, **$p < 0.05$ vs. the control without insulin, and †$p < 0.05$, ††$p < 0.01$, between with or without insulin treatment groups.

2.2.4 Effect of PJT extracts on C2C12 myotubes

Insulin had no significant effect on glucose consumption in the presence or absence of PJT extracts (Fig. 2-7A). This study also investigated the effect of PJT extract on gene expressions responsible for fatty acid oxidation and thermogenesis. HP increased the expression of uncoupling protein 3 (*UCP3*) gene to almost same extent as insulin (Fig. 2-7B). PJT significantly upregulated carnitine palmitoyltransferase 1 alpha (*CPT1α)* and *RORC*. *GLUT4* expression level significantly increased with both insulin and WP. When compared with the control, HP suppressed *GLUT4*, and EE was comparable to that of the control.

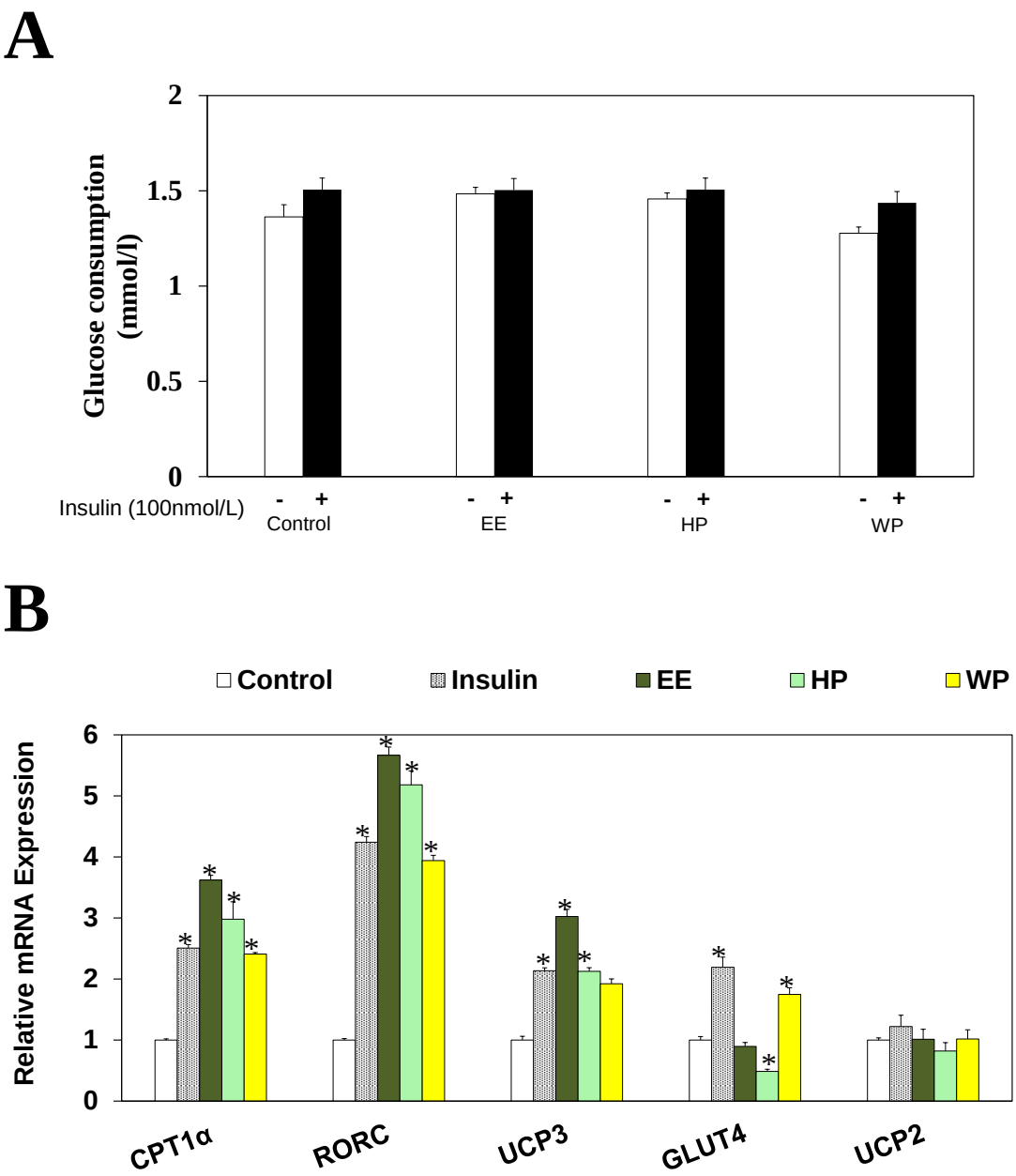

Figure 2-7 Effect of PJT extracts on C2C12 myotubes. Cells were cultured with EE (50 μg/mL), HP (11 μg/mL), or WP (37 μg/mL) in the serum-free medium for 24 h. Glucose consumption was assessed (A). Cells without insulin or treatment (control), insulin only (100 nmol/L), or treated with EE, HP, or WP (50 μg/mL; without insulin) for 24 h and qPCR was performed with values expressed as fold-change over control (B). All data are given as mean ± S.E.M. in three independent experiments. *$p < 0.05$ vs. the control.

2.2.5 HPLC analysis of the PJT extracts

The chromatogram of EE (Fig. 2-8A) possess of a wide spectrum of different compounds either with hydrophilic or hydrophobicity. The chromatogram of HP was similar to the latter part of the EE chromatogram (Fig. 2-8B). The WP was similar to that of the former portion of the EE chromatogram (Fig. 2-8C).

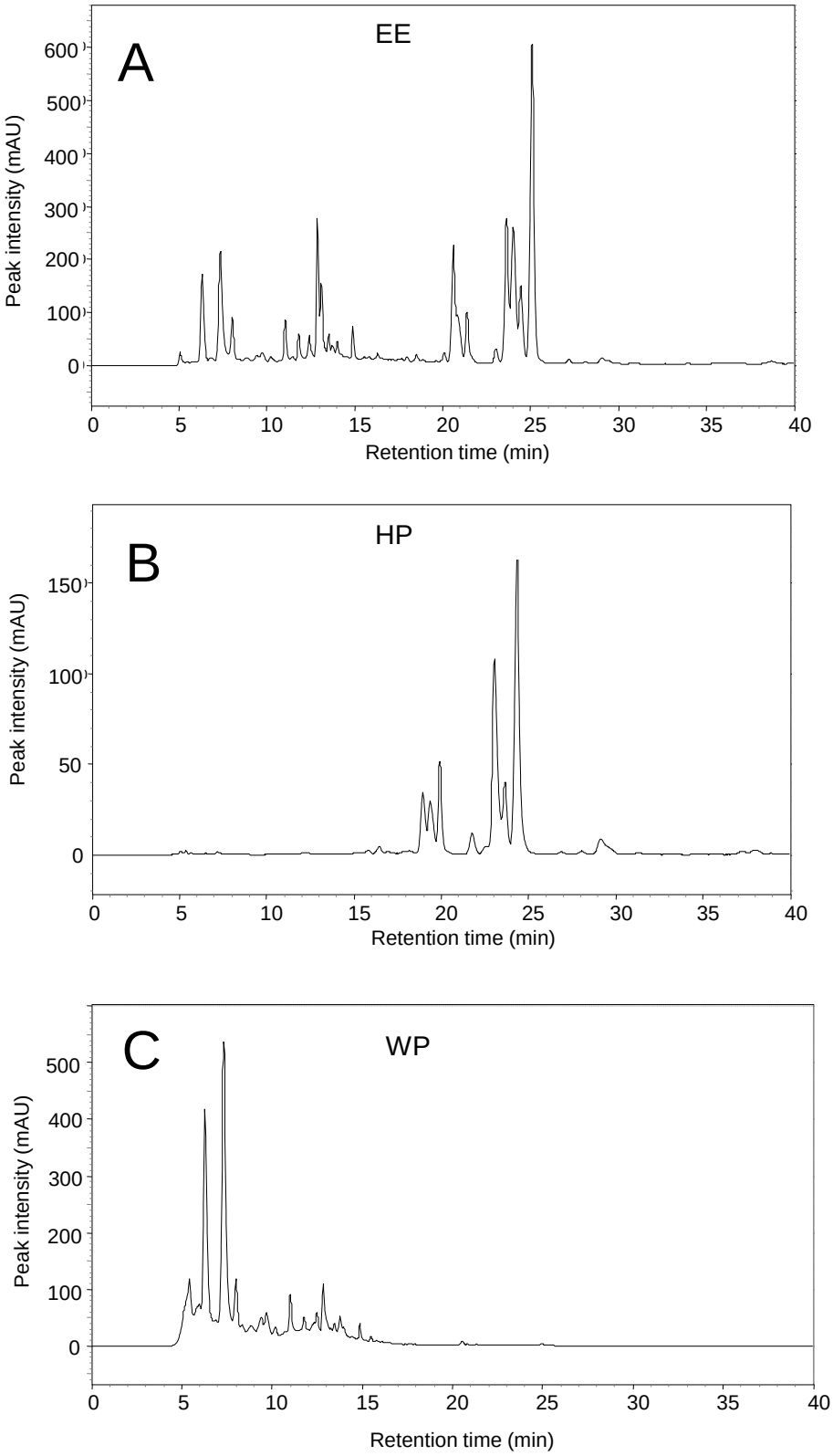

Figure 2-8 HPLC Chromatographs of PJT extracts.

2.3 Discussion

In this study, I further fractionated PJT EE into HP and residual WP as a partial purification to identify anti-obesity related compound(s). The results of this study demonstrated for the first time, that partially purified HP exerts a lipid lowering activity by attenuating lipid accumulation *in vitro*. This study suggests that the anti-obesity mechanism of PJT postulated in previous *in vivo* study (Nukitrangsan *et al.*, 2012b) needs a revision as the partially purified fractions of PJT directly modulated lipid metabolism in adipocytes, hepatocytes and myotubes to inhibit adiposity.

Using 3T3-L1 preadipocytes as the adipose cell model, I found that the HP modulated lipid metabolism during the late stage of adipocyte development and significantly suppressed the TG content. This finding suggests that the HP having an ability to reduce the lipid content during the late stage of the adipocytes. On the other hand, the WP was comparable to that of the control in both 3T3-L1 and HepG2 cells, suggesting the occurrence of compounds in the crude extract to counteract the anti-obesity activity.

In the adipogenic gene network, *PPARγ* is considered as the key regulator of adipogenesis (Fu *et al.*, 2005; Rosen and MacDougald, 2006). Many studies have justified the inhibition of adipogenesis by downregulation of *PPARγ* expression (Gosmann *et al.*, 2012; Ahn *et al.*, 2012). In contrast, several reports have shown the beneficial effects of upregulation of *PPARγ* expression, such as improving type 2 diabetes (Willson *et al.*, 1996) and decreasing serum cholesterol, high density lipid and TGs (Searcy *et al.*, 2012; Chang and Cho, 2012). In my study, HP enhanced the genesis of small adipocytes, which may offset the adverse effects of fat accumulation by increasing lipolysis and thereby decreasing triacylglycerol storage in adipocytes. The downregulation of *PEG1/MEST*, an adipocyte size marker gene, further confirms the above suggestion and improve fatty acid metabolism within adipocytes.

The increase in *FABP4*, an extensive marker for differentiated adipocytes and a carrier for fatty acids indicates an upregulation of fatty acid transportation suggesting that the HP enhanced the ability of cells to process and metabolize fatty acids via energy production in mitochondria (Strand *et al.*, 2012). *LPL* was significantly upregulated by HP,

suggesting the hydrolysis of triglycerides in mature adipocytes (Raichur *et al.*, 2007). However, this observation is contradicting with several other studies, possibly due to either the use of difference in the treatments that are tested, difference in the cell differentiation process or difference in the target point of the inhibition process (Zhang *et al.*, 2012; Yoon *et al.*, 2015; Lee *et al.*, 2007). HP also inhibited fatty acid synthesis via the downregulation of *FASN* expression in HepG2 (Li *et al.*, 2013). *SREBP1c* was also significantly downregulated by the HP which indicates inhibition in lipogenesis. Taken together, these results unequivocally demonstrated *in vitro* that phytochemicals in HP play a crucial role in the gene modulation to attenuate the adiposity.

Moreover, this study showed an acceleration of *CPT1α* expression in HP-treated myotubes, suggesting an increase in fatty acid β-oxidation in muscle cells (Bandyopadhyay *et al.*, 2012). UCPs, the mitochondrial membrane transporters that uncouple substrate oxidation from ATP synthesis (Raichur *et al.*, 2007), showed a significantly increased level of mRNA (*UCP3*) explaining the adaptive thermogenesis in myotubes due to the HP (Schrauwen and Hesselink, 2002).

The chromatogram of HP appears to be associated with the aromatic compounds of comparatively higher hydrophobicity. The present study shows the similarity between the HP and latter part of the EE chromatograms which suggests the possible compound(s) that may be associated with the antiobesity in HP.

Conclusion

This study indicated that partially purified HP regulate lipid metabolism related gene network and energy production *in vitro* to inhibit adipogenesis which may be the primary mechanism of action for the anti-obesity activity of PJT.

CHAPTER III

Isolation of Pteryxin; a coumarin in *Peucedanum japonicum* Thunb attenuates adipogenesis by modulating adipogenic gene network *in vitro*

Introduction

In the previous chapter, I showed that the anti-obesity activity in EE was partially purified into the hexane phase (HP) demonstrating anti-obesity activity in 3T3-L1 adipocytes and HepG2 hepatocytes, with an improved energy expenditure profile in C2C12 myotubes. However, it remained unexplored of the active compound(s) in PJT responsible for the anti-obesity effect.

Thus, in the present study, I examined the following:

1. Isolation of the active compound in PJT.
2. Effect of the active compound to inhibit lipid accumulation.
3. Elucidation of the molecular mechanisms related to inhibition of lipid accumulation *in vitro*.

3.1 Materials and methods

3.1.1 Plant materials, purification and identification of active compound

The PJT used in this study was ground and extracted as described in Chapter II. The yield of EE (11%) of the starting material was further suspended in water and partitioned into *n*-hexane (4×1: 1 v/v). The HP approximate yield was 3.3%, subjected to open column chromatography (CC) for rough fractionation. The CC was performed on silica gel 40 µm 60 Å (26×100 mm; Yamazen Corporation, Japan) column. The starting eluent was hexane (100%), thereby changed stepwise with the following eluents, respectively.

1st – hexane 100% (Fr1)

2nd - hexane-[CH_2Cl_2:methanol (MeOH)] 90:(9.5:0.5) (Fr2, Fr3 and Fr4)

3rd - hexane-[CH_2Cl_2:methanol (MeOH)] 50:(47.5:2.5) (Fr5 and Fr6)

4th - CH_2Cl_2:MeOH (95:5) and (Fr7, Fr8 and Fr9)

5th - MeOH-HCOOH (99.5:0.5) (Fr10 and Fr11) and obtained eleven fractions altogether. These fractions (Fr1 to Fr11) were screened for its adipogenic effect by the TG assay and found Fr3 having the maximum lipid accumulation inhibition activity in 3T3-L1 cells.

The Fr3 (1.3%) was further subjected to HPLC on a silica gel column into twelve fractions (Fr3-1 to -12). HPLC was performed on a Shimadzu HPLC 10A system on a silica gel column (10 × 250 mm, 5SL-II; Cosmosil, Nacalai Tesque, INC., Japan). The mobile phases were hexane as the starting eluent and 0.5% HCOOH in CH_2Cl_2:MeOH (94.5:5.0) as the limiting eluent. The gradient program of the limiting eluent is as follows: 0–5 min, 10%, and 5–30 min, 10% to 50%, 30–40 min, 50% to 10% with a flow rate of 2.0 mL/min and with detection at a wavelength of 322 nm.

All isolated fractions were evaporated, dissolved in 99.5% ethanol 1:0.1 (w/v) and stored at –20˚C until further use. The fractions were screened against lipid accumulation in 3T3-L1 adipocytes and found Fr3-8 having the strongest effect on anti-adipogenesis.

As the next step, this purified active component in Fr3 (Fr3-8; 0.15%) was collected in large quantity and subjected to direct electron ionization-mass spectrometry (EI-MS). EI-MS was performed on a gas chromatogram mass spectrometer (GCMS-QP 2010; Shimadzu Kyoto, Japan) using a direct inlet system. Thereafter, ^{1}H-nuclear magnetic resonance (NMR), ^{13}C-NMR, heteronuclear multiple quantum coherence (HMQC), and heteronuclear multiple bond correlation (HMBC) were carried out for the identification of the chemical structure. ^{1}H-NMR, ^{13}C-NMR, HMQC and HMBC were measured using a 5 mm probe. The operating frequencies were 400.13 MHz for ^{1}H-NMR and 100.62 MHz for ^{13}C-NMR spectra.

3.1.2 Cell culture

3.1.2.1 3T3-L1 preadipocyte culture

For adipogenesis, 3T3-L1 preadipocytes were cultured in 24-well plates at a density of 1×10^4 cells/well in DMEM supplemented in 10% BCS and cells were grown up to confluence as described in Chapter II. The culture medium was then changed to DMEM supplemented with 10% FBS, 10 µg/mL insulin, and HP (50 µg/mL), chlorogenic acid (CGA; 10 µg/mL) or active compound (10, 15, or 20 µg/mL) from Day 2–6. The culture medium was replaced every 2 days.

To investigate the time course of the effect of active compound on adipogenesis, differentiation was triggered by active compound at different time intervals. Cells were harvested on Day 6 for analyses.

3.1.2.2 HepG2 hepatocyte culture

HepG2 cells were cultured as described in Chapter II. For experiments, cells were seeded in 24-well plates at a density of 5×10^4 cells/well, and maintained in serum-free DMEM containing 1% bovine serum albumin overnight. HepG2 cells were then subsequently treated with insulin (1 μM), HP (50 μg/mL), CGA (10 μg/mL) or active compound (10, 15, or 20 μg/mL) for another 24 h.

3.1.3 Triglyceride analysis

At the end of the treatment period, 3T3-L1 and HepG2 cells were washed with phosphate saline buffer (Wako) and harvested into 10% Triton X-100 solution in 1.5 mL tubes and lysed by brief sonication. Then the cell containing tubes were centrifuged at 5,000 rpm for 3 min. The supernatant were transferred to new collection tubes. 20 μL of each sample was mixed with 300 μL enzyme and vortex for 15-20 s. As the final step, incubated at 37°C for 5 min. The TG content was quantified using a commercial enzymatic kit (Wako) as mentioned in Chapter II.

3.1.4 Total RNA extraction and Quantitative real-time PCR

To obtain total RNA, the cells were seeded in 3.0 cm dishes with following densities:

- ✓ 3T3-L1 preadipocytes at 3×10^4 cells/dish
- ✓ HepG2 at 15×10^4 cells/dish.

Total RNA extraction, cDNA synthesis, and qPCR were performed as described in Chapter II.

3.1.5 Statistical analyses

All results were expressed as the mean ± S.E.M. The statistical significance of the difference between the means of control and treatment groups was determined by Dunnett's test. The significance of the difference between the means of two groups was determined by Student's *t*–test. Differences were considered significant at $p < 0.05$.

3.2 Results

3.2.1 Screening of the different fractions of PJT HP

Figure 3-1A shows the highest inhibition of the lipid content of the Fr3. Thus, Fr3 was further fractionated into twelve fractions (Fr3-1 to -12) using the HPLC system. The screening of the fractionation of Fr3 shows the strongest inhibitory activity in the Fr3-8, inhibiting the lipid accumulation by 45.9% in 3T3-L1 adipocytes.

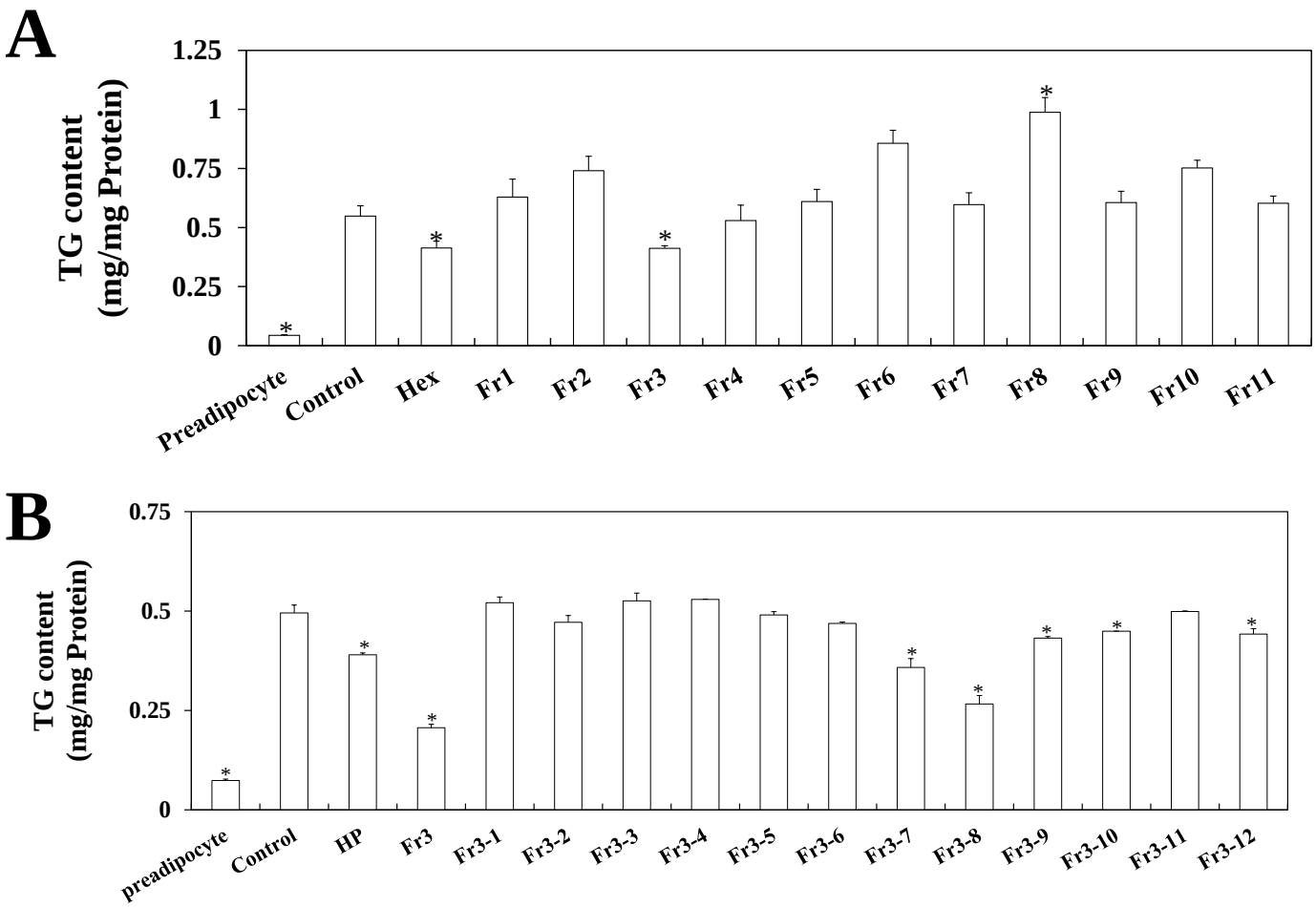

Figure 3-1 Partial purification of PJT HP to identify inhibitory effects of different fractions using 3T3-L1 cells. HP fractions (A) and Fr3 fractions (B) were screened for inhibition of adipogenesis. All data are given as mean± S.E.M. in three independent experiments. *$p < 0.05$ vs. the control.

3.2.2 Chemical structure elucidation

EI-MS analysis of the active compound found the $[M-1]^+$ ion at *m/z* 385. Next, the ^{1}H-NMR revealed the high purity of the compound. The ^{13}C-NMR (Fig. 3-2A) and the 2-D structure analysis were used to identify the chemical structure of the active component (Fig. 3-2B) as pteryxin (Chen *et al.*, 1996b; Akihisa *et al.*, 2003).

A

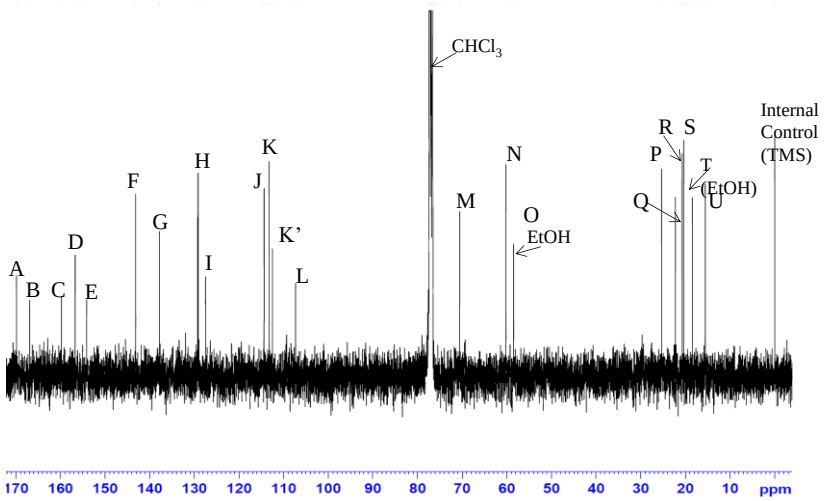

B

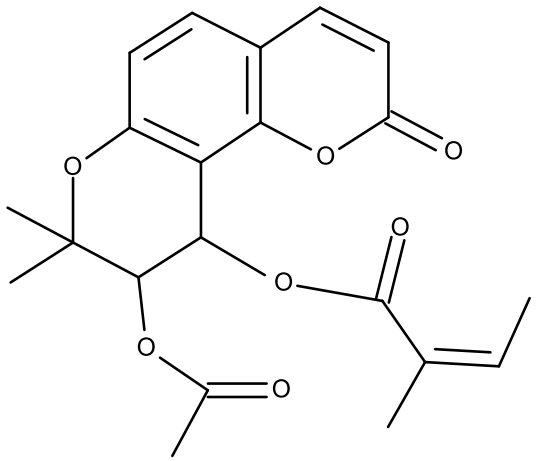

(±)-cis-3'-acetyl-4'-angeloylkhellactone ($C_{21}H_{22}O_7$) MW: 386

Figure 3-2 Identification of the Fr3-8. The ^{13}C-NMR chromatogram of the Fr 3-8 (A). Chemical structure of (±)-pteryxin, which was earlier identified as Fr 3-8 (B).

3.2.3 Effect of pteryxin in the adipocytes

I investigated the effect of pteryxin against chlorogenic acid in 3T3-L1 cells (Fig. 3-3A). A dose-dependent suppression was observed and the TG level in CGA was comparable to the lowest dose of pteryxin.

Next, to obtain insight on the activity of pteryxin during the adipogenic process, I examined the time course of the adipocyte differentiation in the presence of pteryxin (Fig. 3-3B). The results indicated that the lipid accumulation was rather significantly blocked when pteryxin-treatment was administered between Day 0 and Day 2 (Fig. 3-3C). Importantly, pteryxin exerted the ability of suppressing the lipid accumulation at any given time point during the adipogenic process.

A

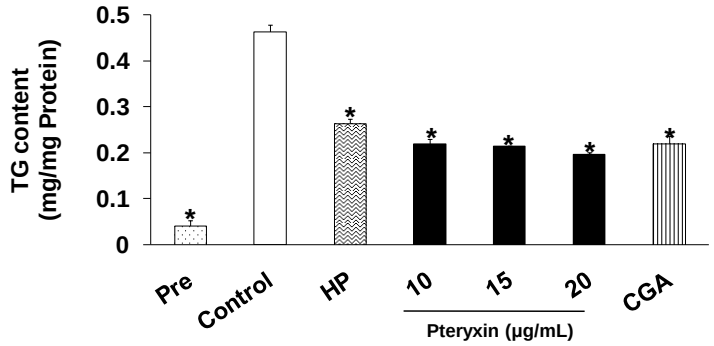

B

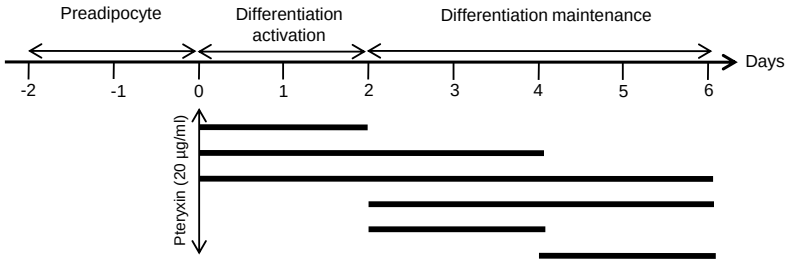

C

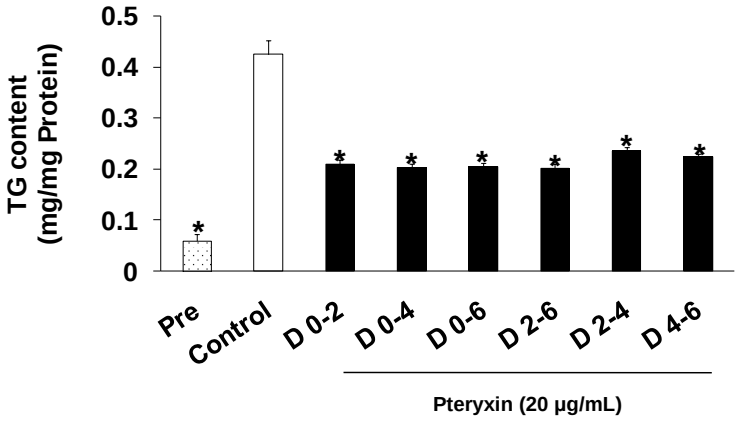

Figure 3-3 Suppression of lipid content by pteryxin in 3T3-L1 cells. Pre; non-differentiated cells, HP; hexane phase of PJT (50 μg/mL), CGA; chlorogenic acid (10 μg/mL).

Furthermore, during the analysis of the gene expressions of the adipocytes, 3T3-L1 preadipocytes were differentiated and treated with 20 μg/mL pteryxin during Day 2–6. Pteryxin showed a lower *PPARγ* expression than the HP-treatment, however significantly higher than the control (Fig. 3-4). Pteryxin decreased the master regulator of fatty acid synthesis, *SREBP1c* and its downstream target genes acyl-CoA carboxylase-1 (*ACC1)* and pyruvate dehydrogenase kinase 4 (*PDK4*) expression levels. *RORC* expression was upregulated significantly by HP and pteryxin.

For an easier interpretation of data, the qPCR values were expressed as fold-change over control. Comparisons between treatments with the control were analyzed by Dunnett's test (*$p < 0.05$), and a particular treatment vs. control was analyzed by Student's *t*-test (†$p < 0.05$, ††$p < 0.01$).

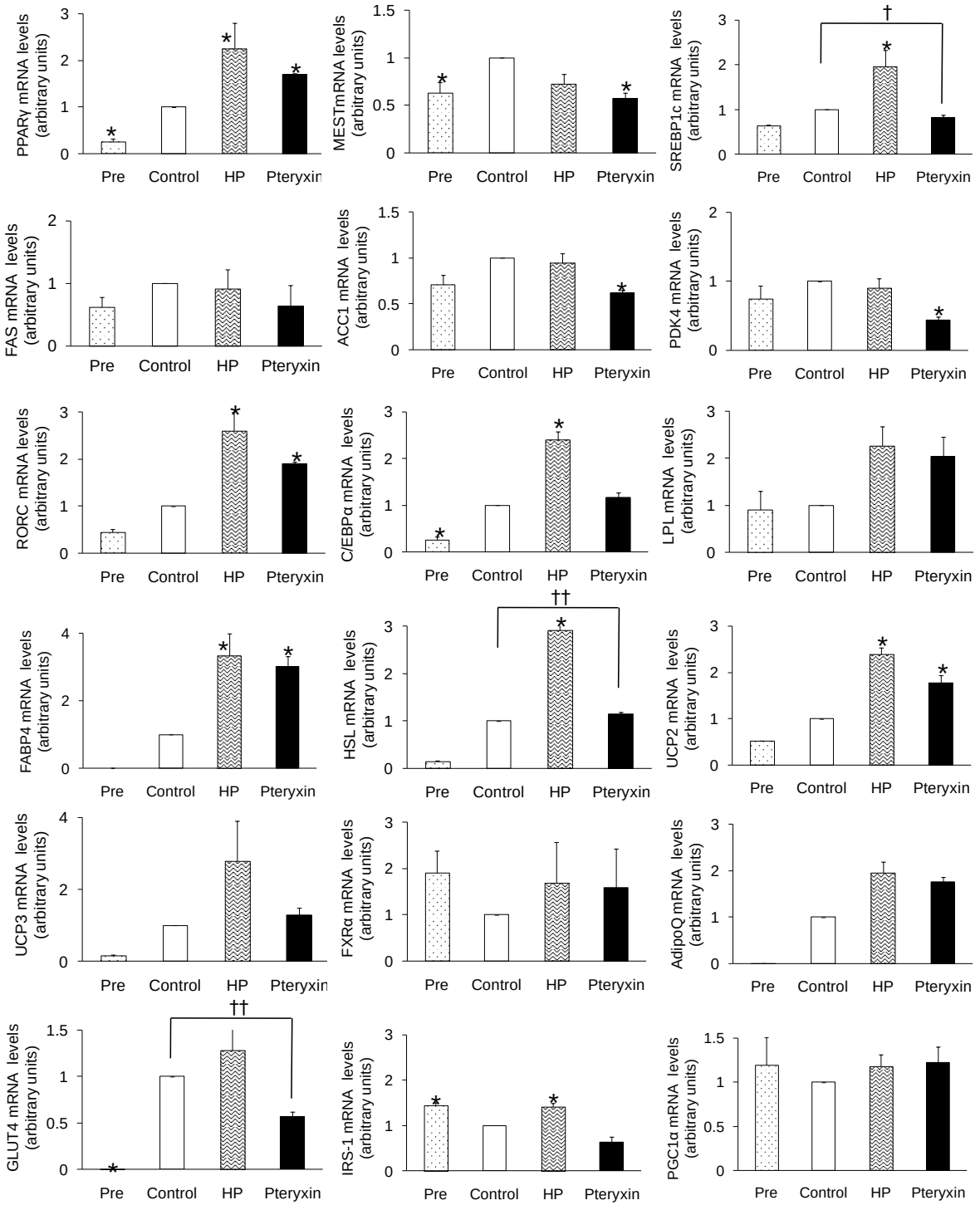

Figure 3-4 Effect of pteryxin on the adipogenic gene network. Pre; non-differentiated cells, HP; hexane phase (50 μg/mL), Pteryxin 20 μg/mL.

3.2.4 Effect of pteryxin on HepG2 hepatocytes

HepG2 cells were treated with different doses of pteryxin. Pteryxin showed an inhibition in the lipogenesis at 10, 15 and 20 µg/mL, respectively (Fig. 3-5A).

CGA values were comparative to that of the control group. Further, the gene expression data revealed that the *SREBP1* (*hSREBP1*) expression was suppressed due to pteryxin (Fig. 3-5B). Pteryxin significantly reduced *FASN* (*hFASN*) expression, stearoyl-CoA desaturase (*hSCD*), and acetyl-CoA-carboxylase-1 (*hACC1*). A lipolytic gene, human PPARα (*hPPARα*) was significantly upregulated by the pteryxin-treatment.

A

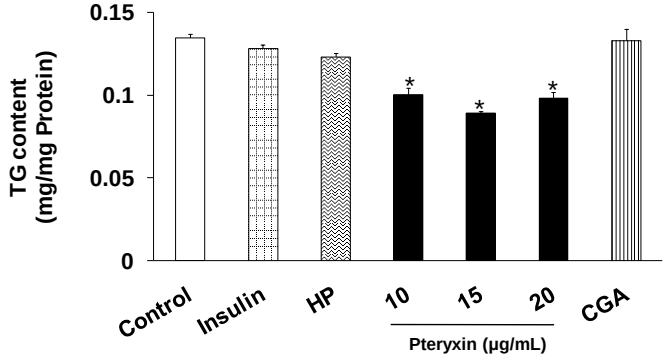

B

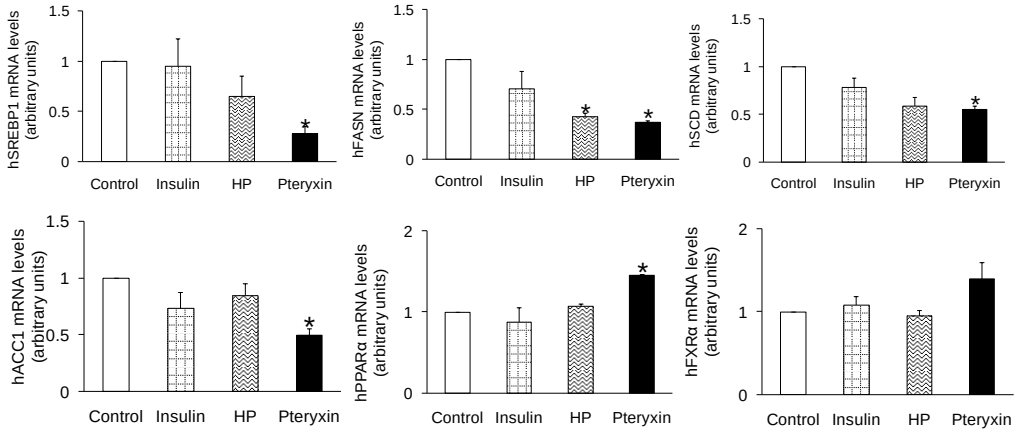

Figure 3-5 Effect of pteryxin on HepG2 hepatocytes. Cells were treated with insulin (1 μM), HP (50 μg/mL), chlorogenic acid (CGA; 10 μg/mL), or pteryxin (10, 15, 20 μg/mL) for 24 h in serum-free medium. TG content was measured in each treatment (A) and expression of lipogenic genes were assessed by qPCR with values expressed as fold-change over control (B). Data are represented as mean ± S.E.M. in three independent experiments. Asterisk indicates a significant difference between control and treatment groups tested by Dunnett's test. *$p < 0.05$ versus control.

3.3 Discussion

In the present study, I isolated the anti-obesity responsible compound, pteryxin, a known natural coumarin in PJT, and found its strong inhibitory properties towards lipid accumulation. However, the suppressive effect of pteryxin on HepG2 was lower compared with that on 3T3-L1 cells. Pteryxin has been previously identified as an antiplatelet aggregation constituent, however its biological activities against obesity have not been reported (Chen *et al.*, 1996b).

In the purification process of HP, I found that the ability of Fr3 to suppress adipogenesis was higher than that of HP. This indicates the availability of counteract compounds in the HP, possibly the Fr3-1 to Fr3-6. In the investigation of the effects of pteryxin on the gene modulation pattern, pteryxin enhanced the *AdipoQ* expression level as previously reported for ascofuranone (Chang and Cho, 2012) and suggests pteryxin as a potential therapeutic agent for obesity (Ohara *et al.*, 2009; Alappat and Awad, 2010). Pteryxin led to formation of small adipocytes, by the downregulation of MEST, an adipocyte size marker gene (Takahashi *et al.*, 2005), which may further increase the lipolytic activity, and decreasing TG storage in adipocytes.

The suppression of lipogenic genes such as, *ACC1/hACC1*, and *hSCD* have attenuated TG accumulation in both pteryxin-treated adipocyte and hepatocyte. Moreover, pteryxin accelerated the direct fatty acid β-oxidation via activation of *hPPARα* (Bandyopadhyay *et al.*, 2012) in HepG2 cells. Taken together, these results demonstrated that pteryxin play a crucial role in the gene modulation to attenuate the adiposity and lipogenesis *in vitro*. Furthermore, the reason to use CGA as a positive control is that CGA is a main constituent in coffee (Shimoda *et al.*, 2006) was previously identified in PJT (Nukitrangsan *et al.*, 2012b). While some studies explained the activity of CGA in stimulating the glucose uptake in 3T3-L1 adipocytes without inducing significant adipogenesis (Alonso-Castro *et al.*, 2008), some exhibited anti-obesity properties in HFD induced obese mice (Cho *et al.*, 2010). In agreement with some reports on CGA leading to insulin resistance and lipogenesis in hepatocytes, my study showed no TG suppression in hepatocytes in the present investigation (Frank *et al.*, 2003).

Conclusion

This study clearly demonstrates for the first time, that pteryxin downregulated the transcription factors for lipid synthesis in the differentiated adipocytes and in hepatocytes, playing a crucial role in regulating lipid metabolism related gene expressions. The results provide an insight on the activity of pteryxin involved in suppressing obesity. Thus, my study suggests pteryxin as a potential natural compound to be used as an anti-obesity drug in the pharmaceutical industry.

CHAPTER IV

Pteryxin containing *Peucedanum japonicum* Thunb extracts and their respective anti-obesity effects: An *in vivo* study

Introduction

In the previous Chapters, I demonstrated that PJT HP plays an important role in the regulation of lipid metabolism and energy production *in vitro*. Furthermore, pteryxin, a coumarin isolated from the HP showed its activity against obesity *in vitro* for the first time (Nugara *et al.*, 2014a; Nugara *et al.*, 2014b). Pteryxin attenuated TG content in both 3T3-L1 adipocytes and HepG2 hepatocytes in a dose-dependent manner. However, the anti-obesity activity of pteryxin rich-HP *in vivo* remained unexplored.

Thus, in the present study, I investigated the following:

1. The inhibitory effects of pteryxin enriched HP on weight gain and several physiological parameters in C57BL/6 mice.
2. Effect of the HP on lipid metabolism-related gene parameters in WAT, liver and muscle tissue.

4.1 Materials and methods

4.1.1 Animals and diets

I used twenty 3-week old male C57BL/6 mice purchased from Japan SLC, Inc. (Shizuoka, Japan) randomly assigned into four groups of five animals allocated for each treatment. Adaptation period was one-week and the animals were fed a semi-synthetic, HFD prepared according to the AIN-76 formulation (Table 4-1). The EE was used 0.40% in the diet, whereas HP 0.12% and WP 0.27% doses were obtained according to the fractionation ratio of EE compensating for sucrose in the diet. Mice were kept in individual plastic cages, maintained at 24°C on a 12 h light-dark cycle with controlled humidity and ventilation. The mice were allowed free access to group-specific diets and water for 4 weeks. Feces were collected during the last three days before sacrifice. At the end of the feeding period, mice were sacrificed after a 6 h fast under anesthesia with pentobarbital sodium salt. Serum, liver tissue, white adipose tissue (WAT), brown adipose tissue (BAT) and soleus muscle tissue samples were excised, weighed and stored at −80°C immediately after collection.

4.1.2 Preparation of PJT extracts

The dried PJT leaves powder (200 g) was extracted with 1 L of ethanol for 6 h at ambient temperature. Extracts were then centrifuged at 3,000 × g for 10 min to remove insoluble materials from the solvent. EE was then further fractionated as described in Chapter II. The approximate yields of HP and residual water phase (WP) were 3.3% and 7.0% of PJT powder (w/w), respectively. To obtain the relative anti-obesity activities of HP and WP, their mixing ratios in EE were incorporated into the respective doses in the experiment diet.

Table 4-1 Composition of experimental high-fat diets

		PJT extract (g/100 g diet)		
	Control*	**EE†**	**HP‡**	**WP§**
Casein	20.0	20.0	20.0	20.0
Corn starch	15.0	15.0	15.0	15.0
Sucrose	38.0	37.6	37.9	37.7
Cellulose	7.0	7.0	7.0	7.0
Mineral mixture	3.5	3.5	3.5	3.5
Vitamin mixture	1.0	1.0	1.0	1.0
DL-Methionine	0.3	0.3	0.3	0.3
Choline bitartrate	0.2	0.2	0.2	0.2
Corn oil	15.0	15.0	15.0	15.0
EE	-	0.4	-	-
HP	-	-	0.1	-
WP	-	-	-	0.3

*The control group was fed with the modified AIN-76 diet (HFD).
†HFD was supplemented with PJT ethanol extract (EE).
‡EE was further fractionated into hexane phase (HP) and supplemented in the HFD.
§HFD was supplemented with the residual water phase (WP).

4.1.3 HPLC analyses for PJT extracts

The HPLC samples (EE, HP and WP) were pretreated using a Sep-Pak vac silica 6 cc column (Waters Corporation, Milford, Massachusetts, USA), dried, dissolved in DMSO and obtained at 82.4, 6.1 and 69.9 μg/mL, respectively. Next, 1 μL from each of these samples was applied to a Cosmosil 2.5 Cholester silica gel column (2.0 mm I.D. × 100 mm, Nacalai Tesque, Inc., Kyoto, Japan) and analyzed using the Shimadzu SPD-M20A system (Shimadzu, Kyoto, Japan). The HPLC conditions are given below:

- The mobile phases were 20 mM, pH 2.5 phosphate buffer (Nacalai Tesque) as the starting eluent and acetonitrile as the limiting eluent.
- Gradient program of the acetonitrile:
  - 0–15 min, 38%,
  - 15–18 min, 90%
  - 18-21 min, 38%,
- Flow rate: 0.4 mL/min
- Wavelength: 323 nm

Using the above mentioned conditions, purified pteryxin was analyzed as the reference chromatogram. The amount of pteryxin in each extract was quantified by using Visnadine (MW–388.41), purchased from Sigma Aldrich Co., St. Louis, USA, as a standard with a comparative structure and molecular weight to pteryxin.

4.1.4 Biochemical analyses

The physiological parameters were tested as follows:

- TC, TG and glucose levels in serum were determined using a commercial enzymatic kit (Wako Pure Chemical Industries Ltd.).
- Serum insulin was measured using an enzyme-linked immunosorbent assay kit (Morinaga Institute of Biological Science, Inc., Yokohama, Japan).
- Total lipids were extracted from the liver tissue by Folch method (Folch *et al.*, 1957)
- Liver levels of TC was determined by Shoenheimer-Sperry method (Sperry and Webb, 1950) and TG by Fletcher's method (Fletcher, 1968).
- TC, TG and the lipid in feces were extracted and quantified using commercial kits (Wako Pure Chemical Industries Ltd.).

All experiments using commercial kits followed the respective manufacturers' protocol.

4.1.5 RNA preparation and Quantitative real-time PCR

Total RNA was extracted from 30 mg of liver, epididymal adipose and soleus muscle tissues by using RNeasy Lipid Tissue Mini Kit (Qiagen, CA, USA). The cDNA was synthesized by using approximately 5 μg of total RNA as a template, using PrimeScript™ First Strand cDNA Synthesis kit (Takara BIO Inc., Shiga, Japan). The qPCR was performed on the Step One Plus ™ Real-Time PCR System using SYBR GREEN® master mix as discussed in previous chapters. The mRNA levels of all genes were normalized using *ACTB* for WAT, *GAPDH* for liver tissue and cyclophilin a (*CYPa)* for soleus muscle, as internal controls.

4.1.6 Statistical analyses and calculation

The insulin resistance index (homeostasis model assessment, HOMA-IR) was calculated according to the formula as follows (Katsuki *et al.*, 2001):

HOMA-IR = plasma glucose (mM) × plasma insulin (mU/L)/22.5

All results are expressed as mean ± S.E.M. The statistical significance of the differences between the mean of the control group and the means of the treatment groups were determined by Dunnett's test. Differences were considered to be significant at $p < 0.05$.

4.2 Results

4.2.1 HPLC of EE, HP and WP

EE consisted of the highest pteryxin peak area higher than HP and WP (Fig. 4-1A). The peak of pteryxin (Fig. 4-1D) was observed in all EE, HP and WP chromatograms. The presence of pteryxin in EE, HP and WP extracts was quantified as 24, 178 and 12 mg/g extract, respectively, using visnadine as the standard (Fig. 4-2).

Based on the above quantification, I determined the pteryxin availability in EE, HP and WP diets as 290 ±0.50, 650 ±0.89 and 94 ±0.85 μg/mouse/day, respectively. Comparing the diet amount offered to each group of treatment mice for 4 weeks, showed the highest pteryxin availability in the HP extract diet.

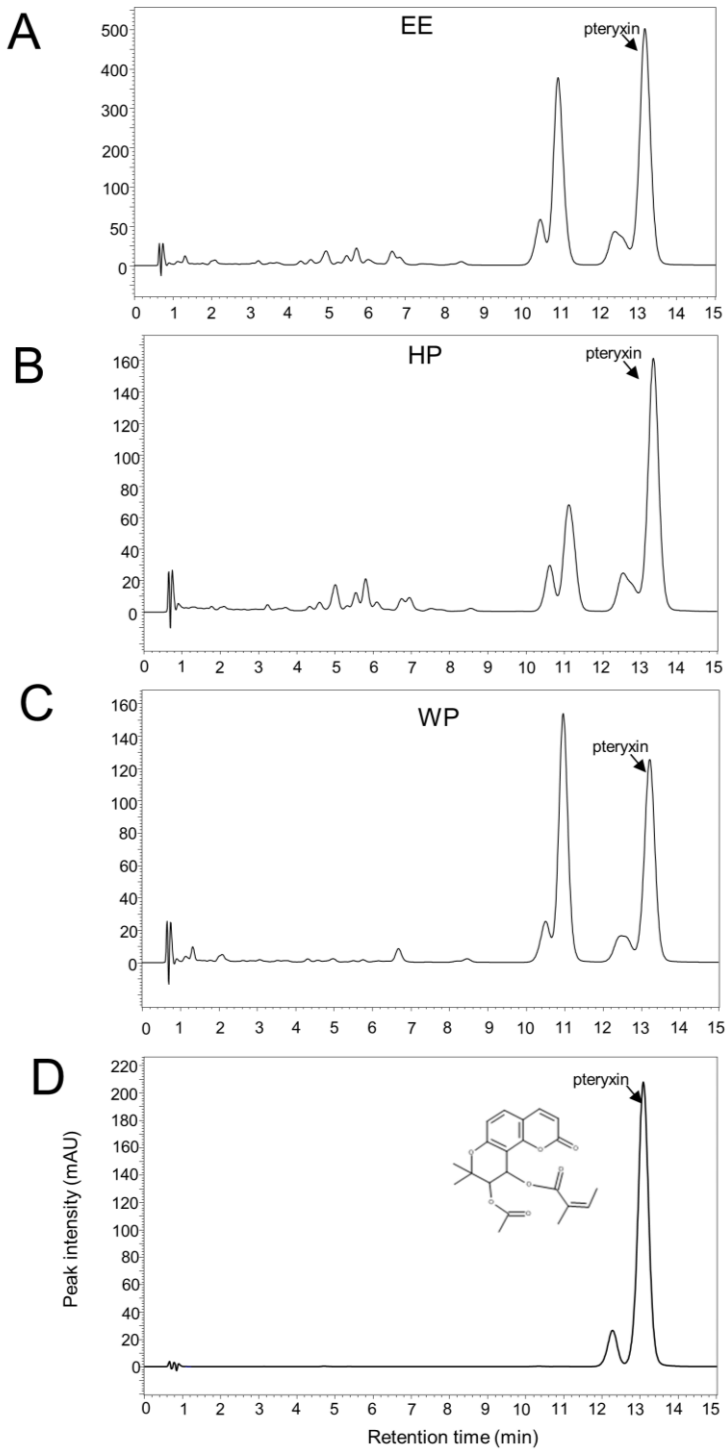

Figure 4-1 Analytical HPLC chromatogram for EE, HP WP and pteryxin.

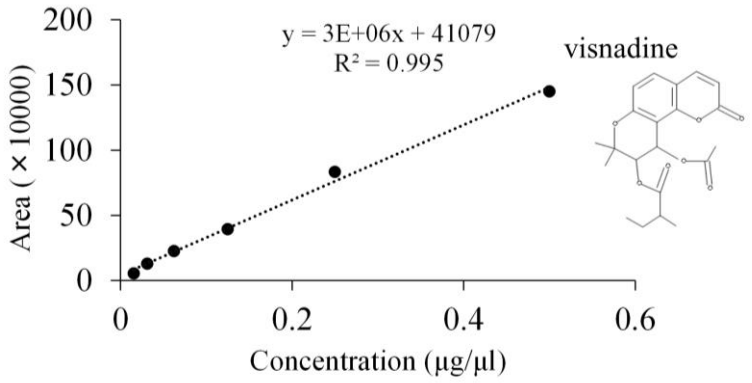

Figure 4-2 Standard curve of visnadine for the quantification of pteryxin.

4.2.2 Effect of HP on physiological parameters in mice

The initial body weight and the food intake showed no significant difference between the groups (Table 4-2). A significant decrease in the final body weight was observed after 4 weeks of the experiment due to the EE and HP treatments. The body weight with the WP treatment was comparable with that of the control group. The epididymal WAT was significantly reduced in the EE and HP groups.

Serum TG and HOMA-IR were reduced in the HP-treated mice (Table 4-3). The hepatic TG levels were reduced in the EE-treated mice. The mice fed with EE, HP or WP did not show any higher fecal excretion of TG.

Table 4-2 Effect of PJT on growth parameters in C57BL/6 mice

Index	Dietary group[†]			
	Control	**EE**	**HP**	**WP**
Food intake (g/day)	3.04±0.01	3.02±0.01	3.02±0.01	3.05±0.01
Energy intake (kcal/day)	12.98±0.02	12.89±0.02	12.89±0.04	13.02±0.02
Initial body weight (g)	13.96±0.72	13.90±0.32	13.94±0.55	13.93±0.63
Final body weight (g)	26.92±0.92	23.95±0.91[a]	24.05±0.43[a]	26.85±0.36
Liver weight (g/100 g body weight)	4.09±0.10	3.99±0.13	3.91±0.11	4.02±0.23
WAT (g/100 g body weight)	7.93±0.42	5.73±0.63	6.16±0.80	6.41±0.55
Abdominal fat	6.75±0.56	4.97±0.55	5.20±0.62	5.43±0.41
Epididymal fat	1.59±0.13	0.88±0.13[a]	0.84±0.18[a]	0.99±0.18[a]
Perirenal fat	3.34±0.34	2.65±0.34	2.90±0.36	2.86±0.26
Omental fat	1.82±0.28	1.45±0.20	1.47±0.12	1.58±0.12
Subcutaneous fat	1.18±0.26	0.75±0.23	0.95±0.28	0.98±0.25
BAT (g/100 g body weight)	0.14±0.02	0.12±0.02	0.10±0.02	0.14±0.02

[†]Values are means ± S.E.M. of five mice.
[a]Significant difference from the control group, $p < 0.05$.

Table 4-3 Effect of PJT on lipid metabolism related parameters in C57BL/6 mice

Index	Dietary group†			
	Control	**EE**	**HP**	**WP**
Serum				
Total cholesterol (mg/dl)	104.38±9.92	94.40±11.95	97.60±8.32	110.70±6.21
Triglyceride (mg/dl)	90.88±6.94	88.38±11.24	67.96±6.99	77.00±8.72
Glucose (mg/dl)	188.79±46.57	152.46±13.68	97.29±18.71	185.07±25.5
Insulin (ng/ml)	0.91±0.12	0.71±0.05	0.85±0.12	0.90±0.13
HOMA-IR	0.48±0.18	0.20±0.04	0.22±0.06	0.46±0.10
Liver lipid (mg/g liver)				
Total cholesterol	4.58±0.17	4.15±0.19	4.60±0.07	4.84±0.16
Triglyceride	67.87±2.07	48.94±2.85	63.01±2.71	58.14±3.85
Fecal excretion (mg/day)				
Total cholesterol	3.86±0.30	3.52±0.36	4.50±0.35	4.19±0.41
Triglyceride	0.23±0.04	0.31±0.05	0.20±0.03	0.18±0.02
Bile acid	1.10±0.11	1.05±0.07	0.85±0.06	0.88±0.10

†Values are means ± S.E.M. of five mice. The significance was checked by Dunnett's test, *$p < 0.05$.

4.2.3 Effect of PJT extracts on lipid metabolism-related gene parameters

In the previous studies on PJT, microarray analysis of gene expressions showed several significantly modulated genes related to lipid metabolism in PJT diet-fed liver tissue of C57BL/6 mice (Nukitrangsan *et al.*, 2011). Therefore, in this study I investigated the effect of HP on these selected lipid metabolism-related genes in WAT, the liver and soleus muscle.

4.2.3.1 Gene regulation pattern in WAT

Figure 4-3 explains the regulation pattern of genes due to the PJT fractions. The key lipogenic activator, *SREBP1c*, showed an upregulation in WP-treatment. The *PPARγ*, *RORC* and *FXRα* gene expressions showed an increasing trend in WAT possibly due to pteryxin-rich HP, as it was observed in Chapter II (Nugara *et al.*, 2014a). The *MEST*, tended to reduce due to HP. Adipose triglyceride lipase (*ATGL*), which is involved in the initial step of TG hydrolysis (Smirnova *et al.*, 2006), was increased due to all fractions.

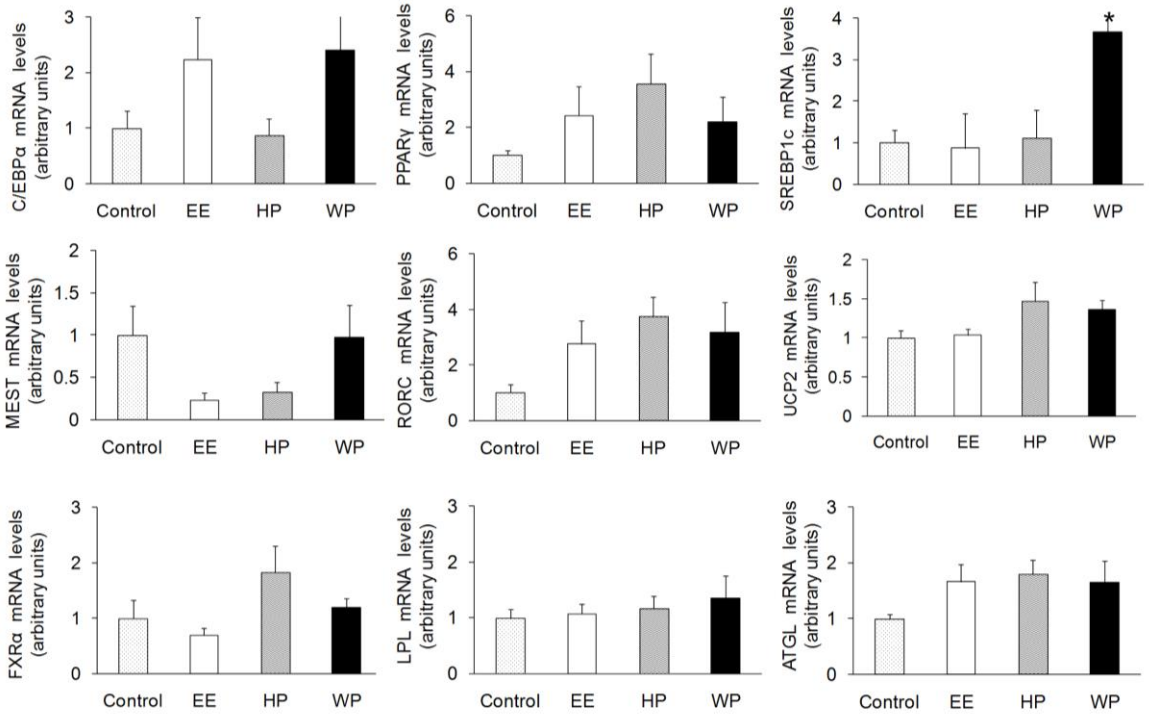

Figure 4-3 Gene expression in WAT of mice fed with a HFD and PJT fractions. The real-time reactions were performed in triplicate for all target genes and *ACTB* as a housekeeping control. Data are shown as means ± S.E.M. for five mice. Asterisk denotes statistical significance between the control group and treatment groups assessed by Dunnett's test (*$p < 0.05$). EE; ethanol extract, HP; hexane phase, WP; water phase of PJT.

4.2.3.2 Gene regulation pattern in liver tissue

The gene expressions of *SREBP1c* and *FAS* were significantly downregulated by HP (Fig. 4-4). Similarly, the EE and WP treatments suppressed the *SREBP1c* expression level. The insulin induced gene 2 (*INSIG2*) and cytochrome P450, family 7, subfamily a, polypeptide 1 (*CYP7A1*) expression levels showed a reducing tendency by HP.

The pre-B-cell colony-enhancing factor 1 (*PBEF1*) was highest in the WP treatment, and HP- and EE-treatments were comparable with the control.

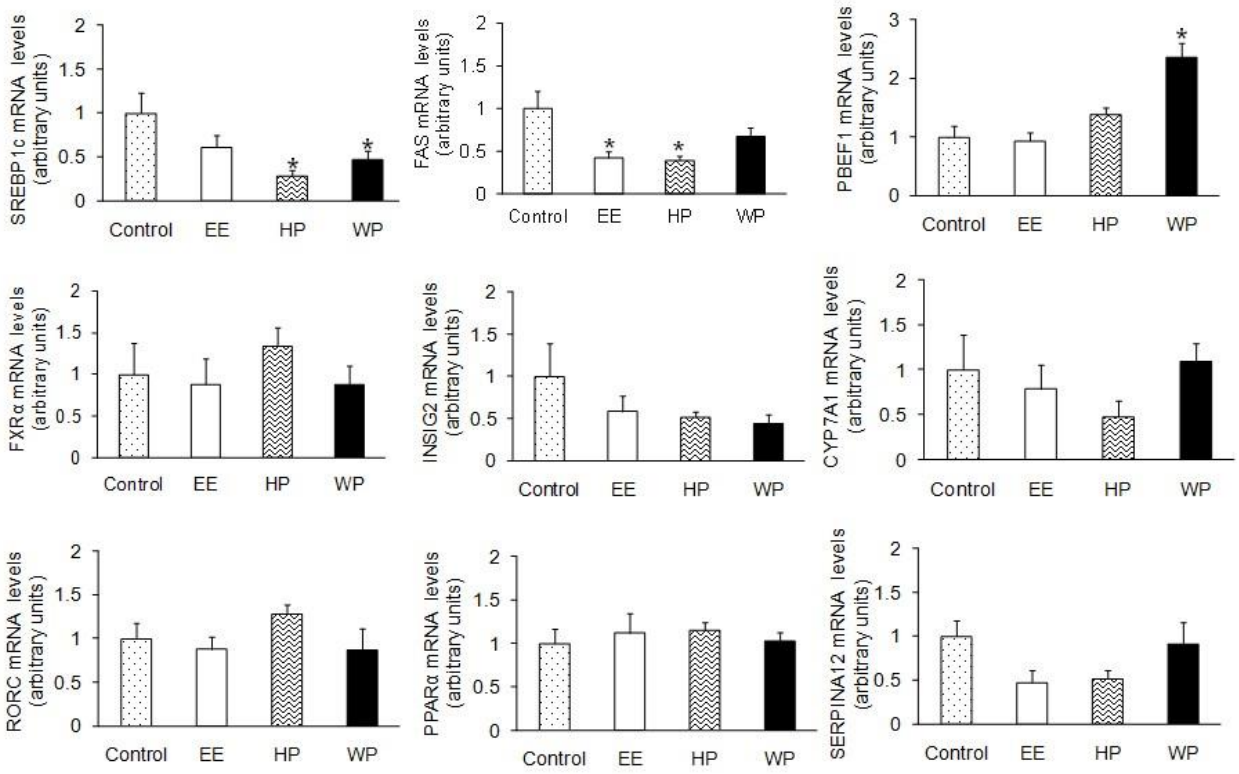

Figure 4-4 Gene expression in the liver tissue of mice fed with a HFD containing different PJT extracts. The real-time reactions were performed in triplicate for all target genes and *GAPDH* as a housekeeping control. Data are shown as means ± S.E.M. for five mice. Asterisk denotes statistical significance between the control group and treatment groups assessed by Dunnett's test (*$p < 0.05$). EE; ethanol extract, HP; hexane phase, WP; water phase of PJT.

4.2.3.3 Gene regulation pattern in muscle tissue

The *UCP2* mRNA level tended to increase in muscle in the HP group (Fig. 4-5). This was contrary to the previous *in vitro* results. The *GLUT4* expression showed a tendency to increase compared with the other treatment groups. However, *CPT1* α and β did not show any alteration, failing to clarify its involvement in the lipid lowering activity.

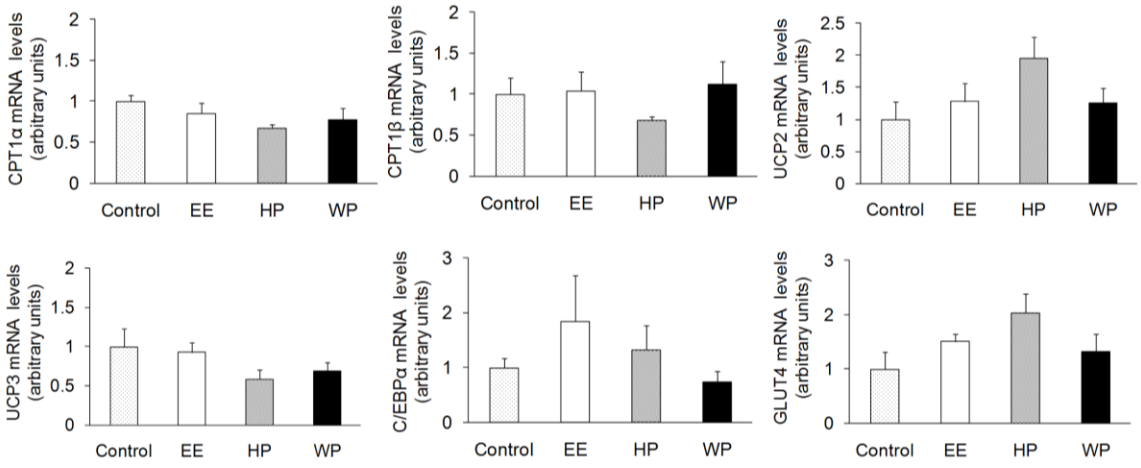

Figure 4-5 Gene expression in muscle tissue of mice fed with a HFD and PJT fractions. The real-time reactions were performed in triplicate for all target genes and *CYPa* as a housekeeping control. Data are shown as means ± S.E.M. for five mice. Asterisk denotes statistical significance between control group and treatment groups assessed by Dunnett's test (*$p < 0.05$).

4.3 Discussion

This study examined the effects of PJT EE, HP and WP treatments on HFD-fed mice in the lipid-lowering mechanisms *in vivo*. Thus, the data demonstrated that HP having the ability of reducing body weight of mice after 4 weeks of treatment period. Even though the HP concentration in diet was the least, its effect in the process of attenuation in body weight was highest, along with lowest fat accumulation in the epididymal and subcutaneous WAT, indicating the strength of pteryxin rich HP. This observation suggested that the effectiveness of HP as an anti-obesity treatment was due to its largely available coumarin, pteryxin.

Moreover, the results suggested that HP regulated gene expression levels pertaining to TG formation and storage in the liver and improved the energy expenditure in muscle tissue. The availability of pteryxin in the EE was 50% lower than HP, however, EE also showed a mitigation of obesity in HFD fed mice indicating the activity of EE was strong and comparable to HP, suggesting the highly effective inhibitory properties of pteryxin at a partially purified stage. However, due to the many and/or strong counterattack compounds in the WP has suppressed the effect of pteryxin in the WP.

Previous studies have elaborated anti-diabetic effects of EE (Nukitrangsan *et al.*, 2012a). Hence, the improvement in insulin resistance due to HP in our study would probably be a consequence of the observed improvement in the WAT profile. A further investigation of pteryxin as a single compound in an *in vivo* study will be required to confirm the above results.

Also, the fecal TG excretion in the treatment groups was comparable with that of the control group, indicating the involvement of possible modulation of a lipogenic gene network due to HP, as observed in the previous chapters (Nugara *et al.*, 2014a; Nugara *et al.*, 2014b).

Moreover, this study attempted to increase understanding of how HP regulates gene expression related to adipogenesis. The production of small adipocytes, which could be attributed to the increased levels of *PPARγ*, may have suppressed the fat accumulation in adipose tissue and the gene expression of adipocytes size marker gene *MEST* (Takahashi *et*

al., 2005) in the HP-fed group, as observed in the Chapter II. *C/EBPα* showed similar expression pattern to that of pteryxin *in vitro*, suggesting the uninterrupted delivery of pteryxin into the animal's body as it was observed for acetylangeloylkhellactone and praeruptorin A, which possess a khellactone backbone similar to that of pteryxin, increase arterial blood flow *in vivo* (Takeuchi *et al.*, 1991).

The expression of *RORC* and *FXRα* in liver showed an upregulation pattern, with no statistical significance and yet concordant with the HP *in vitro* results and indicates the acceleration of activity in β-oxidation of fatty acids due to HP (Raichur *et al.*, 2007). This could have probably led to the repression of *CYP7A1* and *INSIG2* to enhance degradation of 3-hydroxy-3-methyl-glutaryl-coenyme A (HMG-CoA) reductase, the rate-limiting enzyme in cholesterol biosynthesis (Faust *et al.*, 1982; Hubbert *et al.*, 2007). Nevertheless, *PBEF1* also known as visfatin positively correlates with the development of obesity (Johansson *et al.*, 2008) showed a significant increase in the WP suggesting its contribution towards obesity due to the minute quantity of pteryxin in WP and compounds that have counterattacked pteryxin activity. Contributing to the above fact, the WP showed serine peptidase inhibitor, clade A, member 12 (*SERPINA12*), commonly known as vaspin expression levels similar to that of the control indicating its correlation with body fat mass (Youn *et al.*, 2008). Further, *FAS* showed significant repression due to EE and HP, corresponding with the *in vitro* study on HP in Chapter II. Taken together, our data suggest that modulation of gene expression plays a partial, yet important role in attenuating lipid accumulation in WAT and the liver in the presence of HP, possibly due to its major constituent, pteryxin.

In muscle tissue *in vivo*, the *UCP2* level showed a tendency to increase due to HP in the muscle tissue. Although *GLUT4* was upregulated in the muscle tissue, we found the least expression level due to the HP treatment in the C2C12 cells (Nugara *et al.*, 2014b). The mechanisms behind this observation currently remain unknown.

Conclusion

This study demonstrated that pteryxin rich HP rather than WP had higher anti-obesity activity in WAT, the liver and muscle tissue *in vivo*, suggesting that the anti-obesity activity of PJT is largely due to pteryxin.

CHAPTER V

The multifaceted pteryxin-mediated molecular mechanisms to inhibit adipogenesis in 3T3-L1 cells

Introduction

In the previous chapters, I emphasized on the isolation of the pteryxin from the HP of PJT and dose-dependent anti-obesity effects of pteryxin *in vitro*. Thus, as the next step, I was intrigued to find on the molecular mechanisms related to pteryxin at lower and upper-limit doses in 3T3-L1 cells against adipogenesis.

In the present study, I examined the following:

1. The gene expression modulation pattern of pteryxin during the entire adipogenic process.
2. The transcriptomic analysis to elucidate target molecules of pteryxin and the bio-candidate markers during the entire adipogenic period.
3. The gene expression modulation patterns with time in the preadipocyte stage.
4. The transcriptomic analysis and target molecules identification in the preadipocyte stage in the presence of pteryxin.

5.1 Materials and methods

5.1.1 Pteryxin purification

The PJT HP was fractionated by open column chromatography and the Fr3 was collected to a new collection tube. Fr3 was dried, re-dissolved in CH_2Cl and used as the starting material for the HPLC fractionation (Nugara *et al.*, 2014b). In the HPLC program, Fr3-8 was collected as purified pteryxin. The purified pteryxin was dried, re-dissolved in 100% ethanol to obtain 10 µg/µL concentration, and stored at −20°C for further use. Nevertheless, the purified pteryxin was tested on 3T3-L1 cells against adipogenesis to confirm its activity.

5.1.2 Cell culture

The 3T3-L1 preadipocytes were cultured in 24-well plates at a density of 1×10^4 cells/well as it was described in Chapters II and III. The culture medium was then changed to DMEM supplemented with 10% FBS, 10 µg/mL insulin, and pteryxin (20 or 50 µg/mL) from 2 to 6 days.

To investigate the effect of pteryxin on the preadipocyte stage, pteryxin (20 or 50 µg/mL) was maintained in the medium only during Day 0 to Day 2 and harvested the cells either at Day 1 or Day 2 for further analyses. The below illustration gives a better understanding of the treatments and time durations that they were maintained in the medium before the cells were harvested for further experiments (Fig. 5-1):

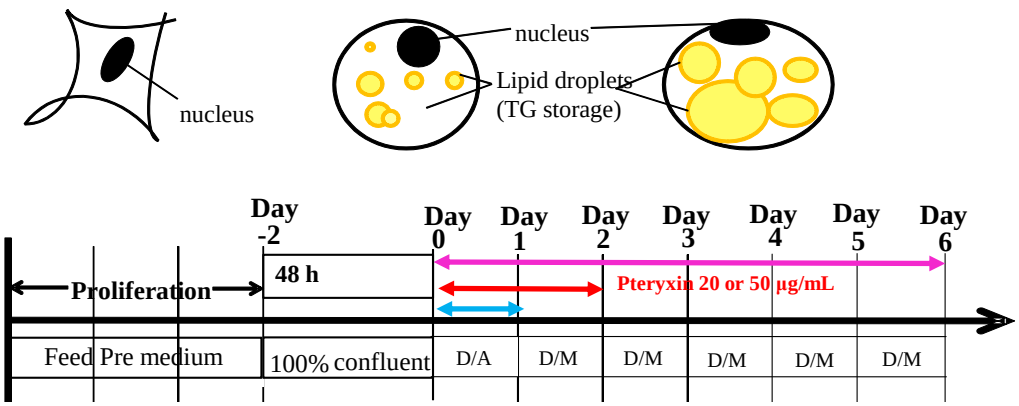

Figure 5-1 Schedule of treatments along the adipogenic process in 3T3-L1 cells.

5.1.3 Quantitative real-time PCR

To obtain total RNA, the 3T3-L1 cells were seeded in 3.0 cm dishes with 3×10^4 cells/dish. The cells were treated with the above pteryxin concentrations during Day 0–1 (24 h), Day 0–2 (48 h) or from Day 0–6, (6 days). Total RNA were extracted, cDNA were synthesized and subjected to qPCR as mentioned in Chapters II and III.

5.1.4 Protein extraction and Western blotting

In the presence of pteryxin for 24 h, 48 h or 6 days, the cells were washed twice with cold PBS and harvested in 1,000 µL accutase (Sigma Aldrich). The harvested cells were then transferred to 1.5 mL tubes, cell number per treatment were counted and centrifuged at 3,000 rpm for 5 min at 4°C. After removal of the supernatant, cells were washed with cold PBS followed by centrifuge at 13,000 rpm for 1 min. The remnants were carefully removed and resuspended the pellet in PRO-PREP solution (iNtRON Biotechnology Inc.). The volume of resuspension buffer depends on the amount of cells per treatment (according to the manufacturer's protocol). The cells were incubated for 20 min at −20°C. Next, the cell suspension was centrifuged at 13,000 rpm for 5 min at 4°C. Finally, the supernatant was transferred to new collection tube and measured the protein concentration using Quant-iT protein kit according to manufacturer's protocol. Equal amounts of protein for each sample were applied to either 5% (for ACC and phospho-ACC) or 10% (all other protein expressions except ACC) polyacrylamide commercial gels (e-PAGEL; ATTO Corporation) and were electrophoretically transferred to polyvinylidene difluoride membranes (PVDF). For ACC, phospho-ACC, p38 mitogen-activated protein kinase (MAPK) and phospho-p38 MAPK, 20 µg of protein was used, for the rest of expressions, 10 µg of protein was used. After electrophoresis, the separated proteins were transferred to the pre-treated PVDF membranes. The nonspecific binding sites in the membranes were blocked using Blocking One (Nacalai Tesque) at room temperature for 1 h. After blocking, the membrane was incubated with primary antibody with 1: 5,000-dilution for β-actin, 1: 2,000-dilution for

phospho-extracellular signal-regulated kinase (ERK) 1/2, 1: 1,000-dilution for ERK1/2, ACC and phospho-ACC, 1:500-dilution for p38 MAPK and 1: 200-dilution for AMP-activated protein kinase (AMPK), phospho-AMPK and phospho-p38 MAPK overnight at 4°C followed by a horseradish peroxidase-conjugated secondary antibody (anti-rabbit – 1: 100,000; anti-mouse – 1: 250,000). Peroxidase activity was visualized by ECL detection kit (GE Healthcare, Life Sciences). The expression of each protein was presented as fold against the control. All measurements were normalized to the levels of β-actin. The density of specific bands was calculated by ImageJ image analysis software (NIH, Bethesda, MD, USA).

5.1.5 Next Generation Sequencing and transcriptome analysis

On Day 6, the control and pteryxin treated cells were harvested, followed by total RNA extraction as described in 5.1.3. The mRNA were synthesized using Ambion Poly(A) Purist MAG Kit (Life Technologies) according to manufacturer's protocol. cDNA libraries were then synthesized from the mRNA using Ambion SOLiD Total RNA-Seq Kit (Life Technologies) and then subjected to 5500xl SOLiD (at Open Research Center, Okinawa Science and Technology Promotion Center) to construct transcript sequences according to the standard protocol for 75-base fragment sequencing followed by evaluation of expression levels. For the gene expression analysis of samples on Day 1 (24 h with pteryxin 20 or 50 μg/mL) the total RNA were extracted as explained above. The prepared total RNA samples were sent to BGI Health Japan Co. Ltd., for the NGS analysis by HiSeq 2000 Illumina NGS. The data processing was carried out as follows:

Reference sequence set was based on Affimetrix Gene Chip Mouse Genome 430 2.0 array (MGI Data and Statistical Reports, 2015; NCBI Reference Sequence Database, 2015). Read from SOLiD (short sequences) were trimmed and filtered according to the quality value (QV). Each read was trimmed from 3'-end when QV of the base was < 20; after trimming, any reads with length < 50bp or mean QV < 20 were discarded. Mapping the filtered SOLiD reads onto the reference sequences (allowing up to 2.5% of mismatch) using the BWA software version no.0.6.1-r104 (Li and Durbin, 2010).

Numbers of mapped reads per reference sequences were counted. Count data were normalized between samples using "upper quartile" (Bullard *et al.*, 2010). Fold changes of gene expression level was calculated between samples. Genes with zero-values for both samples were removed from analysis. Moreover, the fold change of a gene was recorded as '1' (i.e., equivalent between the two samples) when not significant in fisher exact test (based on count data before normalization) after false discovery rate (FDR) adjustment of p-values (Benjamini *et al.*, 2001). This test filtered results to avoid false positives apart from biological significance.

Magnitudes of fold changes were rounded up to 50 times either positive or negative. The ratio (fold change) were used as direct input data for the ingenuity pathway analysis (IPA®; Qiagen Ingenuity, CA) which is a web based software that is used to identify new targets, interactions in the different metabolic pathways, and important biomarkers in a dataset obtained from 'omics experiments.

5.1.6 Statistical analyses

All results were expressed as the mean ±S.E.M. The statistical significance of the difference between the means of control and treatment groups was determined by Dunnett's test or Student's *t*-test. Differences were considered significant at $p < 0.05$.

5.2 Results

5.2.1 Effect of different doses of pteryxin on the gene modulation pattern of adipogenesis

In the presence of 20 and 50 µg/mL from Day 0–6 in 3T3-L1 cells, inhibited the adipogenesis. However, the gene modulation patterns of the two doses showed contradictory information indicating different target points in response to the two doses (Fig. 5-2). The major adipogenic transcription factors *PPARγ* and *C/EBPα* were inhibited due to the 50 µg/mL dosage suggesting pteryxin ability to repress adipogenesis. The downstream target genes of *PPARγ* and *C/EBPα*, *FABP4*, *LPL*, *MEST* and *Glut4* were also suppressed due to the higher dose of pteryxin. The *UCP*s were upregulated due to the lower dose (20 µg/mL), whilst the *PGC1α* and *CPT1α* were upregulated due to the higher dose (50 µg/mL).

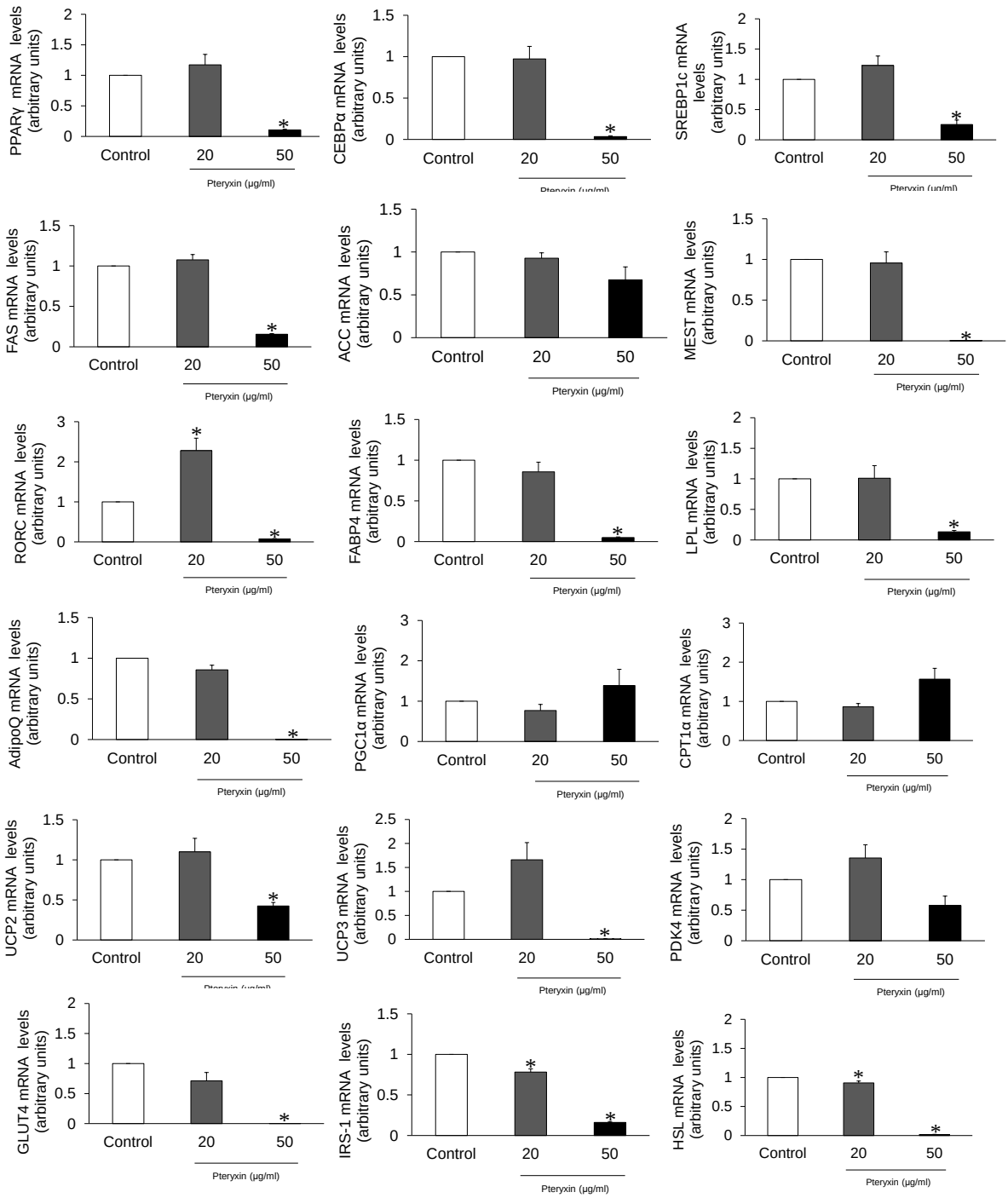

Figure 5-2 Effect of pteryxin (20 or 50 μg/mL) on the adipogenic gene network in 3T3-L1 cells. 3T3-L1 preadipocytes were differentiated and treated with 20 or 50 μg/mL pteryxin during Day 0-6. The qPCR was performed with values expressed as fold-change over control. Values are mean ± S.E.M. in three independent experiments. Comparisons between treatments with the control were analyzed by Dunnett's test (*$p < 0.05$).

5.2.2 Effect of different doses of pteryxin in adipogenesis – Pathway analysis via IPA

As illustrated in the Fig. 5-3, in the presence of pteryxin 20 µg/mL, the IPA results suggested that the preadipocytes were not affected by pteryxin. However, at the adipocyte stage, the leptin gene showed a 50-fold downregulation due to pteryxin. On the other hand, 50 µg/mL pteryxin was able to interfere both in the preadipocyte and adipocytes stages (Fig. 5-4). In the preadipocyte stage, the WNT5a non-canonical pathway was downregulated. The frizzled receptors indicated a downregulation due to pteryxin irrespective of the dosage. In concordance with our qPCR results, the *PPARγ* and *CEBPα* were downregulated throughout the adipogenic process. Moreover, the upstream of *PPARγ*, SMAD 1/5/8 was upregulated due to 50 µg/mL pteryxin.

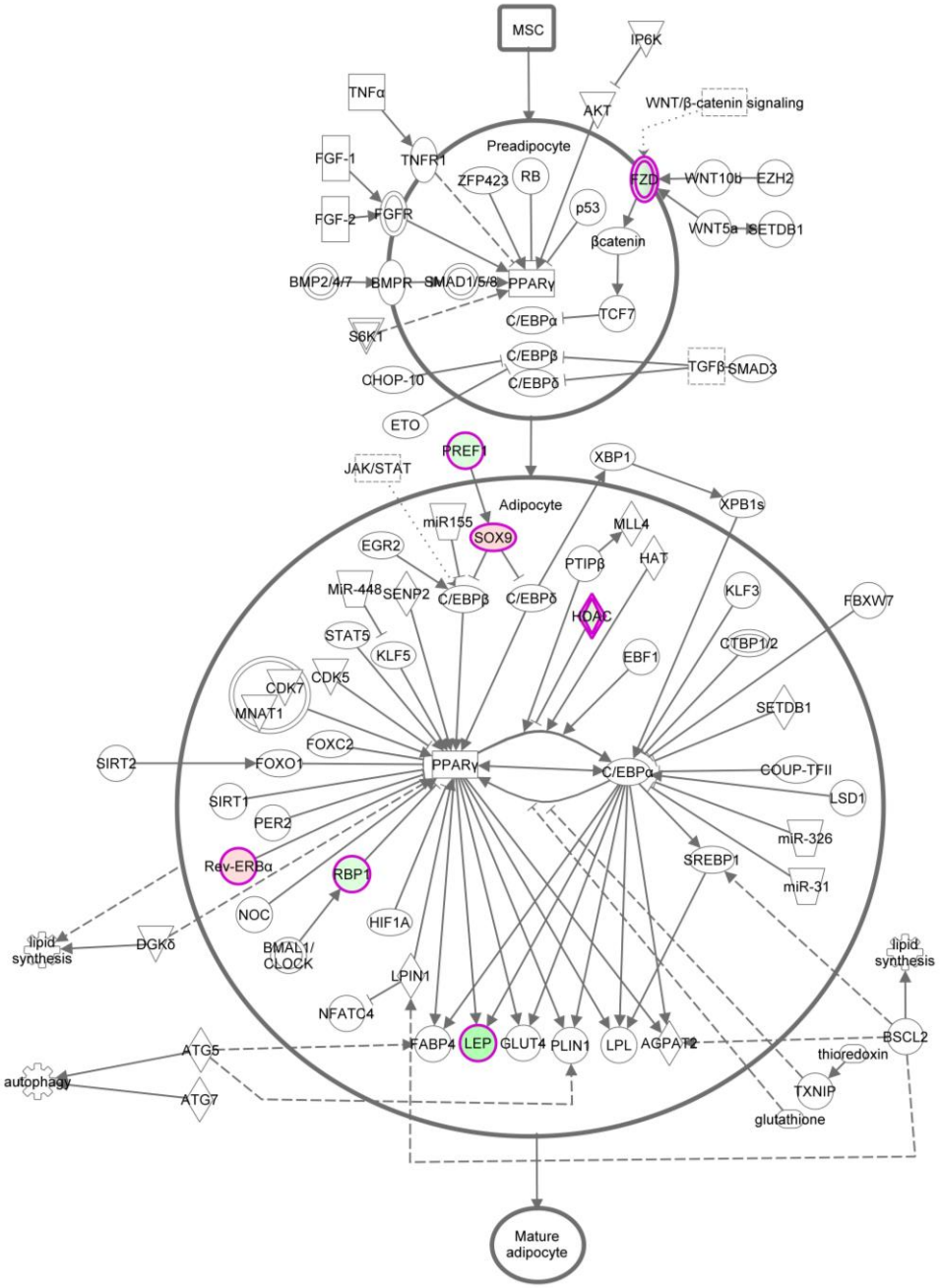

Figure 5-3 Effect of pteryxin (20 μg/mL) on the adipogenic pathway analysis. 3T3-L1 preadipocytes were differentiated and treated with 20 μg/mL pteryxin during Day 0–6. The mRNA were subjected to SOLiD NGS, data were normalized and calculated the fold-change as explained in the ***Materials and Methods***. The processed data were subjected to IPA for pathway, biomarker and target search. The pink color indicates the upregulated genes and green for the downregulated genes. The brightness of color of each target indicates the prominence of that particular gene.

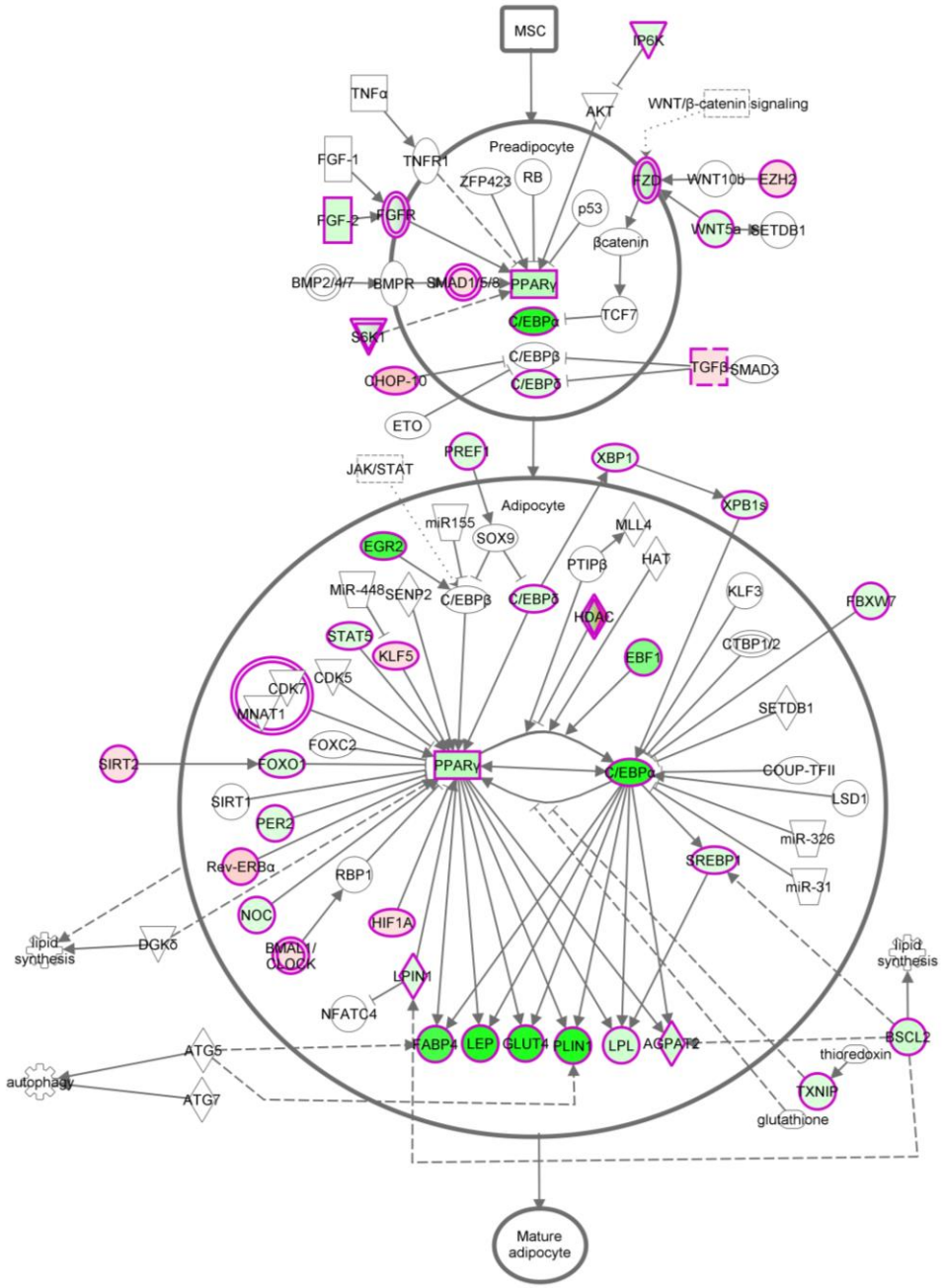

Figure 5-4 Effect of pteryxin (50 μg/mL) on the adipogenic pathway analysis. 3T3-L1 preadipocytes were differentiated and treated with 50 μg/mL pteryxin during Day 0–6. The mRNA were subjected to SOLiD NGS, data were normalized and calculated the fold-change as explained in the ***Materials and methods***. The processed data were subjected to IPA for pathway, biomarker and target search. The pink color indicates the upregulated genes/receptors and green for the downregulated genes/receptors. The brightness of color of each target indicates the prominence of that particular gene.

Furthermore, the AMPK signaling pathway was influenced by the higher dose of pteryxin, with 45-fold downregulation of adiponectin and 50-fold downregulation of leptin gene. The *Glut4* and *HSL* genes were also downregulated (Fig. 5-5). The G-proteins indicated to be upregulated to a lesser extent whereas *IRS-1/2*, phosphoinositide3 kinase (PI3K) and p38 MAPK have tended to be downregulated.

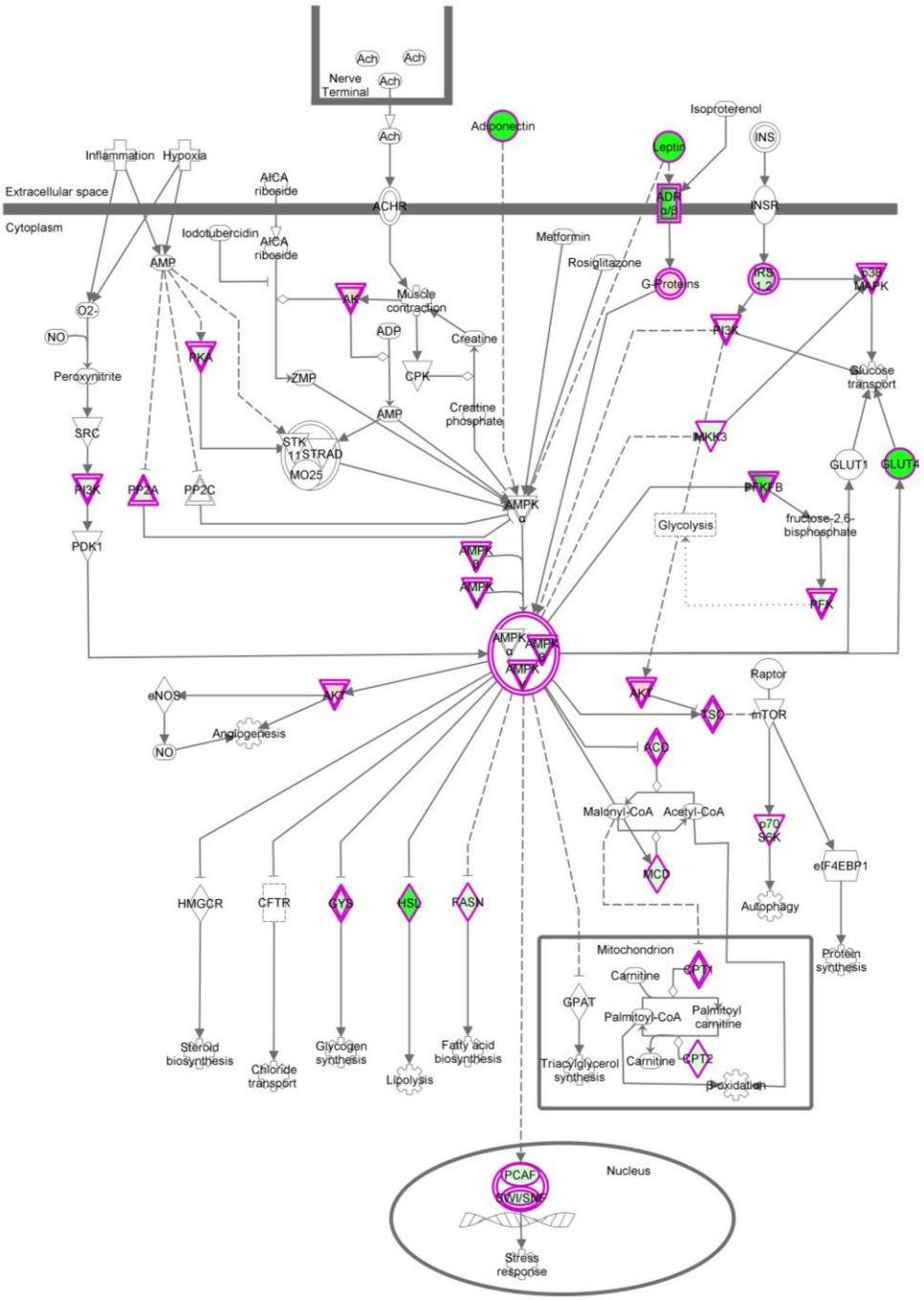

Figure 5-5 Effect of pteryxin (50 μg/mL) on the AMPK Pathway. 3T3-L1 preadipocytes were differentiated and treated with 50 μg/mL pteryxin during Day 0–6. The mRNA were subjected to SOLiD NGS. The processed data were subjected to IPA for pathway, biomarker and target search. The pink color indicates the upregulated and green for the downregulated genes/receptors/proteins. The brightness of color of each target indicates the prominence of that particular gene.

5.2.3 The effect of pteryxin in AMPK and ERK1/2-mediated MAPK signaling pathways

To further elucidate the molecular mechanism of the suppressive effect of pteryxin, I investigated the possibility of pteryxin acting as an activator of either AMPK or ERK1/2. Thus, I investigated the phosphorylation of AMPK, ERK1/2, p38 MAP kinase when the cells were cultured for 6 days in the pteryxin medium. As shown in Fig. 5-6, 20 μg/mL pteryxin significantly increased the phosphorylation of ERK1/2. The AMPK phosphorylation was triggered when the cells were cultured in 50 μg/mL pteryxin. Moreover, the phosphorylation of p38 MAPK was downregulated indicating the suppression of the p38 activity in the presence of pteryxin irrespective of the dosage.

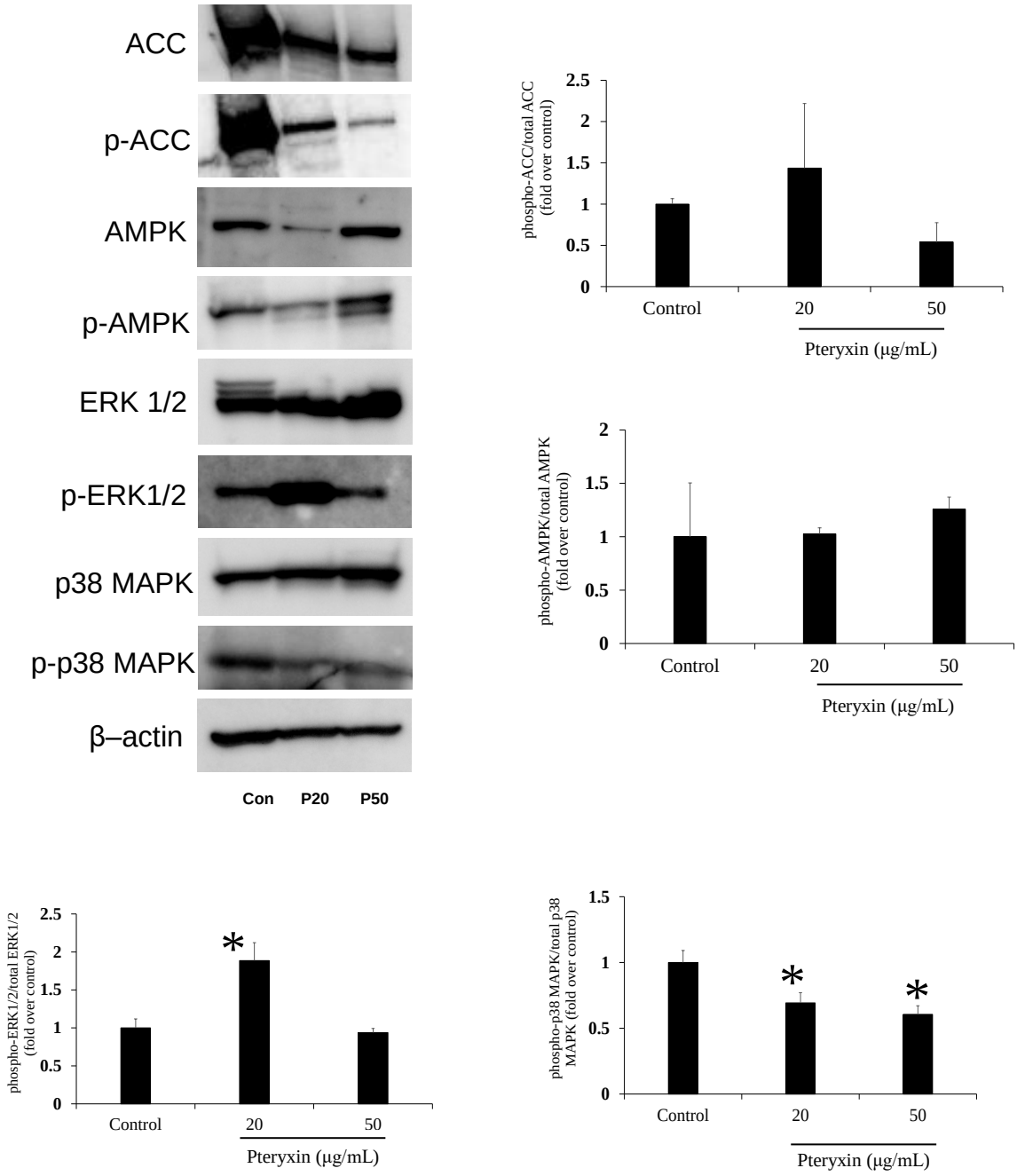

Figure 5-6 Effect of pteryxin on the molecular mechanism to suppress adipogenesis. 3T3-L1 preadipocytes were differentiated and treated with 20 or 50 μg/mL pteryxin during Day 0–6. The protein were extracted and protein expressions were assessed by western blot. All values were normalized to that of β-actin levels. Phosphorylated protein levels were quantified by ImageJ software and normalized to total proteins. Values are represented as mean ± S.E.M. of three independent experiments. Fold changes of protein expressions were obtained against the control group. Significance was tested vs. control by Dunnett's test and $*p < 0.05$.

5.2.4 Anti-adipogenic activity of pteryxin at preadipocyte stage

To identify the mechanism of pteryxin in the early phase of the adipogenesis, pteryxin was added to the medium at Day 0 and maintained either 24 (Day 0–1) or 48 h (Day 0–2). At each time point, the cells were harvested for total RNA extraction and its gene modulation pattern was observed (Fig. 5-7). It was evident that, *PPARγ* was downregulated more, by the 50 μg/mL dose along with time. Pteryxin at 50 μg/mL, *C/EBPα*, was completely downregulated at 48 h. Similarly, *SREBP1c* expression significantly reduced at 50 μg/mL after 48 h. However, after 24 h, the *ACC* and *FAS* showed downregulation irrespective of the pteryxin dose. Pteryxin at 20 μg/mL, significantly reduced the fatty acid transporter gene, *FABP4*. However, 50 μg/mL pteryxin, increased the *FABP4* expression during the first 24 h and thereby reduced after 48 h. Moreover, pteryxin downregulated the *HSL* levels at 48 h irrespective of the dosage. On the other hand, pteryxin at 24 h, showed increasing trend in the *UCP* gene expression levels. Further, pteryxin 20 and 50 μg/mL upregulated the key regulator of energy production *PGC1α*.

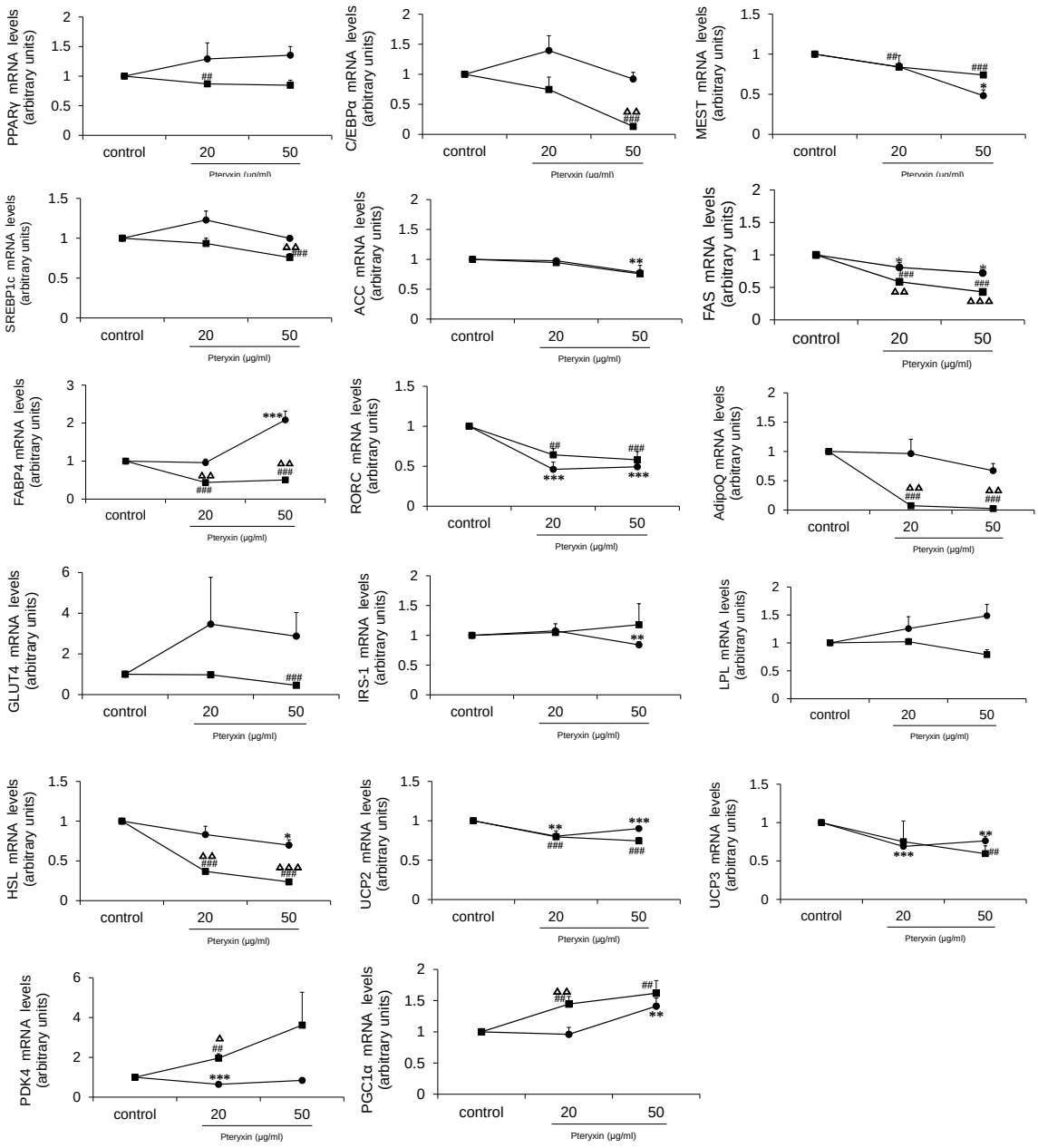

Figure 5-7 Effect of pteryxin (20 and 50 μg/mL) during the preadipocyte conversion period in 3T3-L1 cells. 3T3-L1 preadipocytes were differentiated with pteryxin during Day 0–2. Cells were harvested at 24 h and 48 h, total RNA were extracted, cDNA were synthesized and subjected to qPCR. Values expressed as fold-change over control. Closed circular (●) indicates values at 24 h and closed square (■) indicates values at 48 h. Values are mean ± S.E.M. in three independent experiments vs. control 24 h, *$p < 0.05$, **$0.01 < p < 0.05$, ***$p < 0.01$; vs. control 48 h, #$p < 0.05$, ##$0.01 < p < 0.05$, ###$p < 0.01$; vs. pteryxin 20 μg/mL 24 h, Δ$p < 0.05$, ΔΔ$0.01 < p < 0.05$, ΔΔΔ$p < 0.01$.

5.2.5 Pteryxin alters the lipogenic molecular mechanisms at early adipogenesis – Pathway analysis via IPA

I was also intrigued to examine the target points of different metabolic pathways due to pteryxin. Thus, the data of the Illumina NGS were analyzed by IPA. The 20 μg/mL pteryxin directly affected on the oxidation of lipids by downregulating negative regulatory genes on fatty acid oxidation (Fig. 5-8), however no effects were identified in the adipogenesis at preadipocyte stage. The *ABCA1* was downregulated by 2.1-fold whereas the *KI* was reduced by 3.3-fold. The *Aldh1a7* and *TP63* were reduced by 2.4- and 2.1-fold, respectively when compared with the control values.

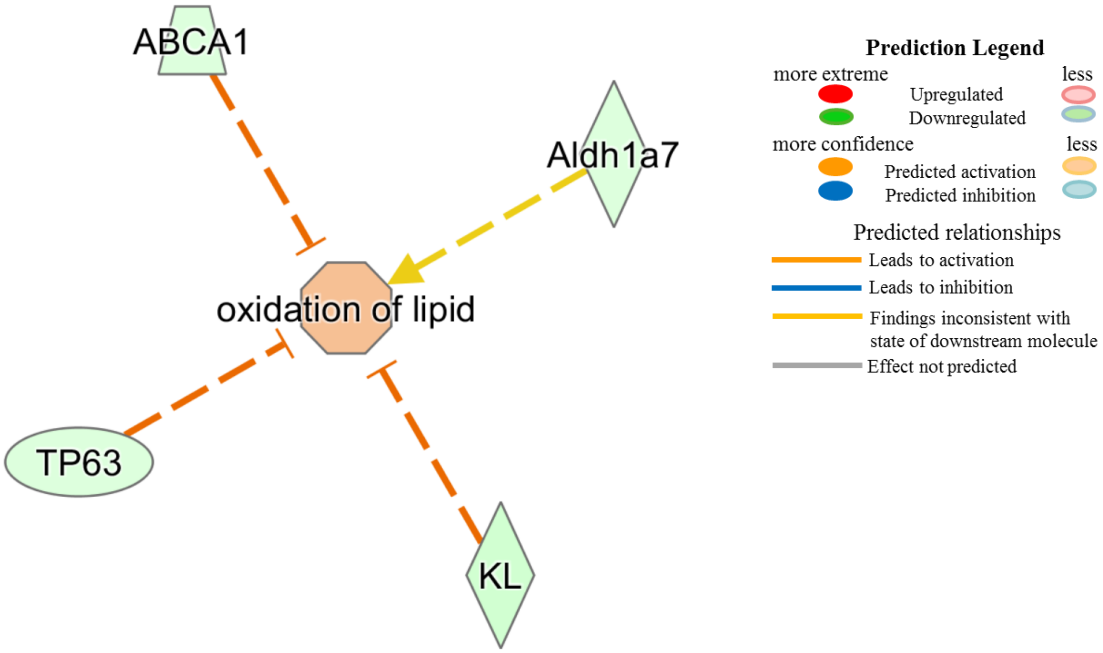

Figure 5-8 Pteryxin (20 μg/mL) affecting the oxidation of lipids during the early adipogenesis. 3T3-L1 preadipocytes were treated with 20 μg/mL pteryxin during Day 0–1 (24 h). The obtained data from Illumina NGS were filtered and mapped as explained in the ***Materials and Methods*** in Chapter V. The processed data were subjected to IPA for pathway, biomarker and target search. *ABCA1*, ATP-binding cassette subfamily A, member 1; *Aldh1a7*, aldehyde dehydrogenase 1A7; *KL*, klotho; *TP63*, tumor protein 63.

At 50 μg/mL, pteryxin was able to reduce the differentiation of adipocytes, adipogenesis in cells (Fig. 5-9A), insulin resistance (Fig. 5-9B) and obesity (Fig. 5-9C) during the first 24 h of the early adipogenesis. The *CMKLR1, IGF1, DUSP9* and *LIPE* were downregulated by 7.4-, 4.4-, 2.8- and 2.1-fold, respectively. Pteryxin 50 μg/mL, upregulated the CA6 by 13.0-fold. *ADM* also indicated of a 5.9-fold upregulation when compared with the control.

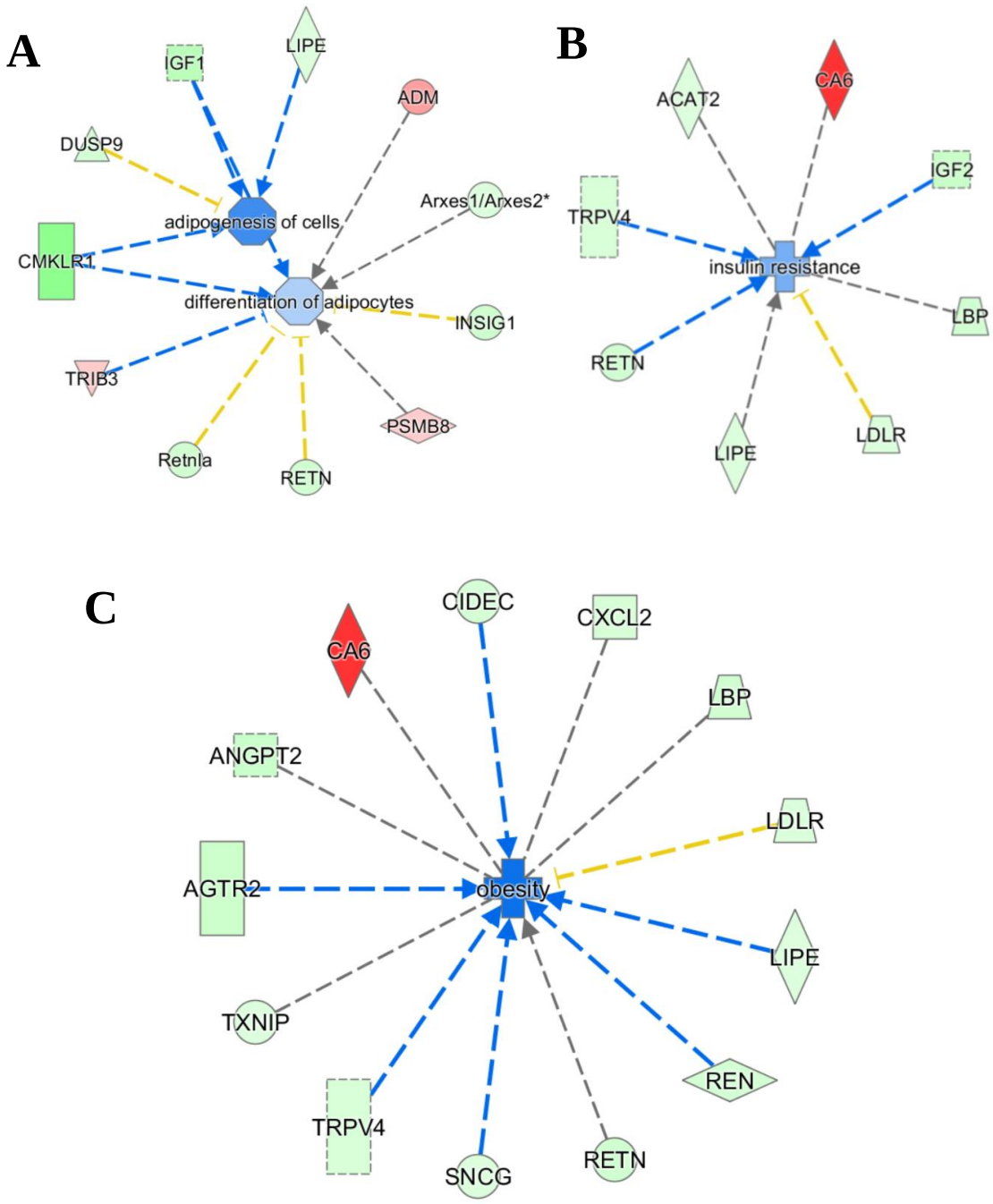

Figure 5-9 Effect of pteryxin (50 μg/mL) on different adipogenic pathways during the early adipogenesis. 3T3-L1 preadipocytes were treated with 20 μg/mL pteryxin during Day 0–1 (24 h). The obtained data from Illumina NGS were filtered and mapped. The processed data were subjected to IPA for pathway, biomarker and target search. *IGF*, insulin like growth factor; *LIPE*, hormone sensitive lipase; *ADM*, adrenomedullin; *Arxes1/Arxes2*, adipocyte-related X-chromosome expressed sequence 1/ adipocyte-related X-chromosome sequence2;

Insig1, insulin induced gene 1; *PSMB8*, 20s proteasome; *RETN*, resistin; Retnla, resistin like alpha; *TRIB3*, tribbles pseudokinase; *CMKLR1*, chemerin chemokine like receptor 1; *DUSP9*, dual specificity phosphatase; *CA6*, carbonic anhydrase 6; *LBP*, lipopolysaccharide binding protein; *LDLR*, low density lipoprotein receptor; TRPV4, Ion (Ca^{+2}) transport protein; *ACAT2*, acetyl CoA-acetyltransferase 2; *CIDEC*, cell death inducing DFFA-like factor C (adipocyte specific); *CXCL2*, chemokine ligand 2; *REN*, renin; *SNCG*, Synuclein gene; *TXNIP*, thioredoxin interacting protein; *AGTR2*, angiotensin II receptor type 2; *ANGPT2*, angiopoietin 2.

Moreover, 50 µg/mL pteryxin affected on the carbohydrate metabolism. The quantity and the release of carbohydrates were reduced while the uptake of the D-glucose was upregulated due to pteryxin (Fig. 5-10).

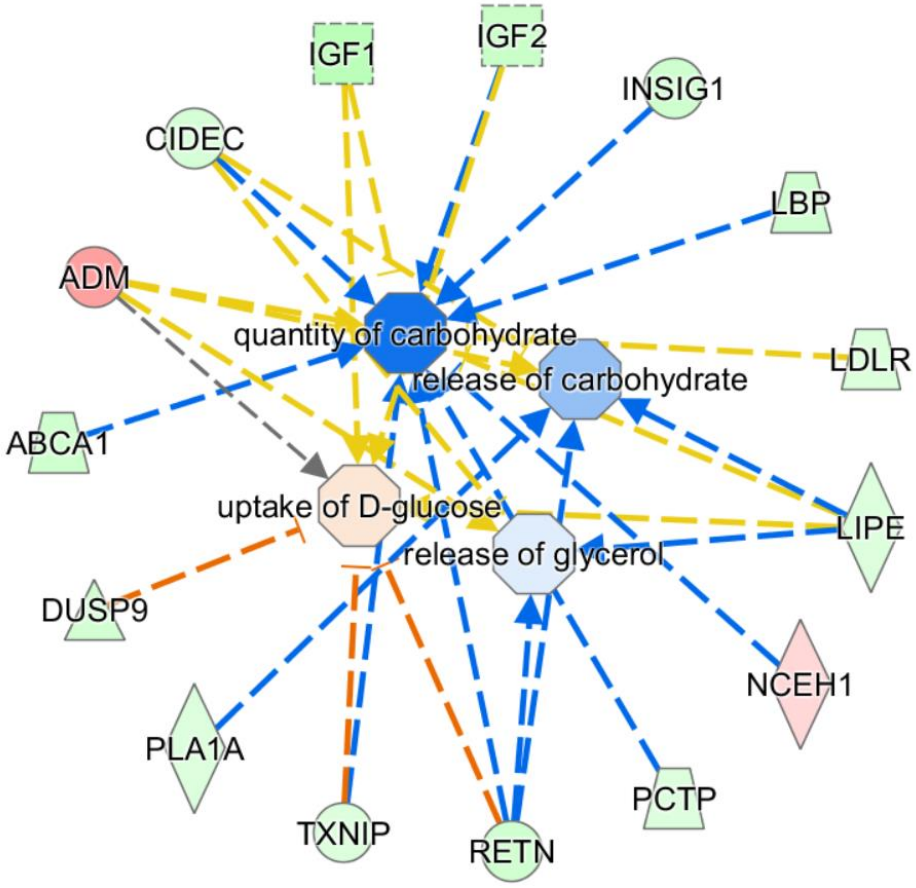

Figure 5-10 Pteryxin (50 µg/mL) affecting on the carbohydrate metabolism during the early adipogenesis. 3T3-L1 preadipocytes were treated with 20 µg/mL pteryxin during Day 0–1 (24 h). The obtained data from Illumina NGS were filtered and mapped. The processed data were subjected to IPA for pathway, biomarker and target search. *IGF*, insulin like growth factor; *Insig1*, insulin induced gene 1; *LBP*, lipopolysaccharide binding protein; *LDLR*, low density lipoprotein receptor; *LIPE*, hormone sensitive lipase; *NCEH1*, neutral cholesterol ester hydrolase 1; *PCTP*, phosphatidylcholine transfer protein; *RETN*, resistin; *TXNIP*, thioredoxin interacting protein; *PLA1A*, phospholipase A1 Member A; *DUSP9*, dual specificity phosphatase; *ABCA1*, ATP-binding cassette subfamily A, member 1; *ADM*, adrenomedullin; *CIDEC*, cell death inducing DFFA-like factor C (adipocyte specific).

5.3 Discussion

This investigation identify a unique role of pteryxin in regulating adipogenesis under two different concentrations. Pteryxin at lower dose (20 μg/mL) regulated the ERK1/2 signaling pathway and switch to AMPK signaling transduction at the higher dose (50 μg/mL). Moreover, this study provides an in-depth understanding of the different molecular mechanisms of action in the early and late adipogenesis in the presence of the two doses. Pteryxin at 50 μg/mL was effective at the preadipocyte stage and suppressed the adipocyte differentiation. Thus, these results provide new insights into an understanding of the different faces of pteryxin to repress the adipogenesis *in vitro*.

At the 20 μg/mL dose, pteryxin was able to increase the ERK1/2 signaling pathway. ERK1/2 signaling pathway is the center of a complex signaling network that regulates pivotal cellular processes including proliferation, differentiation and survival (Procaccia *et al.*, 2010). Studies have shown that ERK1/2 are required for the adipocyte differentiation (Sale *et al.*, 1995). However, the function of ERK in adipogenesis has to be timely regulated, which has to be switched-on in the proliferation stage and switched-off at adipocyte maturity stage in order to maintain mature adipocytes. Several studies have shown that inhibition of ERK1/2 activity during the mitotic clonal expansion (MCE) step occurs post-confluent. The precise suppression of ERKs at the MCE has led to blocking of adipocyte differentiation (Tang *et al.*, 2003). Pteryxin at the lower dose (20 μg/mL) increased the ERK1/2 activity throughout the adipogenesis and inhibited adipogenesis (Sakaue *et al.*, 2004; Jeong *et al.*, 2015) as it was observed in diallyl trisulfide (Lii *et al.*, 2012). Furthermore, *PPARγ*, substrate of ERK (Camp and Tafuri, 1997) decreases its transcriptional activity by the ERK phosphorylation, thereby inhibiting adipocyte differentiation justify the downregulating trend of the *PPARγ* when compared with HP in the previous chapters (Nugara *et al.*, 2014b).

AMPK is known to be involved in the regulation of adipogenesis and energy homeostasis (Carling *et al.*, 2011). The activation of AMPK suppressed the adipogenesis (Hardie, 2011). Pteryxin 50 μg/mL, enhanced the phosphorylation of AMPK, thereby decreasing the accumulation of intracellular lipids in 3T3-L1 cells. However, the regulatory

mechanism related to pteryxin has not been identified. Thus, in this study I revealed the pteryxin-mediated suppression of adipogenesis either via ERK1/2 or AMPK signaling pathway depending on the dose. In addition, our unpublished results indicated no apparent cell cytotoxicity against pteryxin at 50 μg/mL dose. Adipocyte differentiation is a cascade of different genetic modulation patterns, and confirming the qPCR results, pteryxin at 50 μg/mL suppressed major transcription factors *PPARγ* and *C/EBPα* according to the IPA results. However, SOLiD NGS results showed a 50-fold downregulation in the leptin gene expression indicating the correlation between leptin gene and the adipocyte volume (Zhang *et al.*, 2002; Li *et al.*, 2004) and ability of reducing obesity by pteryxin higher dose (Chen *et al.*, 1996a). The Wnt family proteins, secreted from glycoproteins, participate in many cellular developments functions such as cell proliferation, cell migration and differentiation (Gordon and Nusse, 2006). The Wnt family functions through two major pathways: canonical (β-catenin-related) and non-canonical (not β-catenin-related) based on intracellular Ca^{2+} release and the activation of phospholipase C and protein kinase C (Topol *et al.*, 2003). Studies have shown that Wnt10b activates the Wnt/β-catenin pathway and maintain the preadipocytes in undifferentiated state (Ross *et al.*, 2000). However the roles of non-canonical pathways in the adipogenesis are not well understood. Nishizuka et al. have demonstrated that the inhibition of Wnt4a and Wnt5a expression in 3T3-L1 cells prevented the TG accumulation and decreased the adipogenic gene expressions (Nishizuka *et al.*, 2008). In concordance, these results indicated that higher dose of pteryxin downregulated Wnt5a, *PPARγ* and *C/EBPα* in the preadipocyte stage decreasing the adipogenesis. Moreover, the co-receptor for Wnt, frizzled receptor (Fz) also indicated a downregulation in the pathway search suggesting that less availability of active binding site for Wnt may have led to less signaling competence of Wnt5a (Gordon and Nusse, 2006). Further, the lower dose of pteryxin accelerated *CPT1α*, which is the key regulator of β-oxidation, further stimulated by reduction of *ACC2,* and/or activating *PGC1α* (Schreurs *et al.*, 2010), suggesting its activity towards inhibition of adipogenesis.

The role of pteryxin in the preadipocyte stage showed its positive effect in repressing adipogenesis both in the 24 and 48 h. However, the effect was prominent in the presence of 50 μg/mL for 24 h or 20 μg/mL for 48 h. The pattern of gene regulation was closer to the observations that of 50 μg/mL after 6 days. Pteryxin showed an increasing trend in the key

regulator of energy metabolism, *PGC1α*, suggesting the acceleration of conversion from free fatty acids to ATP. Further strengthening this suggestion, the 13-fold increase of *CA6* which was the hallmark among the upregulated genes showed its activity in the maintenance of pH homeostasis by catalyzing the reversible reaction $CO_2 + H_2O \leftrightarrow HCO_3^- + H^+$ (Kivela *et al.*, 1999) in the energy conversion process. However, some studies have shown the acceleration of *CA*s providing bicarbonates for the elevated levels of lipogenesis (Chegwidden and Spencer, 1996). KL protein is correlated with adipogenesis, whereas pteryxin lower dose has reduced its expression by 3.3-fold and suppressed the adipogenesis (Chihara *et al.*, 2006). Moreover, *ABCA1*, a key regulator for cholesterol homeostasis showed a downregulation, thereby reducing the lipid accumulation (De Haan *et al.*, 2014) and increased the lipid peroxidation (Shao and Heinecke, 2009). In the presence of pteryxin 50 μg/mL, *IGF-1*, also known as an inducer for differentiation (Hwang *et al.*, 1997) downregulated in IPA results by 4.4-fold showing the repressive effects of pteryxin higher dose. Further confirming the suppressive effects of higher dose pteryxin on the differentiation at proliferation stage, *CMKLR1*, a recent novel adipocyte-derived molecule showed 7.4-fold downregulation. Pteryxin 50 μg/mL after 24 h in the culture medium, increased the uptake of glucose levels during the preadipocyte stage, similar to the findings reported by other groups in rodent cell lines (Hauner *et al.*, 1998; Tordjman *et al.*, 1989; Garcia de Herreros and Birnbaum, 1989), whilst the quantity of carbohydrates were more prominently retarded.

Conclusion

In summary, I showed the different mechanisms of pteryxin to inhibit adipogenesis both in preadipocyte and adipocyte stages indicating its unique characteristics to adjust the target molecules depending on the dose. This study is the first to demonstrate an in-depth molecular mechanisms related to pteryxin in the attenuation of adipogenesis in 3T3-L1 cell line.

CHAPTER VI

GENERAL CONCLUSIONS

Obesity has become one of the critical factors contributing to world's crisis. *Peucedanum japonicum* Thunb (PJT), possessing anti-obesity properties was nominated as a positive candidate for obesity. It was revealed that ethanol extract of PJT being characterized of an anti-diabetic activity by modulation of obesity related lipid parameters. However, PJT as a crude extracts restricted in-depth investigations on mechanisms related to anti-obesity.

Thus, in this study I partially purified the ethanol extract and found that hexane phase consisting of the anti-obesity characteristics that were observed in the ethanol extract (Fig. 6-1). During the purification of the hexane phase, I isolated a previously known coumarin, pteryxin containing the anti-obesity effects for the first time. Pteryxin modulated the gene network to suppress adipogenesis as illustrated in Fig. 6-2.

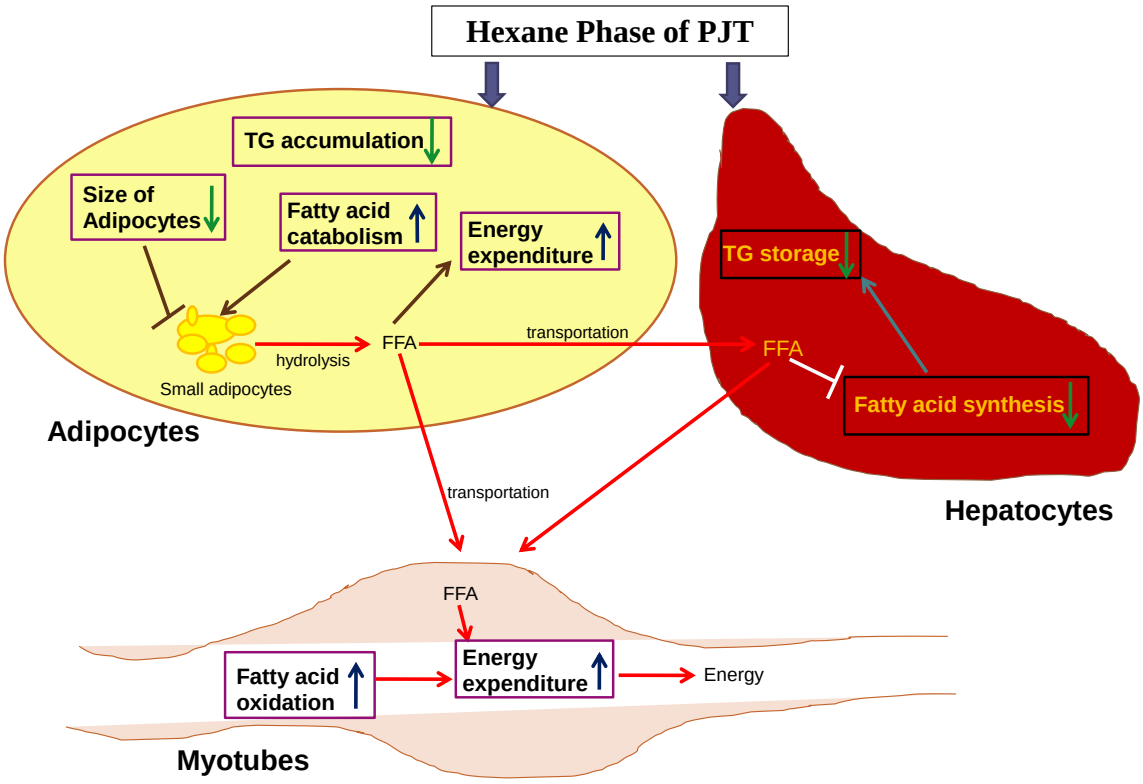

Figure 6-1 Schematic representation of the effect of PJT hexane phase in regulation of adipogenesis-related gene parameters *in vitro*.

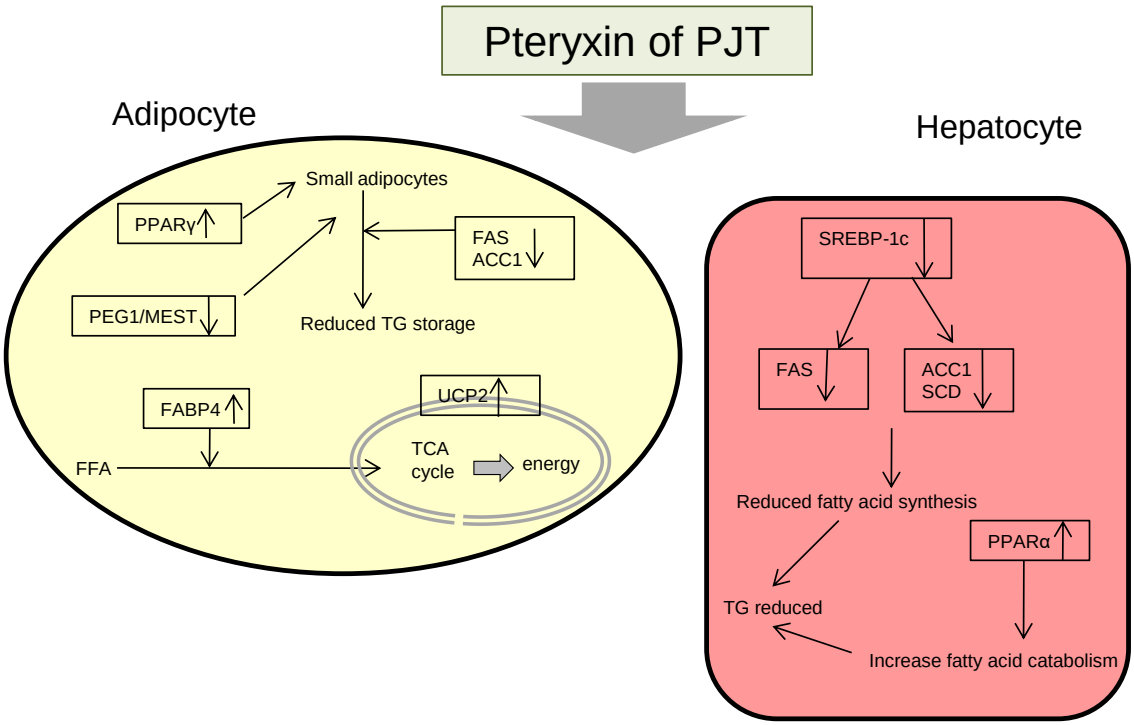

Figure 6-2 Summary illustration of the suppressive effects of pteryxin on adipogenesis and lipogenesis related gene parameters *in vitro*.

Pteryxin not only regulated the anti-adipogenic effect *in vitro* but also *in vivo* when mice were fed with a high-fat diet. Pteryxin containing hexane phase reduced the body weight and impact on several other important physiological parameters very effectively during a 4 week period.

Moreover, pteryxin also showed a unique ability of changing the target molecules to attenuate adipogenesis depending on the dose and the duration of existence in the culture medium *in vitro* and provided great insight on the biomarkers and their respective pathways that pteryxin has affected when compared with other available compounds which possess anti-obesity activity (Fig. 6-3). Further, I have summarized several important characteristics of pteryxin in Table 6-1.

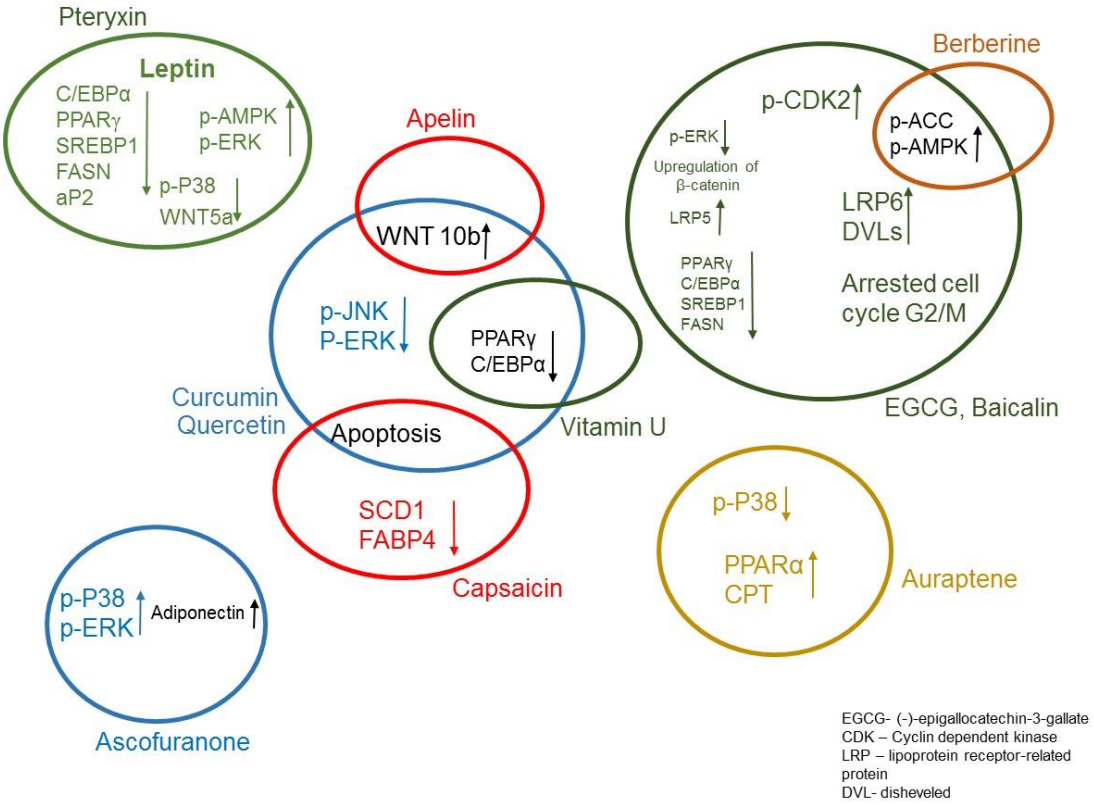

Figure 6-3 Specificity of pteryxin against several other anti-obesity compounds.

Table 6-1 Summary of pteryxin characteristics

Plant name		**Identified Function**		**Reference**
Angelica keiskei	(+)-pteryxin	Antitumor-promoter Scavenging activity for against Nitric oxide		(Akihisa *et al.*, 2003)
Peucedanum japonicum Formosan	(+)-pteryxin	Antiplatelet aggregation		(Chen *et al.*, 1996b)
Peucedanum japonicum Thunb	(+)-pteryxin	Anti-obesity activity		(Nugara *et al.*, 2014b)
	20 μg/mL (+)-pteryxin	*Upregulated genes*	*Downregulated genes*	
		PPARγ, RORC, FABP4, UCP2	SREBP1c, FAS, ACC, MEST	
	50 μg/mL (+)-pteryxin	PGC1α CPT1α	PPARγ, C/EBPα, SREBP1c, MEST, FAS, Adiponectin	Unpublished data

Overall, this study explain and provide very important understanding of the whole regulatory mechanisms related to pteryxin (Fig. 6-4). In addition, a study using purified pteryxin as a single compound in an *in vivo* study in different doses may be a limitation of the present study to investigate the actual complexity of the pteryxin-mediated mechanisms in an animal body.

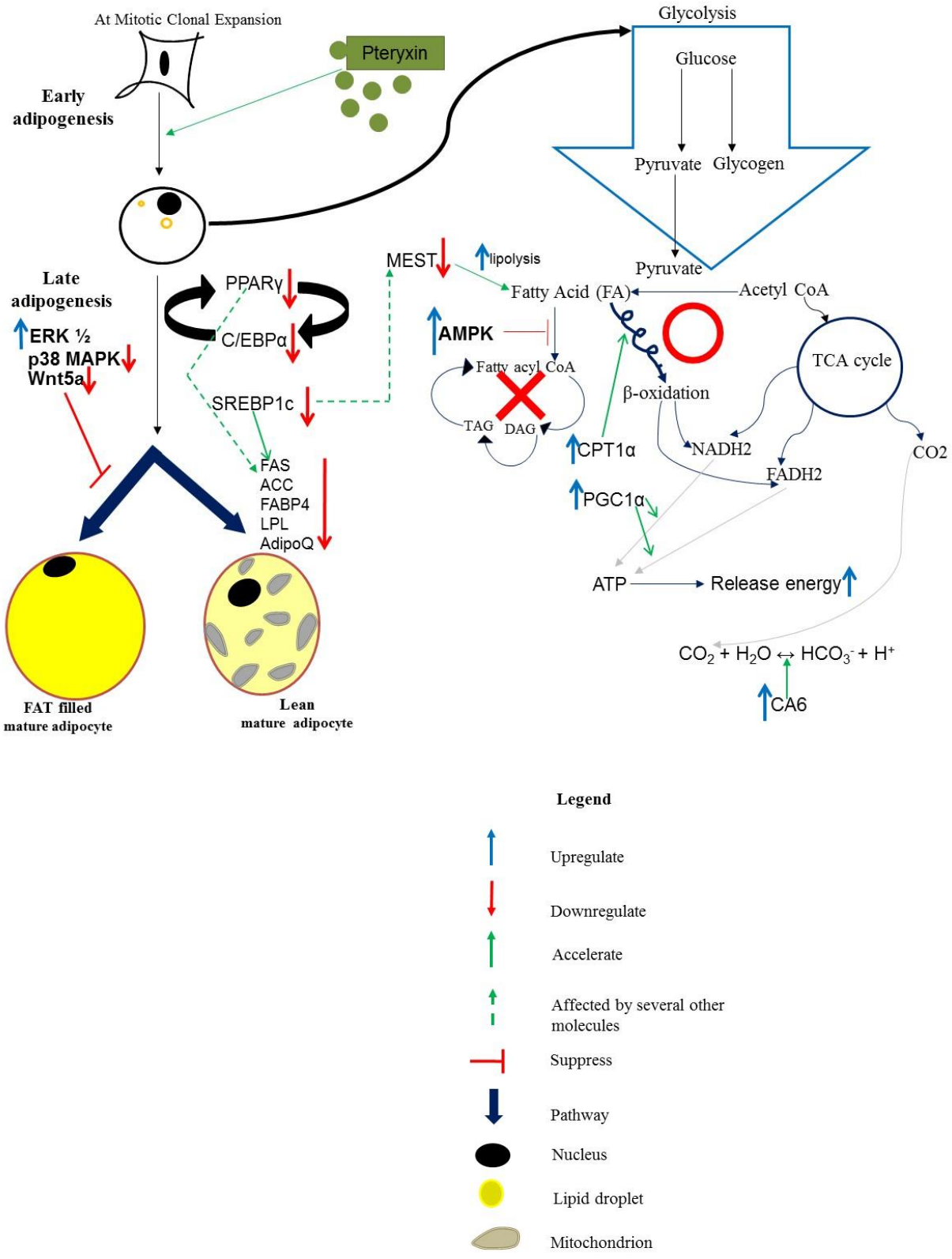

Figure 6-4 Overall mechanism of pteryxin in the adipocytes

References

(1) Ahn, E. K., Lee, J. A., Seo, D. W., Hong, S. S. and Oh, J. S. 2012. 1β-Hydroxy-2-oxopomolic acid isolated from *Agrimonia pilosa* extract inhibits adipogenesis in 3T3-L1 cells. *Biol Pharm Bull,* 35**,** 643-649.

(2) Akihisa, T., Tokuda, H., Ukiya, M., Iizuka, M., Schneider, S., Ogasawara, K., Mukainaka, T., Iwatsuki, K., Suzuki, T. and Nishino, H. 2003. Chalcones, coumarins, and flavanones from the exudate of *Angelica keiskei* and their chemopreventive effects. *Cancer Lett,* 201**,** 133-137.

(3) Alappat, L. and Awad, A. B. 2010. Curcumin and obesity: evidence and mechanisms. *Nutr Rev,* 68**,** 729-738.

(4) Alonso-Castro, A. J., Miranda-Torres, A. C., Gonzalez-Chavez, M. M. and Salazar-Olivo, L. A. 2008. *Cecropia obtusifolia* Bertol and its active compound, chlorogenic acid, stimulate 2-NBDglucose uptake in both insulin-sensitive and insulin-resistant 3T3 adipocytes. *J Ethnopharmacol,* 120**,** 458-464.

(5) Bandyopadhyay, G. K., Vu, C. U., Gentile, S., Lee, H., Biswas, N., Chi, N. W., O'Connor, D. T. and Mahata, S. K. 2012. Catestatin (chromogranin A(352-372)) and novel effects on mobilization of fat from adipose tissue through regulation of adrenergic and leptin signaling. *J Biol Chem,* 287**,** 23141-23151.

(6) Bartelt, A. and Heeren, J. 2014. Adipose tissue browning and metabolic health. *Nat Rev Endocrinol,* 10**,** 24-36.

(7) Benjamini, Y., Drai, D., Elmer, G., Kafkafi, N. and Golani, I. 2001. Controlling the false discovery rate in behavior genetics research. *Behav Brain Res,* 125**,** 279-284.

(8) Bligh, E. G. and Dyer, W. J. 1959. A rapid method of total lipid extraction and purification. *Can J Biochem Physiol,* 37**,** 911-917.

(9) Borch-Johnsen, K. 2007. The metabolic syndrome in a global perspective. The public health impact--secondary publication. *Dan Med Bull,* 54**,** 157-159.

(10) Bullard, J. H., Purdom, E., Hansen, K. D. and Dudoit, S. 2010. Evaluation of statistical methods for normalization and differential expression in mRNA-Seq experiments. *BMC Bioinformatics,* 11**,** 94.

(11) Camp, H. S. and Tafuri, S. R. 1997. Regulation of peroxisome proliferator-activated receptor γ activity by mitogen-activated protein kinase. *J Biol Chem,* 272**,** 10811-10816.

(12) Canto, C., Gerhart-Hines, Z., Feige, J. N., Lagouge, M., Noriega, L., Milne, J. C., Elliott, P. J., Puigserver, P. and Auwerx, J. 2009. AMPK regulates energy expenditure by modulating NAD+ metabolism and SIRT1 activity. *Nature,* 458**,** 1056-1060.

(13) Carling, D., Mayer, F. V., Sanders, M. J. and Gamblin, S. J. 2011. AMP-activated protein kinase: nature's energy sensor. *Nat Chem Biol,* 7**,** 512-518.

(14) Chan, P. T., Fong, W. P., Cheung, Y. L., Huang, Y., Ho, W. K. and Chen, Z. Y. 1999. Jasmine green tea epicatechins are hypolipidemic in hamsters (*Mesocricetus auratus*) fed a high fat diet. *J Nutr,* 129**,** 1094-1101.

(15) Chang, H. P., Wang, M. L., Chan, M. H., Chiu, Y. S. and Chen, Y. H. 2011. Antiobesity activities of indole-3-carbinol in high-fat-diet-induced obese mice. *Nutrition,* 27**,** 463-470.

(16) Chang, Y. C. and Cho, H. J. 2012. Ascofuranone stimulates expression of adiponectin and peroxisome proliferator activated receptor through the modulation of mitogen activated protein kinase family members in 3T3-L1, murine pre-adipocyte cell line. *Biochem Biophys Res Commun,* 422**,** 423-428.

(17) Chegwidden, W. R. and Spencer, I. M. 1996. Carbonic anhydrase provides bicarbonate for de novo lipogenesis in the locust. *Comparative Biochemistry and Physiology B-Biochemistry & Molecular Biology,* 115**,** 247-254.

(18) Chen, H., Charlat, O., Tartaglia, L. A., Woolf, E. A., Weng, X., Ellis, S. J., Lakey, N. D., Culpepper, J., Moore, K. J., Breitbart, R. E., Duyk, G. M., Tepper, R. I. and Morgenstern, J. P. 1996a. Evidence that the diabetes gene encodes the leptin receptor: identification of a mutation in the leptin receptor gene in db/db mice. *Cell,* 84**,** 491-495.

(19) Chen, I. S., Chang, C. T., Sheen, W. S., Teng, C. M., Tsai, I. L., Duh, C. Y. and Ko, F. N. 1996b. Coumarins and antiplatelet aggregation constituents from Formosan *Peucedanum japonicum*. *Phytochemistry,* 41**,** 525-530.

(20) Chihara, Y., Rakugi, H., Ishikawa, K., Ikushima, M., Maekawa, Y., Ohta, J., Kida, I. and Ogihara, T. 2006. Klotho protein promotes adipocyte differentiation. *Endocrinology,* 147**,** 3835-3842.

(21) Cho, A. S., Jeon, S. M., Kim, M. J., Yeo, J., Seo, K. I., Choi, M. S. and Lee, M. K. 2010. Chlorogenic acid exhibits anti-obesity property and improves lipid metabolism in high-fat diet-induced-obese mice. *Food Chem Toxicol,* 48**,** 937-943.

(22) Chung, M. Y., Park, H. J., Manautou, J. E., Koo, S. I. and Bruno, R. S. 2012. Green tea extract protects against nonalcoholic steatohepatitis in ob/ob mice by decreasing oxidative and nitrative stress responses induced by proinflammatory enzymes. *J Nutr Biochem,* 23**,** 361-367.

(23) De Haan, W., Bhattacharjee, A., Ruddle, P., Kang, M. H. and Hayden, M. R. 2014. ABCA1 in adipocytes regulates adipose tissue lipid content, glucose tolerance, and insulin sensitivity. *J Lipid Res,* 55**,** 516-523.

(24) De Simone, G. and D' Addeo, G. 2008. Sibutramine: balancing weight loss benefit and possible cardiovascular risk. *Nutr Metab Cardiovasc Dis,* 18**,** 337-341.

(25) Dixon, J. B., Dixon, M. E., Anderson, M. L., Schachter, L. and O'Brien P, E. 2007. Daytime sleepiness in the obese: not as simple as obstructive sleep apnea. *Obesity (Silver Spring),* 15**,** 2504-2511.

(26) Drew, B. S., Dixon, A. F. and Dixon, J. B. 2007. Obesity management: update on orlistat. *Vasc Health Risk Manag,* 3**,** 817-821.

(27) Faust, J. R., Luskey, K. L., Chin, D. J., Goldstein, J. L. and Brown, M. S. 1982. Regulation of synthesis and degradation of 3-hydroxy-3-methylglutaryl-coenzyme A reductase by low density lipoprotein and 25-hydroxycholesterol in UT-1 cells. *Proc Natl Acad Sci U S A,* 79**,** 5205-5209.

(28) Fisher, F. M., Kleiner, S., Douris, N., Fox, E. C., Mepani, R. J., Verdeguer, F., Wu, J., Kharitonenkov, A., Flier, J. S., Maratos-Flier, E. and Spiegelman, B. M. 2012. FGF21 regulates PGC-1α and browning of white adipose tissues in adaptive thermogenesis. *Genes Dev,* 26**,** 271-281.

(29) Fletcher, M. J. 1968. A colorimetric method for estimating serum triglycerides. *Clin Chim Acta,* 22**,** 393-397.

(30) Folch, J., Lees, M. and Sloane Stanley, G. H. 1957. A simple method for the isolation and purification of total lipides from animal tissues. *J Biol Chem,* 226**,** 497-509.

(31) Frank, J., Kamal-Eldin, A., Razdan, A., Lundh, T. and Vessby, B. 2003. The dietary hydroxycinnamate caffeic acid and its conjugate chlorogenic acid increase vitamin e and cholesterol concentrations in Sprague-Dawley rats. *J Agric Food Chem,* 51**,** 2526-2531.

(32) Fu, M., Sun, T., Bookout, A. L., Downes, M., Yu, R. T., Evans, R. M. and Mangelsdorf, D. J. 2005. A Nuclear Receptor Atlas: 3T3-L1 adipogenesis. *Mol Endocrinol,* 19**,** 2437-2450.

(33) Garcia de Herreros, A. and Birnbaum, M. J. 1989. The acquisition of increased insulin-responsive hexose transport in 3T3-L1 adipocytes correlates with expression of a novel transporter gene. *J Biol Chem,* 264**,** 19994-19999.

(34) Gordon, M. D. and Nusse, R. 2006. Wnt signaling: multiple pathways, multiple receptors, and multiple transcription factors. *J Biol Chem,* 281**,** 22429-22433.

(35) Gosmann, G., Barlette, A. G., Dhamer, T., Arcari, D. P., Santos, J. C., de Camargo, E. R., Acedo, S., Gambero, A., Gnoatto, S. C. and Ribeiro, M. L. 2012. Phenolic compounds from mate (*Ilex paraguariensis*) inhibit adipogenesis in 3T3-L1 preadipocytes. *Plant Foods Hum Nutr,* 67**,** 156-161.

(36) Green, H. and Kehinde, O. 1975. An established preadipose cell line and its differentiation in culture. II. Factors affecting the adipose conversion. *Cell,* 5**,** 19-27.

(37) Hardie, D. G. 2011. AMP-activated protein kinase: a cellular energy sensor with a key role in metabolic disorders and in cancer. *Biochem Soc Trans,* 39**,** 1-13.

(38) Hauner, H., Rohrig, K., Spelleken, M., Liu, L. S. and Eckel, J. 1998. Development of insulin-responsive glucose uptake and GLUT4 expression in differentiating human adipocyte precursor cells. *Int J Obes Relat Metab Disord,* 22**,** 448-453.

(39) Hayata, K., Sakano, K. and Nishinaka, S. 2008. Establishment of new highly insulin-sensitive cell lines and screening of compounds to facilitate glucose consumption. *J Pharmacol Sci,* 108**,** 348-354.

(40) He, W., Barak, Y., Hevener, A., Olson, P., Liao, D., Le, J., Nelson, M., Ong, E., Olefsky, J. M. and Evans, R. M. 2003. Adipose-specific peroxisome proliferator-

activated receptor gamma knockout causes insulin resistance in fat and liver but not in muscle. *Proc Natl Acad Sci U S A,* 100**,** 15712-15717.

(41) Hisamoto, M., Kikuzaki, H. and Nakatani, N. 2004. Constituents of the leaves of *Peucedanum japonicum* Thunb. and their biological activity. *J Agric Food Chem,* 52**,** 445-450.

(42) Hisamoto, M., Kikuzaki, H., Ohigashi, H. and Nakatani, N. 2003. Antioxidant compounds from the leaves of *Peucedanum japonicum* thunb. *J Agric Food Chem,* 51**,** 5255-5261.

(43) Horton, J. D., Goldstein, J. L. and Brown, M. S. 2002. SREBPs: activators of the complete program of cholesterol and fatty acid synthesis in the liver. *J Clin Invest,* 109**,** 1125-1131.

(44) Hubbert, M. L., Zhang, Y., Lee, F. Y. and Edwards, P. A. 2007. Regulation of hepatic Insig-2 by the farnesoid X receptor. *Mol Endocrinol,* 21**,** 1359-1369.

(45) Hung, P. F., Wu, B. T., Chen, H. C., Chen, Y. H., Chen, C. L., Wu, M. H., Liu, H. C., Lee, M. J. and Kao, Y. H. 2005. Antimitogenic effect of green tea (-)-epigallocatechin gallate on 3T3-L1 preadipocytes depends on the ERK and Cdk2 pathways. *Am J Physiol Cell Physiol,* 288**,** C1094-1108.

(46) Hwang, C. S., Loftus, T. M., Mandrup, S. and Lane, M. D. 1997. Adipocyte differentiation and leptin expression. *Annu Rev Cell Dev Biol,* 13**,** 231-259.

(47) Hwang, Y. P., Choi, J. H., Han, E. H., Kim, H. G., Wee, J. H., Jung, K. O., Jung, K. H., Kwon, K. I., Jeong, T. C., Chung, Y. C. and Jeong, H. G. 2011. Purple sweet potato anthocyanins attenuate hepatic lipid accumulation through activating adenosine monophosphate-activated protein kinase in human HepG2 cells and obese mice. *Nutr Res,* 31**,** 896-906.

(48) Japan Society on Obesity and Study. 2014. Available at *http://www.dm-net.co.jp/calendar/2014/021932.php*.

(49) Jeong, S. J., Yoo, S. R., Seo, C. S. and Shin, H. K. 2015. Traditional korean herbal formula Samsoeum attenuates adipogenesis by regulating the phosphorylation of ERK1/2 in 3T3-L1 Cells. *Evid Based Complement Alternat Med,* 2015**,** 893934.

(50) Johansson, L. M., Johansson, L. E. and Ridderstrale, M. 2008. The visfatin (PBEF1) G-948T gene polymorphism is associated with increased high-density lipoprotein cholesterol in obese subjects. *Metabolism,* 57**,** 1558-1562.

(51) Katsuki, A., Sumida, Y., Gabazza, E. C., Murashima, S., Furuta, M., Araki-Sasaki, R., Hori, Y., Yano, Y. and Adachi, Y. 2001. Homeostasis model assessment is a reliable indicator of insulin resistance during follow-up of patients with type 2 diabetes. *Diabetes Care,* 24**,** 362-365.

(52) Kim, H. K., Kim, J. N., Han, S. N., Nam, J. H., Na, H. N. and Ha, T. J. 2012. Black soybean anthocyanins inhibit adipocyte differentiation in 3T3-L1 cells. *Nutr Res,* 32**,** 770-777.

(53) Kim, M. Y., Seguin, P., Ahn, J. K., Kim, J. J., Chun, S. C., Kim, E. H., Seo, S. H., Kang, E. Y., Kim, S. L., Park, Y. J., Ro, H. M. and Chung, I. M. 2008. Phenolic compound concentration and antioxidant activities of edible and medicinal mushrooms from Korea. *J Agric Food Chem,* 56**,** 7265-7270.

(54) Kivela, J., Parkkila, S., Parkkila, A. K., Leinonen, J. and Rajaniemi, H. 1999. Salivary carbonic anhydrase isoenzyme VI. *J Physiol,* 520 Pt 2**,** 315-320.

(55) Koyama, T., Miyata, M., Nishimura, T. and Yazawa, K. 2012. Suppressive effects by leaves of the *Dypsis lutescens* palm on fat accumulation in 3T3-L1 cells and fat absorption in mice. *Biosci Biotechnol Biochem,* 76**,** 189-192.

(56) Lean, M. E. 2001. How does sibutramine work? *Int J Obes Relat Metab Disord,* 25 Suppl 4**,** S8-11.

(57) Lee, J. H., Kim, K. A., Kwon, K. B., Kim, E. K., Lee, Y. R., Song, M. Y., Koo, J. H., Ka, S. O., Park, J. W. and Park, B. H. 2007. Diallyl disulfide accelerates adipogenesis in 3T3-L1 cells. *Int J Mol Med,* 20**,** 59-64.

(58) Lee, M. S., Kim, C. T., Kim, I. H. and Kim, Y. 2011. Effects of capsaicin on lipid catabolism in 3T3-L1 adipocytes. *Phytother Res,* 25**,** 935-939.

(59) Lee, M. S., Kim, D., Jo, K. and Hwang, J. K. 2010. Nordihydroguaiaretic acid protects against high-fat diet-induced fatty liver by activating AMP-activated protein kinase in obese mice. *Biochem Biophys Res Commun,* 401**,** 92-97.

(60) Lehrke, M. and Lazar, M. A. 2005. The many faces of PPARgamma. *Cell,* 123**,** 993-999.

(61) Li, H. and Durbin, R. 2010. Fast and accurate long-read alignment with Burrows-Wheeler transform. *Bioinformatics,* 26**,** 589-595.

(62) Li, Q., Liu, Z., Huang, J., Luo, G., Liang, Q., Wang, D., Ye, X., Wu, C., Wang, L. and Hu, J. 2013. Anti-obesity and hypolipidemic effects of Fuzhuan brick tea water extract in high-fat diet-induced obese rats. *J Sci Food Agric,* 93**,** 1310-1316.

(63) Li, R. Y., Song, H. D., Shi, W. J., Hu, S. M., Yang, Y. S., Tang, J. F., Chen, M. D. and Chen, J. L. 2004. Galanin inhibits leptin expression and secretion in rat adipose tissue and 3T3-L1 adipocytes. *J Mol Endocrinol,* 33**,** 11-19.

(64) Lii, C. K., Huang, C. Y., Chen, H. W., Chow, M. Y., Lin, Y. R., Huang, C. S. and Tsai, C. W. 2012. Diallyl trisulfide suppresses the adipogenesis of 3T3-L1 preadipocytes through ERK activation. *Food Chem Toxicol,* 50**,** 478-484.

(65) Lin, Y. C., Chang, P. F., Yeh, S. J., Liu, K. and Chen, H. C. 2010. Risk factors for liver steatosis in obese children and adolescents. *Pediatr Neonatol,* 51**,** 149-154.

(66) Liu, S., Willett, W. C., Manson, J. E., Hu, F. B., Rosner, B. and Colditz, G. 2003. Relation between changes in intakes of dietary fiber and grain products and changes in weight and development of obesity among middle-aged women. *Am J Clin Nutr,* 78**,** 920-927.

(67) Mackall, J. C., Student, A. K., Polakis, S. E. and Lane, M. D. 1976. Induction of lipogenesis during differentiation in a "preadipocyte" cell line. *J Biol Chem,* 251**,** 6462-6464.

(68) Matson, K. L. and Fallon, R. M. 2012. Treatment of obesity in children and adolescents. *J Pediatr Pharmacol Ther,* 17**,** 45-57.

(69) MGI Data and Statistical Reports. 2015. Available at ftp://ftp.informatics.jax.org/pub/reports/index.html.

(70) Ministry of Health, Labour and Welfare, Japan. 2010. Available at *http://www.mhlw.go.jp/stf/houdou/*.

(71) Nakamura, Y., Hinoi, E., Iezaki, T., Takada, S., Hashizume, S., Takahata, Y., Tsuruta, E., Takahashi, S. and Yoneda, Y. 2013. Repression of adipogenesis through promotion of Wnt/beta-catenin signaling by TIS7 up-regulated in adipocytes under hypoxia. *Biochim Biophys Acta,* 1832**,** 1117-1128.

(72) NCBI Reference Sequence and Database. 2015. Available at http://www.ncbi.nlm.nih.gov/refseq/.

(73) Nishizuka, M., Koyanagi, A., Osada, S. and Imagawa, M. 2008. Wnt4 and Wnt5a promote adipocyte differentiation. *FEBS Lett,* 582**,** 3201-3205.

(74) Nugara, R. N., Inafuku, M., Iwasaki, H. and Oku, H. 2014a. Partially purified *Peucedanum japonicum* Thunb extracts exert anti-obesity effects in vitro. *Nutrition,* 30**,** 575-583.

(75) Nugara, R. N., Inafuku, M., Takara, K., Iwasaki, H. and Oku, H. 2014b. Pteryxin: a coumarin in *Peucedanum japonicum* Thunb leaves exerts antiobesity activity through modulation of adipogenic gene network. *Nutrition,* 30**,** 1177-1184.

(76) Nukitrangsan, N., Okabe, T., Toda, T., Inafuku, M., Iwasaki, H. and Oku, H. 2012a. Anti-obesity Activity of *Peucedanum japonicum* Thunb Extract in Obese Diabetic Animal Model C57BL/6J Ham Slc-*ob/ob* Mice. *Int J LSMR,* 2**,** 28-34.

(77) Nukitrangsan, N., Okabe, T., Toda, T., Inafuku, M., Iwasaki, H. and Oku, H. 2012b. Effect of *Peucedanum japonicum* Thunb extract on high-fat diet-induced obesity and gene expression in mice. *J Oleo Sci,* 61**,** 89-101.

(78) Nukitrangsan, N., Okabe, T., Toda, T., Inafuku, M., Iwasaki, H., Yanagita, T. and Oku, H. 2011. Effect of *Peucedanum japonicum* Thunb on the expression of obesity-related genes in mice on a high-fat diet. *J Oleo Sci*, 60**,** 527-536.

(79) Ohara, K., Uchida, A., Nagasaka, R., Ushio, H. and Ohshima, T. 2009. The effects of hydroxycinnamic acid derivatives on adiponectin secretion. *Phytomedicine,* 16**,** 130-137.

(80) Okabe, T., Toda, T., Nukitrangsan, N., Inafuku, M., Iwasaki, H. and Oku, H. 2011. *Peucedanum japonicum* Thunb inhibits high-fat diet induced obesity in mice. *Phytother Res,* 25**,** 870-877.

(81) Padwal, R. S. and Majumdar, S. R. 2007. Drug treatments for obesity: orlistat, sibutramine, and rimonabant. *Lancet,* 369**,** 71-77.

(82) Papandreou, D., Rousso, I. and Mavromichalis, I. 2007. Update on non-alcoholic fatty liver disease in children. *Clin Nutr,* 26**,** 409-415.

(83) Park, U. H., Jeong, H. S., Jo, E. Y., Park, T., Yoon, S. K., Kim, E. J., Jeong, J. C. and Um, S. J. 2012. Piperine, a component of black pepper, inhibits adipogenesis by antagonizing PPARγ activity in 3T3-L1 cells. *J Agric Food Chem,* 60**,** 3853-3860.

(84) Procaccia, S., Kraus, S. and Seger, R. 2010. Determination of ERK activity: anti-phospho-ERK antibodies and in vitro phosphorylation. *Methods Mol Biol,* 661**,** 39-58.

(85) Raichur, S., Lau, P., Staels, B. and Muscat, G. E. 2007. Retinoid-related orphan receptor γ regulates several genes that control metabolism in skeletal muscle cells: links to modulation of reactive oxygen species production. *J Mol Endocrinol,* 39**,** 29-44.

(86) Rosen, E. D. and MacDougald, O. A. 2006. Adipocyte differentiation from the inside out. *Nat Rev Mol Cell Biol,* 7**,** 885-896.

(87) Rosen, E. D. and Spiegelman, B. M. 2000. Molecular regulation of adipogenesis. *Annu Rev Cell Dev Biol,* 16**,** 145-171.

(88) Ross, S. E., Hemati, N., Longo, K. A., Bennett, C. N., Lucas, P. C., Erickson, R. L. and MacDougald, O. A. 2000. Inhibition of adipogenesis by Wnt signaling. *Science,* 289**,** 950-953.

(89) Sakaue, H., Ogawa, W., Nakamura, T., Mori, T., Nakamura, K. and Kasuga, M. 2004. Role of MAPK phosphatase-1 (MKP-1) in adipocyte differentiation. *J Biol Chem,* 279**,** 39951-39957.

(90) Sale, E. M., Atkinson, P. G. and Sale, G. J. 1995. Requirement of MAP kinase for differentiation of fibroblasts to adipocytes, for insulin activation of p90 S6 kinase and for insulin or serum stimulation of DNA synthesis. *EMBO J,* 14**,** 674-684.

(91) Schrauwen, P. and Hesselink, M. 2002. UCP2 and UCP3 in muscle controlling body metabolism. *J Exp Biol,* 205**,** 2275-2285.

(92) Schreurs, M., Kuipers, F. and van der Leij, F. R. 2010. Regulatory enzymes of mitochondrial β-oxidation as targets for treatment of the metabolic syndrome. *Obes Rev,* 11**,** 380-388.

(93) Searcy, J. L., Phelps, J. T., Pancani, T., Kadish, I., Popovic, J., Anderson, K. L., Beckett, T. L., Murphy, M. P., Chen, K. C., Blalock, E. M., Landfield, P. W., Porter, N. M. and Thibault, O. 2012. Long-term pioglitazone treatment improves learning and

attenuates pathological markers in a mouse model of Alzheimer's disease. *J Alzheimers Dis,* 30**,** 943-961.

(94) Shao, B. and Heinecke, J. W. 2009. HDL, lipid peroxidation, and atherosclerosis. *J Lipid Res,* 50**,** 599-601.

(95) Shen, J. Z., Ma, L. N., Han, Y., Liu, J. X., Yang, W. Q., Chen, L., Liu, Y., Hu, Y. and Jin, M. W. 2012. Pentamethylquercetin generates beneficial effects in monosodium glutamate-induced obese mice and C2C12 myotubes by activating AMP-activated protein kinase. *Diabetologia,* 55**,** 1836-1846.

(96) Shimoda, H., Seki, E. and Aitani, M. 2006. Inhibitory effect of green coffee bean extract on fat accumulation and body weight gain in mice. *BMC Complement Altern Med,* 6**,** 9.

(97) Slovacek, L., Pavlik, V. and Slovackova, B. 2008. The effect of sibutramine therapy on occurrence of depression symptoms among obese patients. *Nutr Metab Cardiovasc Dis,* 18**,** e43-44.

(98) Smirnova, E., Goldberg, E. B., Makarova, K. S., Lin, L., Brown, W. J. and Jackson, C. L. 2006. ATGL has a key role in lipid droplet/adiposome degradation in mammalian cells. *EMBO Rep,* 7**,** 106-113.

(99) Sperry, W. M. and Webb, M. 1950. A revision of the Schoenheimer-Sperry method for cholesterol determination. *J Biol Chem,* 187**,** 97-106.

(100) Strand, D. W., Jiang, M., Murphy, T. A., Yi, Y., Konvinse, K. C., Franco, O. E., Wang, Y., Young, J. D. and Hayward, S. W. 2012. PPAR γ isoforms differentially regulate metabolic networks to mediate mouse prostatic epithelial differentiation. *Cell Death Dis,* 3**,** e361.

(101) Takahashi, M., Kamei, Y. and Ezaki, O. 2005. Mest/Peg1 imprinted gene enlarges adipocytes and is a marker of adipocyte size. *Am J Physiol Endocrinol Metab,* 288**,** E117-124.

(102) Takeuchi, N., Kasama, T., Aida, Y., Oki, J., Maruyama, I., Watanabe, K. and Tobinaga, S. 1991. Pharmacological activities of the prenylcoumarins, developed from folk usage as a medicine of *Peucedanum japonicum* THUNB. *Chem Pharm Bull (Tokyo),* 39**,** 1415-1421.

(103) Tang, Q. Q., Otto, T. C. and Lane, M. D. 2003. Mitotic clonal expansion: a synchronous process required for adipogenesis. *Proc Natl Acad Sci U S A,* 100**,** 44-49.

(104) Taxvig, C., Dreisig, K., Boberg, J., Nellemann, C., Schelde, A. B., Pedersen, D., Boergesen, M., Mandrup, S. and Vinggaard, A. M. 2012. Differential effects of environmental chemicals and food contaminants on adipogenesis, biomarker release and PPAR γ activation. *Mol Cell Endocrinol,* 361**,** 106-115.

(105) Than, A., Cheng, Y., Foh, L. C., Leow, M. K., Lim, S. C., Chuah, Y. J., Kang, Y. and Chen, P. 2012. Apelin inhibits adipogenesis and lipolysis through distinct molecular pathways. *Mol Cell Endocrinol,* 362**,** 227-241.

(106) Thurairajah, P. H., Syn, W. K., Neil, D. A., Stell, D. and Haydon, G. 2005. Orlistat (Xenical)-induced subacute liver failure. *Eur J Gastroenterol Hepatol,* 17**,** 1437-1438.

(107) Topol, L., Jiang, X., Choi, H., Garrett-Beal, L., Carolan, P. J. and Yang, Y. 2003. Wnt-5a inhibits the canonical Wnt pathway by promoting GSK-3-independent beta-catenin degradation. *J Cell Biol,* 162**,** 899-908.

(108) Tordjman, K. M., Leingang, K. A., James, D. E. and Mueckler, M. M. 1989. Differential regulation of two distinct glucose transporter species expressed in 3T3-L1 adipocytes: effect of chronic insulin and tolbutamide treatment. *Proc Natl Acad Sci U S A,* 86**,** 7761-7765.

(109) Uguz, F., Sahingoz, M., Gungor, B., Aksoy, F. and Askin, R. 2015. Weight gain and associated factors in patients using newer antidepressant drugs. *Gen Hosp Psychiatry,* 37**,** 46-48.

(110) Vitali, A., Murano, I., Zingaretti, M. C., Frontini, A., Ricquier, D. and Cinti, S. 2012. The adipose organ of obesity-prone C57BL/6J mice is composed of mixed white and brown adipocytes. *J Lipid Res,* 53**,** 619-629.

(111) Wang, L., Yamasaki, M., Katsube, T., Sun, X., Yamasaki, Y. and Shiwaku, K. 2011. Antiobesity effect of polyphenolic compounds from molokheiya (*Corchorus olitorius* L.) leaves in LDL receptor-deficient mice. *Eur J Nutr,* 50**,** 127-133.

(112) Willson, T. M., Cobb, J. E., Cowan, D. J., Wiethe, R. W., Correa, I. D., Prakash, S. R., Beck, K. D., Moore, L. B., Kliewer, S. A. and Lehmann, J. M. 1996. The structure-

activity relationship between peroxisome proliferator-activated receptor γ agonism and the antihyperglycemic activity of thiazolidinediones. *J Med Chem,* 39**,** 665-668.

(113) World Health Organization. 2014a. Global Status Report on non-communicable diseases. Available at http://www.who.int/nmh/publications/ncd-status-report-2014/en/.

(114) World Health Organization. 2014b. Obesity and Overweight. Available at http://www.who.int/mediacentre/factsheets/fs311/en/.

(115) Yin, J., Hu, R., Chen, M., Tang, J., Li, F., Yang, Y. and Chen, J. 2002. Effects of berberine on glucose metabolism in vitro. *Metabolism,* 51**,** 1439-1443.

(116) Yoon, Y. I., Chung, M. Y., Hwang, J. S., Han, M. S., Goo, T. W. and Yun, E. Y. 2015. *Allomyrina dichotoma* (Arthropoda: Insecta) larvae confer resistance to obesity in mice fed a high-fat diet. *Nutrients,* 7**,** 1978-1991.

(117) Youn, B. S., Kloting, N., Kratzsch, J., Lee, N., Park, J. W., Song, E. S., Ruschke, K., Oberbach, A., Fasshauer, M., Stumvoll, M. and Bluher, M. 2008. Serum vaspin concentrations in human obesity and type 2 diabetes. *Diabetes,* 57**,** 372-377.

(118) Yun, J. W. 2010. Possible anti-obesity therapeutics from nature--a review. *Phytochemistry,* 71**,** 1625-1641.

(119) Zang, M., Zuccollo, A., Hou, X., Nagata, D., Walsh, K., Herscovitz, H., Brecher, P., Ruderman, N. B. and Cohen, R. A. 2004. AMP-activated protein kinase is required for the lipid-lowering effect of metformin in insulin-resistant human HepG2 cells. *J Biol Chem,* 279**,** 47898-47905.

(120) Zhang, X. H., Huang, B., Choi, S. K. and Seo, J. S. 2012. Anti-obesity effect of resveratrol-amplified grape skin extracts on 3T3-L1 adipocytes differentiation. *Nutr Res Pract,* 6**,** 286-293.

(121) Zhang, Y., Guo, K. Y., Diaz, P. A., Heo, M. and Leibel, R. L. 2002. Determinants of leptin gene expression in fat depots of lean mice. *Am J Physiol Regul Integr Comp Physiol,* 282**,** R226-234.